ZMB
Zentrum für Medizinische Biotechnologie
Center of Medical Biotechnology

UNIVERSITÄT DUISBURG ESSEN
Offen im Denken

INVESTIGATING THE ROLE OF THREONINE ASPARTASE 1 IN ESTROGEN-DRIVEN TRANSCRIPTION

Dissertation

zur Erlangung des Doktorgrades

Dr. rer. nat.

der Fakultät für Biologie

an der Universität Duisburg-Essen

vorgelegt von

Lisa Moews

aus Dannenberg

Juli 2022

DOI: 10.17185/duepublico/77038
URN: urn:nbn:de:hbz:465-20231031-140726-6

Die der vorliegenden Arbeit zugrundeliegenden Experimente wurden am Zentrum für medizinische Biotechnologie (ZMB) in der Abteilung für Molekularbiologie II der Universität Duisburg-Essen durchgeführt.

1. Gutachter: Prof. Dr. Shirley Knauer

2. Gutachter: Prof. Dr. Perihan Nalbant

Vorsitzender des Prüfungsausschusses: Prof. Dr. Dominik Boos

Tag der mündlichen Prüfung: 26.09.2022

TABLE OF CONTENTS

ZUSAMMENFASSUNG

Die Protease Threonin Aspartase 1 (Taspase1) ist für die Spaltung diverser Substrate wie z. B. des MLL (Mixed-Lineage Leukemia)-Proteins oder des Transkriptionsfaktors TFIIA verantwortlich und so in unterschiedliche zelluläre Prozesse involviert. Zudem ist eine Überexpression von Taspase1 für Leukämien wie auch verschiedene solide Tumorarten beschrieben. Taspase1 ist hierbei zur Aufrechterhaltung des malignen Phänotyps in vielen Tumoren essentiell, wohingegen die genetische Depletion von Taspase1 im adulten Organismus keine schwerwiegenden Auswirkungen zeigt. Somit stellt diese Protease ein vielversprechendes molekulares Angriffsziel für die Krebstherapie dar. Die mangelnden Kenntnisse über Taspase1 lassen sich u. a. damit begründen, dass bisher nur wenige Interaktionspartner dieser Protease identifiziert wurden. Zudem sind zwar einige Substratproteine der Taspase1 bekannt, diese weisen aber kaum funktionelle Gemeinsamkeiten auf, so dass Taspase1 bisher keine übergeordnete Rolle in einem zellulären Prozess oder Signalweg zugeordnet werden konnte. Daher sollten in dieser Arbeit systematisch weitere stabile und transiente Interaktoren identifiziert werden, um anhand der funktionalen Schnittmenge der bekannten und neu identifizierten Interaktionspartner Rückschlüsse auf die zentrale Funktion und das gesamte Wirkungsspektrum der Taspase1 ziehen zu können.

Mittels co-Immunpräzipitationsexperimenten (co-IPs) und Massenspektrometrie konnten u. a. Nucleolin und Topoisomerase II (Topo II) als neue Bindungspartner der Taspase1 identifiziert werden. Für diese Proteine ist beschrieben, dass sie gemeinsam mit dem bereits bekannten Taspase1-Interaktionspartner Nucleophosmin 1 (NPM1) einen co-Repressorkomplex ausbilden können, der an Promotorbereiche Östrogen-abhängiger Gene bindet, jedoch nach einer Steroidbehandlung wieder dissoziiert. Dieser Befund und zusätzliche Indizien deuteten auf einen Zusammenhang von Taspase1 und der zellulären Östrogenantwort, der im Folgenden weiter untersucht werden sollte. Tatsächlich konnte *TASP1* als östrogen-abhängiges Gen charakterisiert werden, welches nach Östrogenstimulus zyklisch hochreguliert wird. Die Identifizierung eines Östrogen-Response-Elements (ERE) 7,8 kbp strangaufwärts des *TASP1*-Promotors unterstreicht dies ebenfalls.

Es ist bekannt, dass das Enzym Topo II β bei der Transkriptionsinitiation Hormon-regulierter Gene eine essentielle Funktion ausübt. Im Promoterbereich werden durch

Topoisomerasen transiente DNS-Doppelstrangbrüche erzeugt, um so vorhandene topologische Barrieren wie superspiralisierte oder verknotete DNS zu entfernen. In der Tat konnte im Rahmen dieser Arbeit eine direkte Funktion der Taspase1 in diesem essentiellen Prozess der Transkriptionsaktivierung Hormon-induzierter Gene nachgewiesen werden. Mittels co-IP isolierte Taspase1-Komplexe wiesen nach Östrogenexposition eine starke Akkumulation der an diesem Prozess maßgeblich beteiligten Proteine einschließlich Topo II auf.

Da eine östrogenabhängige Assoziation von Topo II mit immunpräzipitierter Taspase1-GFP identifiziert werden konnte, wurde im Folgenden das Zusammenspiel zwischen Taspase1 und Topo II detaillierter untersucht. Zum einen konnte innerhalb der Topo II α-Sequenz eine einfache Taspase1-Konsensus-Spaltsequenz (^{1249}QEDG^{1252}) identifiziert werden. *In vivo*- und *in vitro*-Spaltungsexperimente konnten jedoch nicht bestätigen, dass Topo II α tatsächlich ein Taspase1-Substrat darstellt. Dies schließt allerdings nicht aus, dass eine Taspase1-vermittelte Spaltung von Topo II α unter bestimmten Umgebungsbedingungen dennoch stattfindet. Dies könnte durchaus Gegenstand weiterführender Untersuchungen sein.

Die beobachtete Kolokalisation von Taspase1 und Topo II in 293T- und HeLa-Zellen lieferte einen weiteren Hinweis für einen funktionellen Zusammenhang zwischen den beiden Proteinen. Tatsächlich zeigten *proximity ligation assays*, dass es sich bei der Interaktion von Taspase1 und Topo II vermutlich um eine direkte Protein-Protein-Interaktion handelt. Daraufhin stellte sich die Frage, wie diese direkte Taspase1-Topo II-Wechselwirkung hormoninduzierte DNS-Doppelstrangbruch an Östrogen-abhängigen Promotoren beeinflusst. *In vitro*-Experimente mit rekombinanter Topo II β und Taspase1-His zeigten, dass Taspase1-His in konzentrationsabhängiger Weise die Entstehung Topo II β-katalysierter Doppelstrangbrüche in Plasmid-DNS verstärkt. Mittels Affinitätselektrophorese konnte gezeigt werden, dass Taspase1 an DNS binden kann. Diese neu identifizierte Eigenschaft von Taspase1 könnte eine Erklärung dafür liefern, dass diese Protease in der Lage ist, die enzymatische Aktivität von Topo II β positiv zu beeinflussen. So könnte postuliert werden, dass Taspase1 die Bindung von Topo II an die DNS erleichtert bzw. Topo II zu bestimmten DNS-Sequenzen rekrutiert.

Zudem konnte im Rahmen dieser Arbeit gezeigt werden, dass Taspase1 den Östrogen-Signalweg auch auf weiteren Ebenen beeinflusst. Die Spaltung von Taspase1-Substratproteinen führte zu einer Veränderung der Genexpressionsmuster nach Hormon-Stimulus der Zelle. Beispielsweise führte die Östrogen-Behandlung von 293T-Zellen auch zu einer Erhöhung der H3K4-Methylierung, einer mit Gen-Aktivierung assoziierten epigenetischen Modifikation. Da die Spaltung des MLL-Proteins durch Taspase1 die Voraussetzung für eine effiziente MLL-vermittelte H3K4-Methylierung darstellt, kann geschlussfolgert werden, dass erst die Östrogen-induzierte Hochregulation von Taspase1 den im gleichen Zeitfenster erscheinenden Anstieg der H3K4-Methylierung ermöglicht. Durch diese indirekte Modulation der epigenetischen H3K4-Signatur trägt Taspase1 somit vermutlich auch zur länger andauernden Aktivierung von Östrogen-bedingten genetischen Programmen bei.

Die im Rahmen dieser Arbeit neu identifizierte Funktion von Taspase1 im Östrogen-Signalweg konnte weiterhin durch Taspase1-Depletionsstudien bestätigt werden. Nach siRNA-vermittelter Taspase1-Depletion wurden insbesondere verminderte Expressionsmengen Östrogen-regulierter Gene wie c-fos und c-myc nachgewiesen.

Zusammenfassend konnte in dieser Dissertation Taspase1 einem übergeordneten Signalweg, und zwar dem zellulären Östrogenweg zugeordnet werden. In diesem Kontext wurde Taspase1 als multifunktionaler Koaktivator der Östrogen-vermittelten Transkriptionsaktivierung charakterisiert.

SUMMARY

The protease Threonine aspartase 1 (Taspase1) is involved in diverse cellular processes by proteolytic processing of various substrates including MLL (mixed-lineage leukemia) proteins and transcription factor TFIIA. An overexpression of Taspase1 is described for leukemia, solid tumor types and diverse human cancer cell lines. The genetic depletion of Taspase1 in adult mice causes no apparent deficiencies but especially cancer cells are dependent on Taspase1 expression to maintain their proliferation, classifying Taspase1 as a non-oncogene addiction protease. Thus, this protease represents a promising therapeutic target for anti-cancer therapy. However, previous knowledge of Taspase1 is based on its known substrates and high-throughput screenings that allowed the identification of new potential cleavage targets or interaction partners. The small number of previously known Taspase1 interactors might rely on the fact that transient or context-dependent interactions are easily overlooked. This thesis thus aimed for a better understanding of Taspase1´s sphere of activity and strives to unravel its full range of functions. Therefore, one goal of this project was to search for further transient and stable Taspase1 interaction partners to gain a deeper understanding of its overarching molecular function

As such, co-immunoprecipitation experiments and mass spectrometry allowed to identify novel Taspase1 binding partners Nucleolin and Topoisomerase II (Topo II). Previous studies already revealed that Taspase1's known interaction partner NPM1 together with Nucleolin and Topo II β is able to form a co-repressor complex. The latter is present on promoters of estrogen responsive genes but disassociates rapidly after estrogen treatment. This finding and additional circumstantial evidence suggested a link between Taspase1 and the cellular estrogen response, and therefore further investigations were performed in this regard. Indeed, the *TASP1* gene itself is estrogen-responsive demonstrated as Taspase1 was found to be cyclically upregulated upon estrogen stimulation. This is in accordance with the identification of an estrogen response element (ERE) 7.8 kbp upstream of the *TASP1* promoter in this thesis. It is known that Topo II β function is essential for the transcriptional activation of hormone-inducible genes. The enzyme generates a transient DNA double strand break (DSB) within the promotor region and resolves topological barriers such as DNA supercoils or knots, thereby allowing the transcription machinery to gain rapid access.

In frame of this thesis, Taspase1 could be assigned a direct function in transcriptional activation of estrogen-dependent genes since estrogen treatment leads to a significant increase of Topo II, NPM1, Nucleolin and γH2AX in Taspase1 complexes isolated via co-IPs from chromatin fractions.

As Topo II was identified as an estrogen-dependent component of immunoprecipitated Taspase1-GFP complexes, the possible interplay between Taspase1 and Topo II was subjected to further investigation. Although a shortened Taspase1 cleavage sequence (aa ^{1249}QEDG^{1252}) could be identified in Topo II α, *in vivo* and *in vitro* cleavage experiments could not confirm it as a potential Taspase1 substrate. However, this does not exclude the possibility that Taspase1-mediated cleavage of Topo II α might occurs under certain physiological conditions. Moreover, Taspase1 and Topo II co-localized in 293T- and HeLa cells, again hinting towards a functional interplay between these two proteins. In fact, proximity ligation assays could verify a probably direct interaction between Taspase1 and Topo II. Subsequently, the effect of this interplay on hormone-induced DSBs at estrogen-dependent promotors was investigated *in vivo* and *in vitro* by a Topo II β cleavage assay. It turned out that Taspase1 directly facilitates Topo II β-mediated DSBs in a dose-dependent manner. It was also revealed that Taspase1 is able to directly bind to DNA, which might explain how Taspase1 positively enhances Topo II β-mediated DSBs.

Furthermore, the results of this thesis unravelled further modes of action for Taspase1 to reinforce the cellular estrogen response: methylation of histone H3 lysine 4 (H3K4me) increases after estrogen stimuli correlating with Taspase1 levels. This indicates that Taspase1 might enables H3K4me epigenetic labelling via cleavage-triggered activation of MLL in an estrogen-dependent manner. Hence, it can be concluded that Taspase1 is also responsible for the necessary epigenetic signature that allows the maintenance of the hormone-activated transcriptional program. Furthermore, Taspase1-depletion studies demonstrated a decline of estrogen-regulated gene expression levels such as c-fos and c-myc, thereby validating the pivotal role of Taspase1 in estrogen-driven transcription.

In sum, the results generated in this thesis demonstrate for the first time that Taspase1's sphere of activity is embedded in a specific signaling cascade, namely the cellular estrogen pathway. Taspase1 can thus be newly classified as a multi-functioning co-activator of estrogen-driven transcription.

1 INTRODUCTION

1.1 PROTEASES IN CANCER

Proteases are enzymes, which catalyze the breakdown of peptides and proteins (proteolysis) through hydrolysis of the peptide bond thereby regulating diverse cellular processes (Barrett, 2001; López-Otín and Overall, 2002; Turk, 2006), e.g. angiogenesis, apoptosis, autophagy, blood coagulation, cell-cycle progression, cell proliferation, DNA replication and transcription, immune response, inflammation, migration, neurogenesis, remodeling and wound healing (Barrett, 2001; Sternlicht and Werb, 2001; López-Otín and Overall, 2002; Turk, 2006; López-Otín and Bond, 2008). According to their catalytic mechanism, proteases can be subdivided into five classes: aspartic, cysteine, metallo, serine or threonine proteases (Barrett, 2001; López-Otín and Overall, 2002; Turk, 2006). Serine, cysteine and threonine proteases build an intermediate through proteolysis by using the side chain of the respective amino acid in the active site as a nucleophile, while aspartic and metallo-proteases utilize a water molecule for nucleophilic attack on the substrate carbonyl carbon without forming an intermediate (Barrett, 2001; Lah *et al.*, 2006). Furthermore, proteases can be classified based on their preferred cleavage site within the substrate as exo- or endopeptidases (Barrett, 2001; Turk, 2006; Clausen *et al.*, 2011) or a classification on the basis of structural similarities, which reflect evolutionary relations, is used (Barrett, 2001).

Proteases proteolytically process many different classes of proteins including other enzymes, cytokines, growth factors and hormones (Sternlicht and Werb, 2001; López-Otín and Overall, 2002). The cleavage event can lead for example to an altered activity or localization of the substrate or result in modulated protein-protein interactions (López-Otín and Bond, 2008). Because proteolytic substrate cleavage is irreversible and can determine the cell fate, a tight regulation of proteases is necessary. A possible mechanism to control the action of proteases is the activation of the inactive precursor protein (zymogen) by autoproteolytic cleavage. Two prominent examples for zymogen activation are blood coagulation (Neurath and Walsh, 1976) and caspase activation during apoptosis (Nicholson, 1999). Besides zymogen activation, fine tuning of the activation-mechanism (Doucet and Overall, 2008), post-translational modifications (Cardone *et al.*, 1998; Villamil *et al.*, 2012) and endogenous protease inhibitors, like

serpins (Law *et al.*, 2006) or cystatins (Kopitar-Jerala, 2012), play critical roles in the regulation of proteases.

Over the past few decades, the importance of proteolysis has become increasingly apparent, as proteolysis is critical to maintain cell homeostasis (Barrett, 2001; López-Otín and Overall, 2002), and at least 600 proteases constitute the human degradome (Rawlings *et al.*, 2018; Bond, 2019; Rawlings and Barrett, 2020), which determines the fate of many proteins (López-Otín and Overall, 2002).

The continuously increasing number of newly discovered proteases and their involvement in a variety of processes within the cell elucidate the elementary role of proteases in human biology. Thus, dysregulated proteases lead to pathological conditions and many proteases are associated with human diseases including cancer, cardiovascular diseases, inflammatory and neurodegenerative disorders (Koblinski *et al.*, 2000; López-Otín and Matrisian, 2007; López-Otín and Bond, 2008). Moreover, dysregulation of protease function is associated with all stages of tumorigenesis (Koblinski *et al.*, 2000; Egeblad and Werb, 2002; Borgoño and Diamandis, 2004) and in tumor-microenvironment, proteases are known to be involved in tumor-promoting properties like growth factor signaling pathways, angiogenesis, invasion, metastasis and migration (Mason and Joyce, 2011; Vizovisek *et al.*, 2021). These properties link proteases to the hallmarks of cancer (Figure 1.1) and highlight the importance of the knowledge in proteases, their degradome and possible therapeutic approaches (Lah *et al.*, 2006; López-Otín and Matrisian, 2007; Vizovisek *et al.*, 2021).

Besides the aforementioned tumor-promoting properties, it is known that some proteases display also anti-tumor characteristics (López-Otín and Matrisian, 2007). Several intracellular proteases are involved in signaling cascades that act as protective mechanisms (López-Otín and Matrisian, 2007), such as caspases in apoptosis (Teitz *et al.*, 2000) or deubiquitylases in protein modification removal (Hoeller *et al.*, 2006). Loss-of-function mutations within the genes coding for those proteases are known in different tumors (Teitz *et al.*, 2000; Hoeller *et al.*, 2006) and indicate a tumor suppressor function in those cases (López-Otín and Matrisian, 2007).

Considering their dual role in carcinogenesis, proteases serve as promising drug targets for anti-cancer therapies. One approach to target proteases is to design small synthetic molecules that mimic the amino acid sequence specifically recognized by the

corresponding protease (Lah *et al.*, 2006). Selective inhibitors can then be identified by high-throughput screening of these rationally designed molecules (Lah *et al.*, 2006). First clinical trials with synthetic inhibitors of matrix metalloproteases showed not the expected effects on cancer progression, although the previously performed *in vitro* and animal experiments looked promising (Lah *et al.*, 2006; López-Otín and Matrisian, 2007). Meanwhile, clinical trials of the proteasome inhibitor Bortezomib were more successful and it gained approval as a drug to treat multiple myeloma and mantle cell lymphoma (Kane *et al.*, 2003; Lah *et al.*, 2006; Kane *et al.*, 2007).

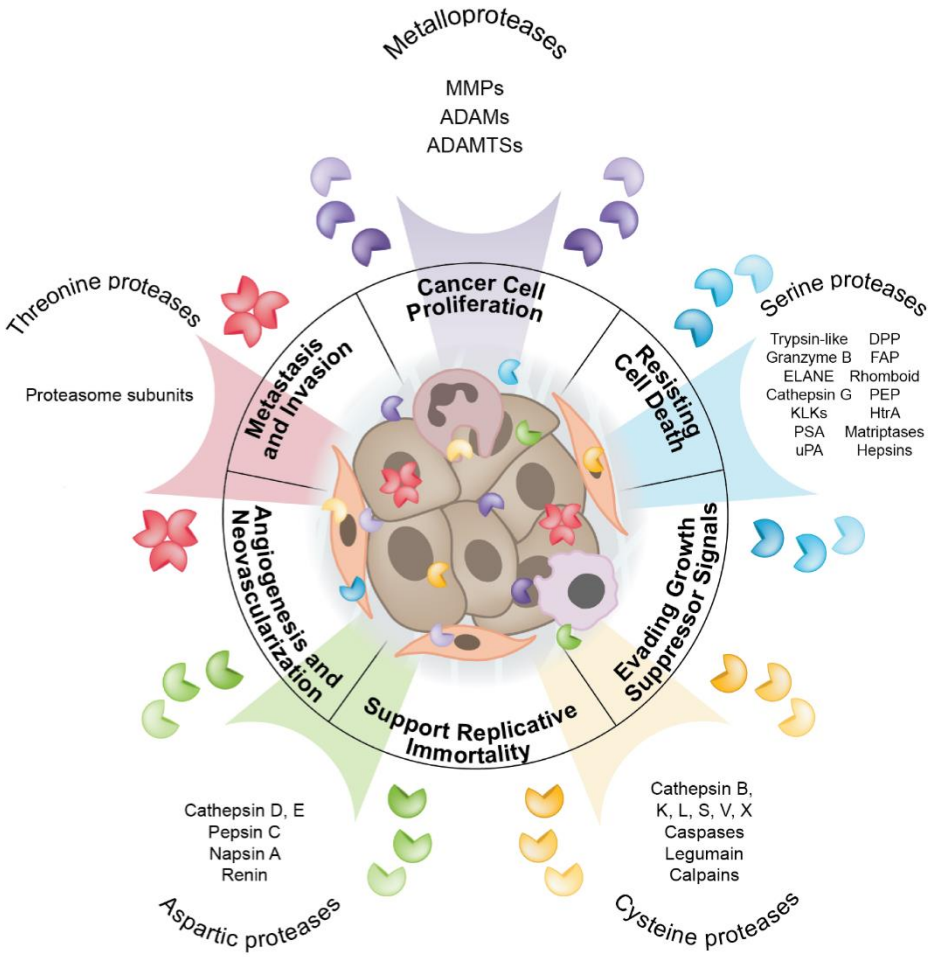

Figure 1.1: Relationship between different protease classes and selected hallmarks of cancer proposed by Hanahan and Weinberg (Hanahan and Weinberg, 2000; Hanahan and Weinberg, 2011) (adapted after (Vizovisek *et al.*, 2021)).

In addition, it must be considered that cells are able to adapt to new situations, so that the function of an inhibited protease can be taken over by other proteases. Therefore, an extensive knowledge of all cancer relevant proteases is required for the development of improved anti-cancer therapies. One prominent example of a so far poorly understood protease is Threonine aspartase 1, which is responsible for the

cleavage of the MLL (Mixed lineage leukemia) protein (Hsieh *et al.*, 2003a). For a better understanding of (patho)biological processes, involvement in diseases but also for the development of target related therapeutics against the respective disease, it is necessary to identify and characterize the responsible protease and get a better insight in its interactome and degradome.

1.2 TASPASE1

1.2.1 PHYSIOLOGICAL ROLE

Taspase1 (Threonine aspartase 1) is an endopeptidase and its corresponding gene, located on chromosome 20p12.1, encodes a protein of 420 amino acids (aa) and a molecular weight of approximately 45 kDa (Hsieh *et al.*, 2003a; Khan *et al.*, 2005). Sequence analysis revealed an asparaginase-2 homology domain within Taspase1. This protease was therefore classified as a member of type II asparaginases, a subfamily of Ntn (N-terminal nucleophile) hydrolases (Hsieh *et al.*, 2003a; Khan *et al.*, 2005). Taspase1 and the other family members share a similar structure: they consists of a central β-sheet sandwich, which is surrounded on both faces with α-helices (Khan *et al.*, 2005). Moreover, Taspase1´s active site contains the catalytically relevant threonine which enables *cis*-proteolytic activity (Hsieh *et al.*, 2003a). But in contrast to all other asparaginases, which hydrolyze the free amino acid asparagine to aspartate, Taspase1 has a unique feature within the family: it is able to act as a protease (Hsieh *et al.*, 2003a). Thus, Taspase1 constitutes a unique class of endopeptidases (Hsieh *et al.*, 2003a; Khan *et al.*, 2005).

Like other proteases, Taspase1 is expressed as a proenzyme and gains its proteolytic activity by autocatalytic *cis*-cleavage between Asp233 and Thr234, thereby generating two subunits, namely the α-subunit (aa 1-233) and the β-subunit (aa 234-420) (Hsieh *et al.*, 2003a). The subunits reassemble into an αββα heterodimer representing Taspase1´s active form (Bier *et al.*, 2012b). The N-terminal Threonine of the mature β-subunit acts as a nucleophile for Taspase1 *trans*-activity (Hsieh *et al.*, 2003a; Bier *et al.*, 2011b; Wünsch *et al.*, 2015). A mutated Taspase1 variant with a replacement of Thr234 by Val (Taspase1^{T234V}) revealed the importance of the Thr234 for Taspase1 *trans*-cleavage activity since the TV mutant showed no *cis*-activity as it was unable to cleave its substrates (Khan *et al.*, 2005; Bier *et al.*, 2012b; Bier *et al.*, 2012a). Taspase1 cleaves specific substrate proteins by hydrolyzing the peptide bond after an aspartate

residue within the conserved peptide motif $Q^3X^2D^1/G^{1´}$ (Hsieh *et al.*, 2003a), which was later refined to $Q^3(F/I/L/V)^2D^1/G^{1'}X^{2'}D^{3'}D^{4'}$ (Hsieh *et al.*, 2003a; Bier *et al.*, 2011b; Wünsch *et al.*, 2015).

With this improved Taspase1 cleavage consensus sequence, a genome-wide bioinformatic screen was performed allowing the prediction of potentially novel Taspase1 targets (Bier *et al.*, 2011b). It revealed 27 putative targets, which confirmed known Taspase1 substrates such as the MLL proteins but also disclosed many new candidates, which are participating in a broad range of biologicals functions including cell cycle and transcriptional regulation, differentiation and apoptosis as well as DNA replication and nuclear transport, and are known to play critical roles in cancer (Bier *et al.*, 2011b). Interestingly, the putative Taspase1 targets are located in the nucleus, in the cytoplasm and in the cell membrane (Bier *et al.*, 2011b).

In fact, Taspase1 is mainly localized inside the nucleus and showed a significant accumulation within the nucleoli (Bier *et al.*, 2011a). *In silico* analysis predicted two basic amino acid clusters within Tapase1's highly conserved C-terminal α-subunit as a potential nuclear localization signal (NLS). Fluorescence microscopy and microinjection of different Tapase1 constructs confirmed the activity of Taspase1´s bipartite NLS (aa ^{197}**KR**N**KRK**LELAERVDTDFMQL**KKRR**^{220}) and demonstrated that for efficient nuclear import both basic clusters are essential (Bier *et al.*, 2011a). An import-deficient Taspase1 variant ($Taspase1_{NLSmut}$) lacks catalytic activity in *cis* and *trans*, while $Taspase1^{T234V}$ localizes to the nucleus but showed no nucleolar accumulation indicating that nuclear import is essential for Taspase1´s activity and that the NLS is required for nuclear and nucleolar localization (Bier *et al.*, 2011a). Considering that Taspase1 cleaves cytosolic substrates, Taspase1 needs transient access to the cytoplasm. However, no nuclear export signal (NES) could be identified within the Tapase1 sequence, but cell fraction analysis disclosed low Tapase1 amounts in the cytoplasm (Bier *et al.*, 2011a). As a nucleolar shuttle protein containing a NES (Wang *et al.*, 2005; Yu *et al.*, 2006) and a nucleolar localization signal (NoLS) (Box *et al.*, 2016) NPM1 (nucleophosmin 1) is able to shuttle between cytoplasm, nucleus and nucleoli (Box *et al.*, 2016). NPM1 is known to be involved in the localization and function of several proteins (Oughtred *et al.*, 2021) such as Nucleolin (Li *et al.*, 1996) and the tumor suppressor ARF (Korgaonkar *et al.*, 2005; Kuo *et al.*, 2008). Co-immunoprecipation experiments verified an interaction between NPM1 and

Taspase1 (Bier *et al.*, 2011a). Furthermore, it was shown that both, Taspase1$_{NLSmut}$ and Taspase1 coupled with a strong NES resulting in a cytoplasmic localized Taspase1 (Taspase1$_{cyt}$), are translocated into the nucleoli upon co-expression of NPM1 (Bier *et al.*, 2011a). Neither Taspase1 subunits alone nor the catalytic inactive Taspase1^{T234V} were able to bind to NPM1 (Bier *et al.*, 2011a). Additionally, co-expression of Taspase1 with a mutated NPM1 (NPM1$_{mut}$), which predominantly localizes to the cytoplasm, results in cytoplasmic localization of Taspase1, while additional treatment with the export inhibitor Leptomycin B prevented this localization shift to the cytosol (Bier *et al.*, 2011a). These data suggest that Taspase1 is actively translocated to the nucleus via the classical Importin-α import pathway and upon activation, the active Taspase1 takes advantage of NPM1 shuttle to gain access to the nucleoli and transiently to the cytoplasm before it is reimported (Bier *et al.*, 2011a). The dynamic Importin-α/NPM1 switch (Figure 1.2) enables Taspase1 to access the cytoplasm in order to cleave its cytoplasmic substrates, despite the lack of a NES (Bier *et al.*, 2011a).

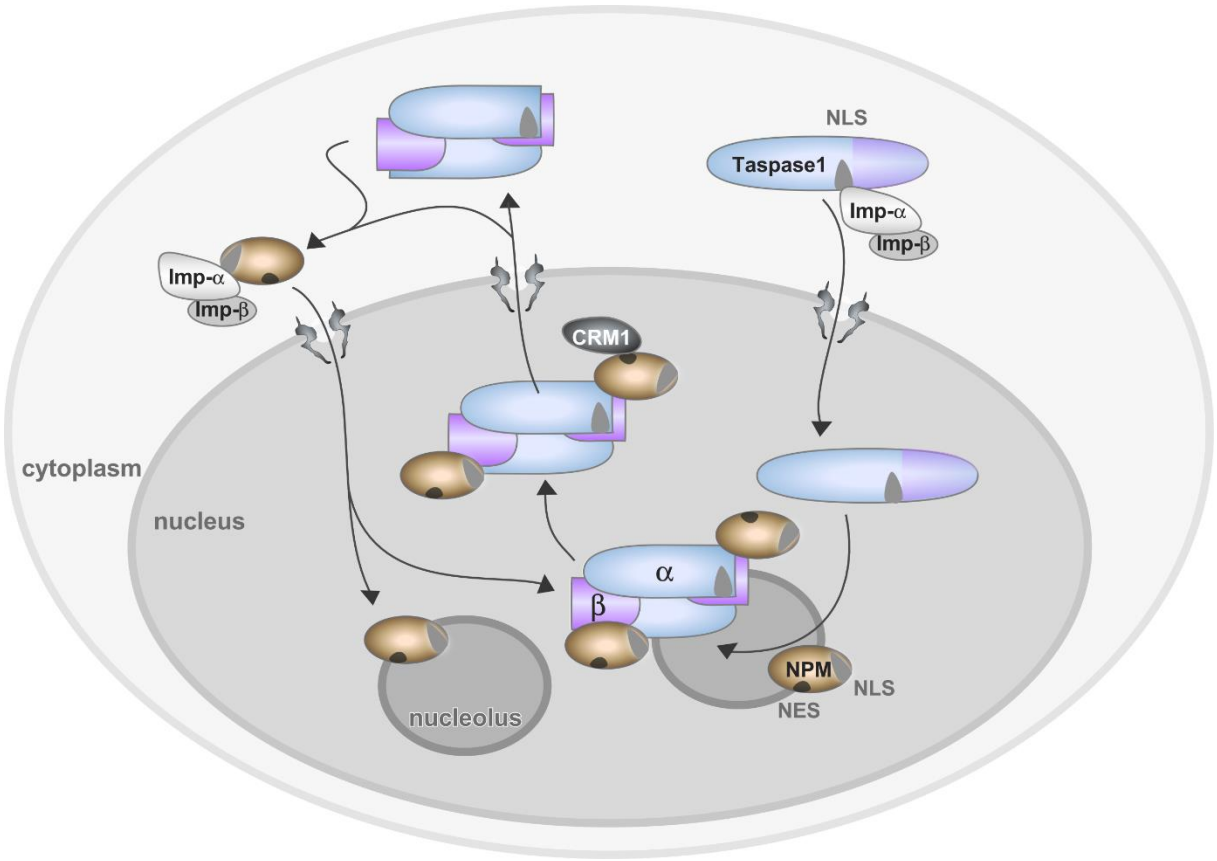

Figure 1.2: The Importin-α/NPM1 switch regulates Taspase1 localization.

Taspase1´s bipartite nuclear localization signal (NLS) is recognized by Importin-α (Imp-α), that mediates the translocation of Taspase1 into the nucleus. After intramolecular autoproteolysis, the active Taspase1

αββα-heterodimer is able to interact with nucleophosmin 1 (NPM1) thereby gaining access to nucleoli and cytoplasm via NPM1´s nucleolar localization signal (NoLS) and its nuclear export signal (NES). The Importin-α/NPM1 switch allows Taspase1 access to its substrates within the different compartments (Bier *et al.*, 2011a).

Even though Taspase1 was discovered about almost 20 years ago, so far little is known about Taspase1´s dagradome, its functional protein interaction network and finally its primary physiological relevance. The previous knowledge is primarily based on the known substrates and the interaction partners identified so far. For a better understanding of Taspase1's activity network and its superior biological function, it is important to identify further substrates and interaction partners to examine Taspase1's sphere of action within this context.

1.2.2 TARGETS AND INTERACTION PARTNERS

1.2.2.1 MLL

In 2003, Taspase1 was first identified and described as the protease that proteolytically processes and activates the MLL protein (Hsieh *et al.*, 2003a) thereby controlling expression of HOX genes and cell cycle regulators (Hsieh *et al.*, 2003b; Hsieh *et al.*, 2003a; Takeda *et al.*, 2006). Taspase1-mediated cleavage of the approximately 500 kDa MLL protein generates a N-terminal 320 kDa fragment and a C-terminal 180 kDa fragment (Hsieh *et al.*, 2003b; Hsieh *et al.*, 2003a). Taspase1 recognizes two highly conserved cleavage sites (CSs) in MLL, namely CS1 (aa ^{2664}QVD/GADD^{2670}) and CS2 (aa ^{2716}QLD/GVDD^{2722}) (Hsieh *et al.*, 2003b), which reflect Taspase1 consensus sequence QXD/GXDD (Bier *et al.*, 2011b). Taspase1 is able to recognize and proteolytically process both CSs but shows a preference for CS2 (Hsieh *et al.*, 2003a). After MLL processing, the generated MLL cleavage fragments dimerize and form a stable complex through the interaction of the FY-rich N- and C-terminal domains as well as the SET (Su(var)3–9, Enhancer of zeste and trithorax) domain (Yokoyama *et al.*, 2002; Hsieh *et al.*, 2003b; Liu *et al.*, 2009), which also ensures the correct nuclear localization (Nakamura *et al.*, 2002; Yokoyama *et al.*, 2002; Hsieh *et al.*, 2003b).

The mature MLL dimer represents the scaffold for the formation of a multi-protein complex as the different conserved domains within MLL facilitate the binding to various proteins and cellular structures such as DNA. The N-terminal located AT-hook motifs

enable the direct binding of AT-rich DNA, such as promotor regions (Zeleznik-Le *et al.*, 1994). But MLL can also bind indirectly to DNA via DNA binding proteins like the tumorsuppressor protein Menin (Hughes *et al.*, 2004; Yokoyama *et al.*, 2004; Krivtsov and Armstrong, 2007). To silence transcription, MLL recruits transcriptional repressors (Xia *et al.*, 2003) and histone deacetylases (Nakamura *et al.*, 2002) via its DNA methyltransferase homology region. For transcriptional activation, MLL contains a transactivation domain that interacts with histone acetyltransferases (Ernst *et al.*, 2001; Dou *et al.*, 2005) and a SET domain which harbours the histone methyltransferase (HMT) activity methylating histone H3 at lysine 4 (H3K4) (Milne *et al.*, 2002; Nakamura *et al.*, 2002). PHD fingers, Cys4-His-Cys3 zinc-finger-like motifs (Fair *et al.*, 2001) allow the interaction with chromatin remodeling factors (Rozenblatt-Rosen *et al.*, 1998) and cell cycle regulators like E2F (Yokoyama *et al.*, 2004; Takeda *et al.*, 2006).

Via the described binding domains at least the core components Ash2, Wdr5, Rbbp5, HCF1 and Dpy30 (Nakamura *et al.*, 2002; Hsieh *et al.*, 2003b) associate with MLL. In addition to these common subunits the protein complex has been shown to interact with further facultative components, such as chromatin-remodeling factors (e.g. histone acetyltransferase, MOF), mRNA-processing factors, the tumor suppressor Menin and also with nuclear hormone receptors (Hess, 2004; Dou *et al.*, 2006; Dreijerink *et al.*, 2006). This multi-protein complex regulates transcription by modification and remodeling of chromatin to create specific epigenetic patterns and to allow access to DNA that leads to the expression or repression of the respective gene (Figure 1.3).

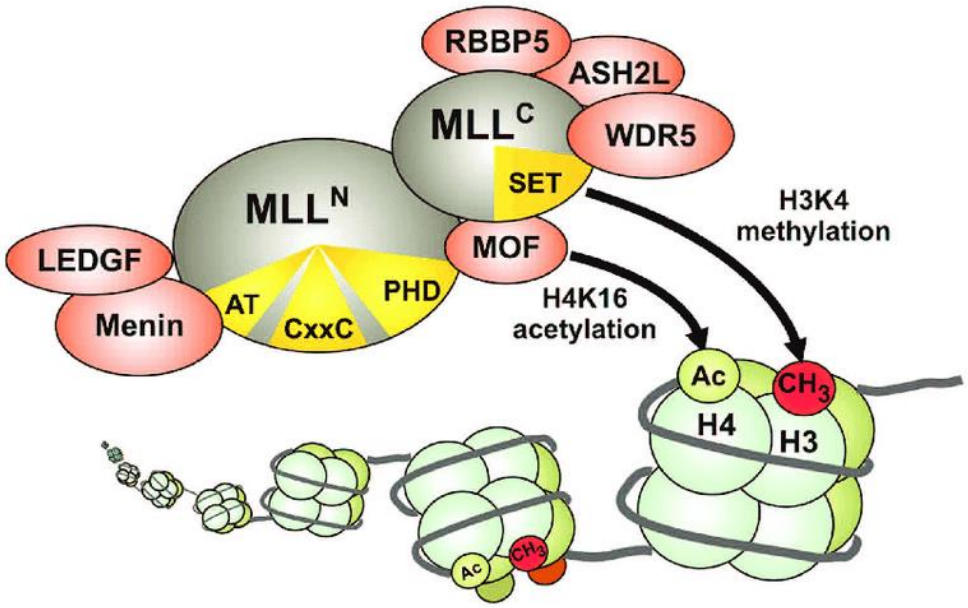

Figure 1.3: Composition and function of MLL multi-protein complex.

After Taspase1-mediated proteolytic processing of MLL, the N-terminal (MLL^N) and C-terminal (MLL^C) fragments of MLL dimerize and form a stable complex. The mature MLL dimer provides the scaffold for the formation of a multi-protein complex. MLL´s different conserved domains (indicated in yellow) facilitate the binding to various proteins. The resulting MLL multi-protein complex ensures transcriptional regulation by modification and remodeling of chromatin. Specific epigenetic patterns regulate access to chromatin leading to maintained expression or repression of the respective genes (Slany, 2009).

Despite MLL´s general role in transcriptional regulation, MLL proteins were identified to coordinate hormone dependent gene regulation, especially the estrogen-driven gene expression (Dreijerink *et al.*, 2006; Ansari *et al.*, 2009; Ansari *et al.*, 2011). Sequence analysis revealed that several MLL proteins contain at least one LXXLL nuclear receptor interaction domain (Ansari *et al.*, 2009). Proteins harboring this motif are known to facilitate the interaction with nuclear receptors (NRs) (Heery *et al.*, 1997), like estrogen receptors (ERs), and play important roles in gene activation after the respective hormone stimulus (Mangelsdorf *et al.*, 1995; Nilsson *et al.*, 2001). Additionally, Menin, which is part of the MLL multi-protein complex (Hughes *et al.*, 2004; Yokoyama *et al.*, 2004), was identified to mediate the recruitment of nuclear receptors to target genes. This fact classifies Menin as a co-activator of ERα mediated gene transcription (Dreijerink *et al.*, 2006). The Menin-MLL complexes are known to target several HOX genes and genes for cyclin-dependent kinase inhibitors (CDKIs) (Hughes *et al.*, 2004; Yokoyama *et al.*, 2004; Milne *et al.*, 2005b).

HOX genes are key regulators in the control of embryonic development (Morgan, 1997; Taylor, 2000). The importance of a proper HOX gene regulation by MLL was demonstrated with MLL knockout mice. During embryonic development, a homozygous MLL knockout ($MLL^{-/-}$) caused death of mouse embryos within day 10.5, reflecting an initially activated HOX gene expression that could not be sustained, presumably because of an insufficient epigenetic gene activation (Yu *et al.*, 1995). Additionally, $MLL^{-/-}$ embryos exhibited deficient hematopoietic stem cell (HSC) activity (Yagi *et al.*, 1998; Ernst *et al.*, 2004). Heterozygous mice ($MLL^{+/-}$) were born anaemic, in smaller size and displayed segment abnormalities and defective hematopoietic precursors (Yu *et al.*, 1995; Yagi *et al.*, 1998).

Taspase1-mediated cleavage of MLL is necessary for MLL HMT activity as demonstrated by $Taspase1^{-/-}$ cells displaying reduced levels of H3K4 methylation and additionally exhibiting only full length MLL, which indicates that Taspase1 is the only protease capable of MLL processing (Takeda *et al.*, 2006). Moreover, $Taspase1^{-/-}$ mice showed classic homeotic transformations and died shortly after birth due to feeding defects, confirming Taspase1´s function in correct body segmentation (Takeda *et al.*, 2006). Interestingly, Taspase1-deficient cells revealed an overexpression of p16Ink4a, but only low amounts of cyclins A, B and E, which is consistent with the fact that $Taspase1^{-/-}$ mice are smaller in size due to poor proliferation (Takeda *et al.*, 2006). It was further demonstrated that MLL interacts with E2F (Yokoyama *et al.*, 2004; Takeda *et al.*, 2006), a cell cycle regulator which leads to the expression of cyclins (Blais and Dynlacht, 2004; Bracken *et al.*, 2004) and HOX genes (Storre *et al.*, 2002). Further studies also revealed a direct activation of cyclins and CDKIs by MLL (Dou *et al.*, 2005; Milne *et al.*, 2005b; Xia *et al.*, 2005; Tyagi *et al.*, 2007). Thus, Taspase1-mediated MLL cleavage seems to play an important role in cell cycle regulation (Milne *et al.*, 2005b; Xia *et al.*, 2005; Takeda *et al.*, 2006; Kotake *et al.*, 2009) and embryonic development (Yu *et al.*, 1998; Ringrose and Paro, 2004; Schuettengruber *et al.*, 2007).

Abnormal regulation of HOX gene expression is sometimes associated with MLL chromosomal translocations in AML (acute myeloid leukemia) (Drabkin *et al.*, 2002; Debernardi *et al.*, 2003). In general, a wide range of MLL chromosomal translocations are associated with acute leukemias (Look, 1997; Daser and Rabbitts, 2004; Meyer *et al.*, 2009; Meyer *et al.*, 2018) as well as therapy-related secondary leukemia resulting from the treatment with DNA Topoisomerase II inhibitors (for further information see

section 1.3) (Pedersen-Bjergaard *et al.*, 1998; Rowley and Olney, 2002; Azarova *et al.*, 2007; Bandele and Osheroff, 2009; Ezoe, 2012). The most MLL chromosomal rearrangements occur within the breakpoint cluster region between exon 8 and 13 (Ayton and Cleary, 2001) on chromosome band 11q23 (Ziemin-van der Poel *et al.*, 1991; Nilson *et al.*, 1996; Rasio *et al.*, 1996; Bailly, 2012) leading to MLL fusion proteins containing the first 8 – 13 exons of MLL and a variable number of exons from the fusion gene partner. The most frequent MLL fusion partner genes are AF4, AF9, AF10, ELL and ENL (Meyer *et al.*, 2006; Liu *et al.*, 2009; Meyer *et al.*, 2018).

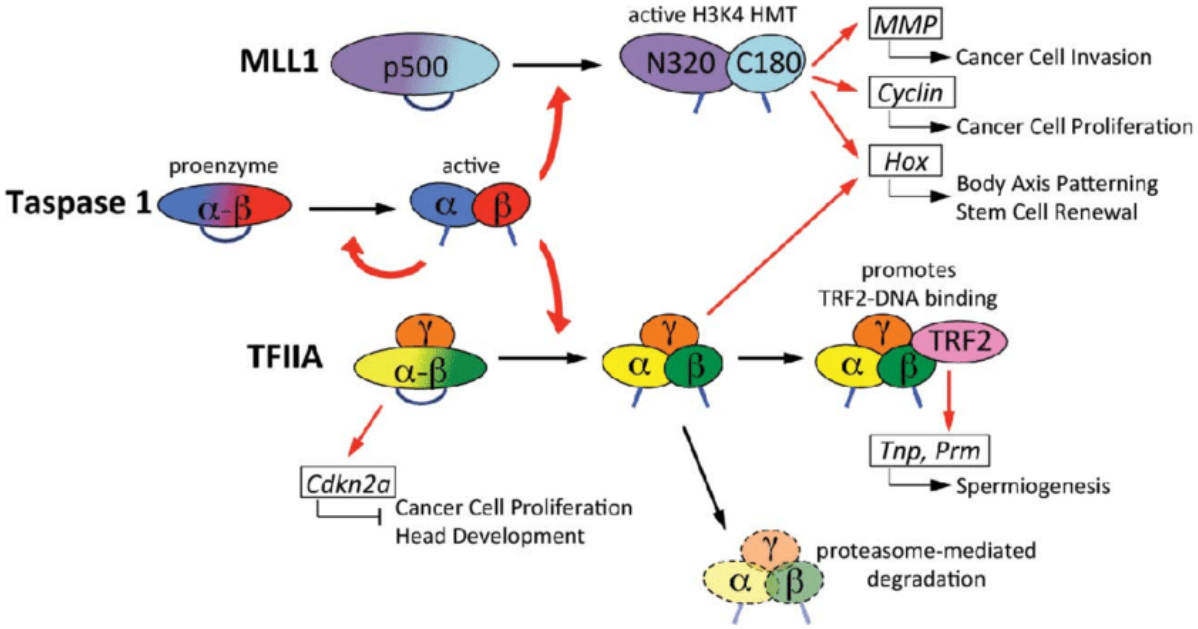

Figure 1.4: Taspase1-mediated cleavage of MLL and TFIIA and its involvement in carcinogenesis.

After intramolecular autoproteolysis of the Taspase1 proenzyme, the active protease is able to cleave its substrates MLL1 and TFIIA. Taspase1-mediated processing of MLL1 generates two subunits, N320 and C180. The reassembled mature MLL1 heterodimer possesses full histone methyltransferase (HMT) activity that creates epigenetic marks at histone H3 lysine 4 (H3K4) and leads to transcriptional activation of various genes including matrix metalloproteases (MMPs), cyclins and HOX genes. The unprocessed transcription factor TFIIA αβ/γ ensures transcriptional activation of the Cdkn2a gene. The cleavage of TFIIA αβ by Taspase1 leads to proteasomal degradation of the resembled TFIIA α/β/γ complex (Niizuma *et al.*, 2015).

1.2.2.2 TFIIA

In 2006, transcription factor IIA (TFIIA) was identified as the second Tapase1 substrate (Zhou *et al.*, 2006). TFIIA belongs to the general transcription factors (GTF), which maintain basal expression of RNA polymerase II (RNA pol II)-dependent genes

(Reese, 2003). The GTFs (TFIIA, B, D, E, F and H) together with RNA pol II and a huge amount of different proteins (like chromatin modifiers and remodelers, co-activators and co-repressors) are part of the preinitiation complex (PIC), which is formed at promotor regions of RNA pol II-dependent genes to initiate transcription (Orphanides *et al.*, 1996; Thomas and Chiang, 2006; Gupta *et al.*, 2016). The formation of the PIC is a defined and highly organized process (Thomas and Chiang, 2006). TFIIA functions as an anti-repressor within the PIC (Imbalzano *et al.*, 1994; Thomas and Chiang, 2006) by interacting with TATA-box binding protein (TBP) and at the same time stabilizing the promotor binding of the whole TFIID complex (Lagrange *et al.*, 1996; Oelgeschläger *et al.*, 1996). But this transcription factor is also able to operate as a transcriptional co-activator by directly associating with other activators, transcriptional co-factors, GTFs and also with their subunits (Thomas and Chiang, 2006).

TFIIA is encoded by two separate genes, *GTF2A1* and *GTF2A2* leading to the transcription of the 55 kDa TFIIA αβ and the 12 kDa TFIIA γ, respectively (DeJong and Roeder, 1993; Ozer *et al.*, 1994; Thomas and Chiang, 2006; Høiby *et al.*, 2007). TFIIA αβ harbors a Taspase1 cleavage site and its proteolysis generates the 35 kDa α-subunit as well as the19 kDa β-subunit, which reassemble to TFIIA α/β (DeJong and Roeder, 1993; Høiby *et al.*, 2007). The γ-subunit is associated with both cleaved TFIIA α/β and uncleaved TFIIA αβ (Høiby *et al.*, 2007). Taspase1 cleavage of TFIIA at aa ^{272}QVD/G^{275} (Zhou *et al.*, 2006) was confirmed by a mutated version of TFIIA with single mutations in the cleavage site (TFIIA^{D274A} and TFIIA^{G275A}), rendering it uncleavable (Zhou *et al.*, 2006). Interestingly, uncleaved TFIIA was less degraded by the ubiquitin-proteasome pathway than the TFIIA α and TFIIA β subunits originating from Taspase1 processing (Høiby *et al.*, 2004). Moreover, mouse embryonic fibroblasts (MEFs) lacking Tapase1 exhibited unprocessed TFIIA αβ/γ, which was transcriptionally active (Zhou *et al.*, 2006). In addition, the investigation of non-cleavable TFIIA αβ revealed a more stabilized complex, which accumulates at the *Cdkn2a* locus (Takeda *et al.*, 2015). This locus encodes for two negative cell cycle regulators p16Ink4a (CDKI) and p19Arf that promotes apoptosis and cell cycle arrest (Sherr, 2001). The mRNA levels of both were increased in embryonic heads of Taspase1$^{-/-}$ mice (Takeda *et al.*, 2015). An additional knockout of p16Ink4a and p19Arf in Taspase1$^{-/-}$ significantly rescued the craniofacial malformations resulting from the

loss of *TASP1* suggesting that their transcription is actively repressed by Taspase1-mediated processing of TFIIA (Takeda *et al.*, 2015).

Taken together, these data lead to the conclusion, that TFIIA function within the cell is controlled by Taspase1 processing to ensure rapid transcriptional adjustment (Høiby *et al.*, 2004; Zhou *et al.*, 2006) especially of cell cycle regulators in proliferative processes, for example in head morphogenesis (Takeda *et al.*, 2015).

1.2.2.3 USF2

The upstream stimulatory factors (USFs) are a family of transcription factors and USF possesses two isoforms, USF1 (43 kDa) and USF2 (44 kDa) (Sawadogo *et al.*, 1988), encoded by two different genes (Gregor *et al.*, 1990; Sirito *et al.*, 1992; Sirito *et al.*, 1994). Whereas USF1 plays a role in immune response and metabolism, USF2 is involved in brain function, embryonic development, fertility, growth and metabolism (Sirito *et al.*, 1998; Corre and Galibert, 2005). The C-terminal domain is highly conserved and comprises two domains: a basic helix-loop-helix (b-HLH) domain and a leucine zipper (LZ), which enables binding of promotors containing E-boxes (5´-CACGTG-3´) and dimerization (Sawadogo and Roeder, 1985; Gregor *et al.*, 1990; Roy *et al.*, 1991). In Addition, USFs have shown to bind pyrimidine-rich initiatior elements within promotors (Roy *et al.*, 1991; Du *et al.*, 1993). A truncated USF, containing the b-HLH domain but no LZ, is able to bind DNA to a lesser extent than full-length USF, but is unable to dimerize with other USFs, indicating that the LZ is necessary for dimerization and effective DNA binding (Gregor *et al.*, 1990). USF1 and USF2 are known to form homo- or heterodimers (Sirito *et al.*, 1992), but occur primarily as USF1/USF2 heterodimers *in vivo* (Viollet *et al.*, 1996). A highly conserved USF-specific region (USR) is located N-terminal to the b-HLH domain and is presumed to play a significant role in transcriptional activation (Groenen *et al.*, 1996; Luo and Sawadogo, 1996; Qyang *et al.*, 1999). The USR together with a part of the basic region are responsible for USF2´s nuclear localization (Luo and Sawadogo, 1996). With a sequence identity of approx. 70 % within the b-HLH-LZ domain (Sirito *et al.*, 1994), USF1 and USF2 exhibit similar properties in DNA binding and transcriptional activity (Sawadogo, 1988; Sirito *et al.*, 1992; Sirito *et al.*, 1994). Furthermore, it was shown that USF is involved in transcription of RNA pol II-dependent genes, by the finding that USF interacts directly with TFIID thereby stabilizing the PIC and leading to a stimulated

transcription (Sawadogo and Roeder, 1985; Carcamo *et al.*, 1989). Interestingly, the N-terminal domain of the isoforms is presumed to be responsible for transcriptional activation and shows the biggest differences in sequence identity (Sirito *et al.*, 1992; Sirito *et al.*, 1994), which emphasizes that the isoforms regulate different genes and suggests also that they are regulated in different ways (Luo and Sawadogo, 1996). This was illustrated by the finding of an increased level of USF2 in USF1$^{-/-}$ knockout mice, whereas USF2$^{-/-}$ mice exhibited a reduced expression of USF1 (Sirito *et al.*, 1998). Further studies with knockout mice revealed the importance of USFs in embryonic development. Newborn mice lacking USF2 were remarkably smaller and displayed a decreased fertility (Vallet *et al.*, 1997; Sirito *et al.*, 1998; Hadsell *et al.*, 2003). The life span of male USF2$^{-/-}$ mice was seriously shortened and more than 50 % of newborn mice die within 48 h after birth, while USF1$^{-/-}$ mice did not show such restrictions (Vallet *et al.*, 1997; Sirito *et al.*, 1998; Hadsell *et al.*, 2003). Moreover, mice with a combined knockout of USF1$^{-/-}$ and USF2$^{-/-}$ were not viable and died during embryogenesis ((Vallet *et al.*, 1997; Sirito *et al.*, 1998; Hadsell *et al.*, 2003). In addition, male USF2$^{-/-}$ mice showed manifested prostate hyperplasia and dysregulated prostate growth (Chen *et al.*, 2006), which is in accordance with the shortened life time of male USF2$^{-/-}$ mice. A tumor suppressor function was ascribed to USF2 in prostate carcinogenesis, since investigations of prostate cancer cell lines showed significantly reduced USF2 protein levels and after USF2 expression tumorigenicity was decreased (Chen *et al.*, 2006). The assumption that USF2 functions as a tumor-suppressor was further supported by the finding that MEFs lacking USF2 showed an increased cell proliferation and this loss-of-function phenotype could be antagonized in a 'rescue experiment' by re-expression of USF2 (Chi *et al.*, 2020). Furthermore, not only a cell proliferation-promoting effect was observed in the absence of USF2, but also an increased invasion and migration potential of the cells (Chi *et al.*, 2020).

In 2011, USF2 was identified and confirmed as a novel Taspase1 substrate (Bier *et al.*, 2011b), but the functional relevance of USF2 cleavage remained unclear. A potential Taspase1-mediated cleavage of USF2 was analyzed by introducing mutations within the putative cleavage sequence of USF2 at aa ^{88}QLD/GQGD^{94} (Bier *et al.*, 2011b). The generated USF2 mutant (USF2^{mut}) was indeed uncleavable suggesting that USF2 cleavage is specifically mediated by Taspase1 (Heiselmayer, 2018). Co-immunoprecipitation (IP) experiments demonstrated a reduced interaction between USF2 and USF1 upon Taspase1-mediated USF2 cleavage (Heiselmayer,

2018). Moreover, reduced levels of cyclin-dependent kinase (CDK) 4 in USF2^{mut} overexpressing cells were observed (Heiselmayer, 2018). The investigation of expression profiles from cells expressing USF1/USF2^{mut} compared with USF1/USF2^{C} demonstrated a reduced expression of proliferating genes and increased levels of pro-apoptotic gene products (Heiselmayer, 2018). In addition, cell viability assays showed that various cancer cell lines overexpressing USF2^{mut} had a decreased cell viability compared to cells expressing a truncated USF2 that resembles the C-terminal part of cleaved USF2 (USF2^{C}), which leads to the conclusion that USF2 is involved in tumor suppression (Heiselmayer, 2018).

Taken together, USF2 cleavage mediated by Taspase1 could also specifically regulate gene transcription during embryonic development similar to the changed TFIIA transcriptional regulation mode after Taspase1 cleavage (Høiby *et al.*, 2004; Zhou *et al.*, 2006).

1.2.2.4 NPM1

In 2011, Bier et al revealed the NPM/Importin α switch (for further information see section 1.2.1 and Figure 1.2), a specific interaction of Taspase1 with nucleophosmin1 and importin α, which enables Taspase1´s nuclear, nucleolar and cytoplasmic translocation (Bier *et al.*, 2011a).

As mentioned before, NPM1 shuttles between cytoplasm, nucleus and nucleoli (Box *et al.*, 2016) and is thereby involved in the localization and function of several proteins (Oughtred *et al.*, 2021). Thus, NPM1 is a multifunctional protein and participates in a broad range of important biological processes like chromatin remodeling (Okuwaki *et al.*, 2001), embryogenesis (Grisendi *et al.*, 2006), maintenance of genome stability (Wang *et al.*, 2005), mRNA processing (Murano *et al.*, 2008), regulation of apoptosis (Ahn *et al.*, 2005), and ribosome biogenesis (Savkur and Olson, 1998). NPM1 mutation or gene disruption by translocation are known to be associated with hematological malignancies (Grisendi *et al.*, 2006; Falini *et al.*, 2007) and particularly 35 % of adult AML patients displayed cytoplasmic localized NPM1 due to a mutation of the NPM1 gene (Falini *et al.*, 2005; Falini *et al.*, 2006). In addition, a high expression of NPM1 is found in proliferating cells (Lin *et al.*, 2006) and an overexpression of NPM1 is frequently associated with various solid tumor types (Grisendi *et al.*, 2006). Especially in human breast cancer and endometrial cancer it was shown that NPM1 level is

increased after E2 induction through the ERα pathway (Skaar *et al.*, 1998; Zhu *et al.*, 2006; Chao *et al.*, 2013; Zhou *et al.*, 2014). To summarize, NPM1 has a dual role as an oncogene as well as a tumor suppressor (Grisendi *et al.*, 2006).

1.2.2.5 FURTHER TARGETS/INTERACTION PARTNERS

A bioinformatic screen with the improved Taspase1 cleavage consensus sequence revealed 27 putative Taspase1 targets (Bier *et al.*, 2011b) of which only MLL (Hsieh *et al.*, 2003b; Hsieh *et al.*, 2003a; Takeda *et al.*, 2006), TFIIA (Zhou *et al.*, 2006), USF2 (Bier *et al.*, 2011b; Heiselmayer, 2018), Myosin1f (Hensel *et al.*, 2022), ALF (Høiby *et al.*, 2004) and REV3L (Wang *et al.*, 2020) have been confirmed so far within a cellular context. It is important to analyze the other putative Taspase1 targets regarding their modulated behavior upon site-specific proteolysis by Taspase1 to get a better understanding of Taspase1´s function.

In 2019, only two protein-protein interactions were annotated for Taspase1 in the BioGRID protein databases, namely MLL (Hsieh *et al.*, 2003a) and the amyloid precursor protein APP (Oláh *et al.*, 2011). As these hits were based on high-throughput methods it is probable that further Taspase1-interacting proteins have been overlooked, because with this kind of approaches it might be difficult to identify interactions that rely on context-dependent or conditional interactions or even on post-translational modifications. Since Taspase1 with its multiple targets and its involvement in cell cycle progression is likely to form transient interactions with diverse binding partners, it is worthwhile focusing on Taspase1’s interaction network, which would help to decipher its complete functionality.

1.2.3 ROLE IN CANCER

The role of Taspase1 in the development of cancer has become obvious because of Taspase1’s upregulated expression in leukemia (for further information see section 1.2.2.1) and in various solid tumor types such as cancer in breast, colon, head and neck cancer or glioblastoma (Takeda *et al.*, 2006; Chen *et al.*, 2010; Bier *et al.*, 2011a; Bier *et al.*, 2012a).

One explanation for Taspase1’s association with cancer is the finding, that this protease is directly involved in cell cycle regulation, as mentioned before. On whole organism level it was observed that Taspase1-deficient mice are clearly smaller than

their wild-type littermates (Takeda *et al.*, 2006; Chen *et al.*, 2010). At cell level it was demonstrated that MEFs deficient for Taspase1 proliferate poorly and exhibit decreased cyclin levels, like cyclin A, B and E, as well as an increased expression of CDKIs and in accordance with this a disrupted cell cycle (Takeda *et al.*, 2006; Chen *et al.*, 2010; Dong *et al.*, 2014; Takeda *et al.*, 2015). The expression of both, cyclins and CDKIs, is regulated by MLL, which is processed only by Taspase1 (Takeda *et al.*, 2006; Tyagi *et al.*, 2007), so this could be a possible explanation for Taspase1's contribution to cell cycle progression. But, the pivotal relevance of Taspase1 for cell cycle progression can by far not fully be explained with the processing of its first discovered and thus far most prominent substrate MLL, which is involved in the expression of cyclins and CDKIs (Milne *et al.*, 2005b; Xia *et al.*, 2005; Tyagi *et al.*, 2007). The observed proliferation defect in Taspase1 knockout mice was significantly more pronounced than in mice, which carry noncleavable MLL alleles, indicating that further functions of Taspase1 may contribute to cell cycle progression (Takeda *et al.*, 2006; Chen *et al.*, 2010).

Furthermore, Taspase1 deficiency also causes a disruption of proliferation in human cancer cell lines and promotes apoptosis due to the increase of several CDKIs and a decrease of anti-apoptotic MCL-1 (Chen *et al.*, 2010; Takeda *et al.*, 2015). This diminished level of MCL-1 was caused by a reduced protein stability due to a decreased expression of the deubiquitinase USP9X (Chen *et al.*, 2010). This led to an increase of ubiquitinated MCL-1 and suggests that Taspase1 stabilizes MCL-1 at protein level (Chen *et al.*, 2010).

In addition to its role in tumor progression, the role of Taspase1 in cancer initiation was underlined by the finding that MEFs lacking Taspase1 (in contrast to normal MEFs) were resistant to oncogenic transformation induced by classic oncogenes like E1A, Myc, p53 and RAS (Takeda *et al.*, 2006). Furthermore, it was shown that transformed cells require Taspase1 to sustain cell proliferation suggesting an important role of Taspase1 in cancer maintenance (Chen *et al.*, 2010), thus justifying Taspase1´s classification as a non-oncogene addiction protease (Takeda *et al.*, 2006; Chen *et al.*, 2010). However, *in vitro* transformation assays revealed, that Taspase1 was not able to produce colonies on soft agar and is therefore not a classical oncogene (Chen *et al.*, 2010).

Interestingly, general protease inhibitors have been studied regarding their effect on Taspase1 activity, but none showed an effect on Taspase1 proteolytic activity (Lee *et al.*, 2009; Knauer *et al.*, 2011; Chen *et al.*, 2012). Even the well-known threonine protease inhibitor Bortezomib, which can inhibit the 26S proteasome (the only other threonine protease in mammals) (Adams and Kauffman, 2004; Chen *et al.*, 2011), has no effect on the proteolytic activity of Taspase1 (Chen *et al.*, 2012; Zheng *et al.*, 2015). Only a few specific Taspase1 inhibitors have been identified, but they are lacking general applicability (Lee *et al.*, 2009; Chen *et al.*, 2012; van den Boom *et al.*, 2014; van den Boom *et al.*, 2020).

Taken together, the above described findings allow the classification of Taspase1 as a non-oncogene addiction protease because it is not alone sufficient for tumor initiation but it is able to activate and maintain tumor properties (Chen *et al.*, 2010). Non-oncogene addiction proteins are promising targets for anti-cancer therapy, because they maintain the transformed phenotype in cancer cells, but are not essential for the survival of healthy cells (Luo *et al.*, 2009). Thus, Taspase1 serves as a highly attractive target for anti-cancer therapy.

So far, Taspase1 can neither be assigned to a specific protein interaction network nor to a specific signaling pathway. It is therefore necessary to investigate the interactome and degradome of Taspase1 in more detail in order to enable a more precise classification of Taspase1 function in the cellular context.

1.3 HUMAN DNA TOPOISOMERASES II ALPHA AND BETA

DNA Topoisomerases form a unique class of enzymes which catalyze supercoiling of DNA or its relaxation by breaking and rejoining of DNA strands. This function is necessary for transcription, DNA replication, chromosome condensation and segregation of daughter chromatids during anaphase (Wang, 1996; Nitiss, 1998; Pommier *et al.*, 2016). DNA Topoisomerases are subdivided in two categories: type I and type II. Whereas type I Topoisomerases achieve the topological changes by creating a single-strand break within the DNA, type II Topoisomerases generate a transient DNA double strand break (DSB) (Champoux, 2001; Wang, 2002; Pommier *et al.*, 2016). According to their structural and mechanistic similarity, the two types are further divided in four subfamilies called IA, IB, IIA and IIB (Wang, 1996; Nitiss, 1998; Champoux, 2001; Wang, 2002; Pommier *et al.*, 2016).

The subfamily IIA is functionally characterized by the capability for (de)catenation and (un)knotting double-stranded DNA as well as relaxation of negative and positive supercoils. This ATP-dependent reaction of type IIA DNA Topoisomerases allows the passage of one intact DNA double helix through another thereby removing knots and tangles (Osheroff *et al.*, 1991; Kellner *et al.*, 2000; McClendon and Osheroff, 2006). The human Topoisomerases consisting of two isoforms – Topoisomerase (short Topo) II α and II β – belong to the subfamily IIA (Tsai-Pflugfelder *et al.*, 1988; Chung *et al.*, 1989; Osheroff *et al.*, 1991; Kellner *et al.*, 2000; McClendon and Osheroff, 2006).

The primary structure of Topo II α and II β consists of three functional domains: an N-terminal ATPase domain, a central DNA binding/cleavage domain (core domain) and a C-terminal domain (CTD) (Jensen and Svejstrup, 1996; Sehested and Jensen, 1996; Mirski *et al.*, 1997; Berger *et al.*, 1998; Mirski *et al.*, 1999; Champoux, 2001). The ATPase domain is responsible for binding of ATP and its hydrolysis (Berger *et al.*, 1998; Champoux, 2001), while the core domain contains the active site tyrosine required for DNA binding and cleavage (Berger *et al.*, 1996). The divergent CTD contains a nuclear localization signal (NLS), which allows the nuclear import of the respective Topo (Jensen and Svejstrup, 1996; Sehested and Jensen, 1996; Mirski *et al.*, 1997; Mirski *et al.*, 1999). However, it has no relevance for catalytic activity *in vitro* (Jensen and Svejstrup, 1996; Sehested and Jensen, 1996; Mirski *et al.*, 1997; Mirski *et al.*, 1999), but contains sites for posttranslational modifications, such as phosphorylation and SUMOylation (Austin and Marsh, 1998; Gilroy and Austin, 2011; Madabhushi, 2018). Both isoforms share an overall sequence identity of 68 %. The ATPase domains as well as the DNA binding/cleavage domains of the two isoforms show with 78 % the highest sequence homology, whereas the CTDs have more divergent sequences with only 37 % sequence identity (Jenkins *et al.*, 1992; Austin *et al.*, 1993; Sng *et al.*, 1999). Despite the high degree of homology, the isoforms differ both genetically and functionally. In terms of molecular mass and gene location, the Topo II α gene is located on chromosome 17q21-22, which encodes for a 170 kDa protein, whereas the Topo II β gene is located on chromosome 3p24 and encodes for a 180 kDa protein (Tsai-Pflugfelder *et al.*, 1988; Austin and Fisher, 1990; Jenkins *et al.*, 1992; Austin *et al.*, 1993). Additionally, both isoforms display distinct expression patterns during cell cycle and accordingly show a different appearance in proliferating tissues. While the level of Topo II β remain constant during cell cycle, Topo II α alters in amount and stability. Through replication (S phase), Topo II α protein level and

stability increases and reaches its peak in late G_2/M phase (Heck and Earnshaw, 1986; Chow and Ross, 1987; Heck *et al.*, 1988; Hsiang *et al.*, 1988; Woessner *et al.*, 1991). After exiting mitosis, Topo II α gets instable and is rapidly degraded demonstrating its involvement in cell division specific events. This is in accordance with the finding that Topo II α is expressed in proliferating tissues as well as tumor tissues and hardly detectable in non-proliferating tissues, whilst Topo II β expression level show no correlation with the proliferation state of the cell (Heck and Earnshaw, 1986; Chow and Ross, 1987; Heck *et al.*, 1988; Hsiang *et al.*, 1988; Woessner *et al.*, 1991). Topo II α and Topo II β localize in the nucleus with an accumulation at the nucleoli, but during mitosis, Topo II α is tightly bound to chromosomes, whereas Topo II β is diffusely distributed in the cytoplasm (Heck *et al.*, 1988; Austin and Marsh, 1998; Bakshi *et al.*, 2001; Christensen *et al.*, 2002; Wang, 2002; Pommier *et al.*, 2016). Interestingly, Topo II α showed a 10-fold stronger binding to positive supercoiled DNA as compared to negative supercoils, while Topo II β showed no preferential binding (McClendon *et al.*, 2005). Nevertheless, studies with isoforms lacking the CTD showed no effect on the general catalytic activity of the respective isoform (Gilroy and Austin, 2011), but 'tail-swap' experiments revealed a clearly inhibited activity in case of Topo II α with the β-CTD and just a slightly stimulated catalytic activity in case of Topo II β with the α-CTD (Meczes *et al.*, 2008). Further experiments with CTD-truncated isoforms demonstrated an increased DNA binding affinity for Topo II β, but not for Topo II α (Gilroy and Austin, 2011). Taken together, these results suggest that the CTD of Topo II β plays a negative regulatory role in Topo II β (Meczes *et al.*, 2008; Madabhushi, 2018). These isoform-specific characteristics suggest isoform-specific cellular functions: whereas Topo II α plays an essential role in chromosome condensation, segregation and replication, Topo II β is absolutely required for transcription (Pommier *et al.*, 2016; Gómez-Herreros, 2019) of hormonally and developmentally regulated genes (Christensen *et al.*, 2002; Ju *et al.*, 2006; Sano *et al.*, 2008; Cowell *et al.*, 2012; Madabhushi, 2018). It was shown that Topo II β induces transient DNA DSBs in regulatory regions of hormone regulated genes upon corresponding hormone stimuli (estrogen, androgens, retinoic acid, insulin and glucocorticoids) and that such scheduled DNA breaks in stimulus-responsive promoters and enhancers enable transcription initiation and also transcriptional elongation (Ju *et al.*, 2006; McNamara *et al.*, 2008; Haffner *et al.*, 2010; Bunch *et al.*, 2015; Trotter *et al.*, 2015).

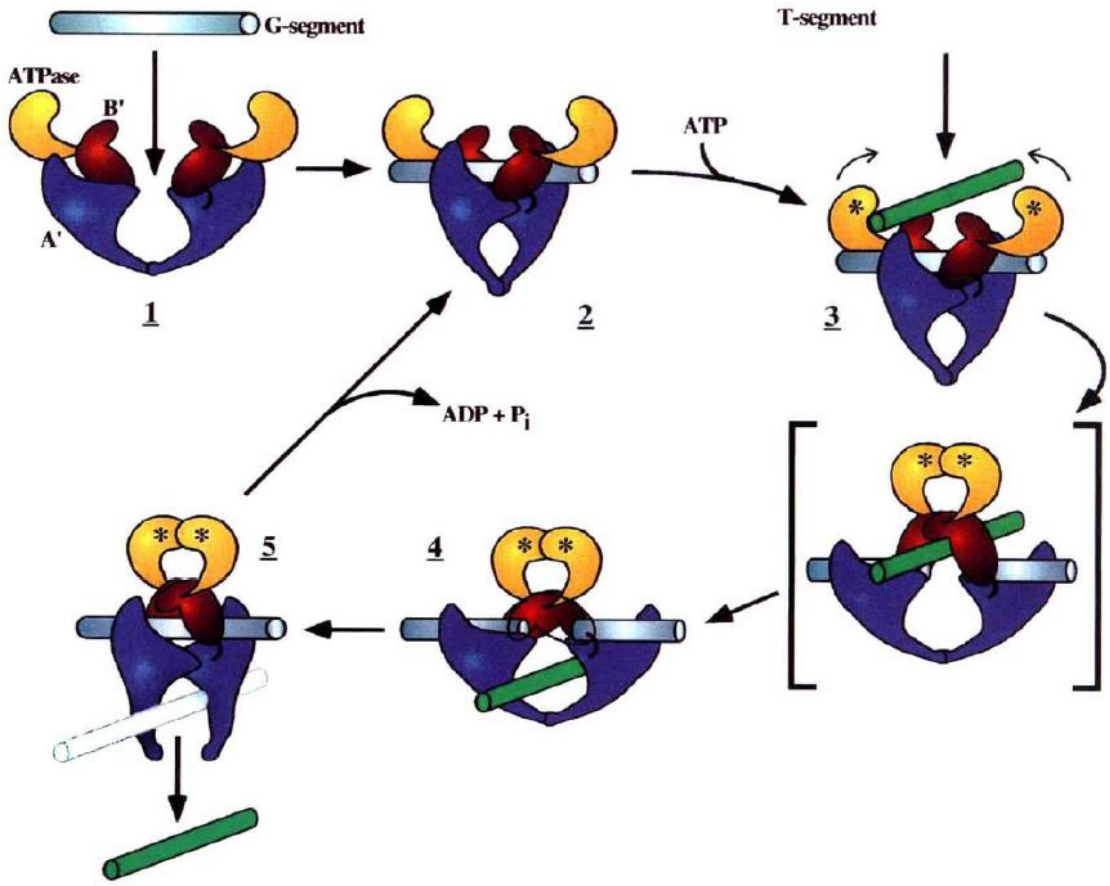

Figure 1.5: The proposed catalytic cycle of Topoisomerase II based on the two-gate model. Dimerized Topo II binds two DNA segments and introduces a double strand break in the so called G-('gate') segment. Subsequently, the intact T-segment DNA (green) is translocated through the cleaved G-segment (pale blue). Then the enzyme ligates the generated DSB and releases the translocated T-segment through a further gate in the protein which hast to be closed with ATP-hydrolysis to initiate a further round of catalysis (Berger *et al.*, 1996).

The Topo II reaction mechanism that catalyzes topological rearrangements of DNA is described in a two-gate model (Figure 1.5) (Berger *et al.*, 1996) and initially requires enzyme dimerization as eukaryotic Topo II proteins function as homodimers (Biersack *et al.*, 1996). The heart-shaped Topo II dimer contains a large central hole recognizing one DNA segment (G-segment), which is bound to the core domain. DNA recognition by Topo II is supposed to be based more on the topological structure of the DNA (like crossovers or nodes) and less on a preferred DNA consensus sequence, allowing the enzyme to operate on numerous sites within a given genome (Osheroff *et al.*, 1991). ATP binds to the ATPase domain and in the presence of Mg^{2+} each strand of the G-segment is cleaved by one active site tyrosine of each monomer generating a transient DSB and a covalently linked enzyme-DNA intermediate (cleavage complex) to maintain genomic integrity (Roca and Wang, 1994; Berger *et al.*, 1996; Bakshi *et al.*,

2001). Undergoing conformational changes, the ATPase domains dimerize and act like a clamp (closed clamp) allowing capture of a second DNA strand (T-segment), which is then transported through the enzyme-cleaved DNA gate (Roca and Wang, 1994; Berger *et al.*, 1996; Bakshi *et al.*, 2001). The DSB within the G-segment is subsequently re-ligated. Afterwards, the bound ATP is hydrolyzed, thereby reopening the ATPase domains (open clamp) and releasing the T-segment. Now the dimeric enzyme is able to initiate a new catalytic cycle (Roca and Wang, 1994; Berger *et al.*, 1996; Bakshi *et al.*, 2001).

The enhanced understanding of the catalytic cycle of Topo II has also led to a better insight into the mechanism of action of Topo II inhibitors. The anticancer drugs targeting Topo II are divided in poisons and catalytic inhibitors (Froelich-Ammon and Osheroff, 1995; Nitiss, 2009). The latter, as the name suggests, inhibit Topo II catalytic activity with different modes of action depending on the drug type. The following types of Topo II inhibitiors are known: those that prevent the binding between Topo II and DNA (e.g. aclarubicin) (Jensen *et al.*, 1990; Sørensen *et al.*, 1992), some that inhibit Topo II mediated ATP hydrolysis (e.g. novobiocin) (Robinson *et al.*, 1993) or drugs that stabilize the noncovalent enzyme-DNA complex thereby preventing the generation of a DSB (e.g. merbarone) (Drake *et al.*, 1989; Andoh and Ishida, 1998; Fortune and Osheroff, 1998). However, Topo II poisons stabilize the covalently bound enzyme-DNA intermediate upon DNA cleavage leading to permanent DSBs. As a result, the accumulation of DSBs ultimately causes cell death (Nitiss, 2009). One prominent example of a Topo II poison is the chemotherapy drug Etoposide (Fortune and Osheroff, 2000; Baldwin and Osheroff, 2005; Deweese and Osheroff, 2009; Vann *et al.*, 2021), which showed antineoplastic activity in AML (acute myeloid leukaemia), breast cancer, gastric cancer, lung cancer, ovarian cancer, Hodgkin's disease and non-Hodgkin's lymphoma (Hande, 1998). In sum, Topo II represents a promising anti-cancer target as it is very active in proliferating cells such as cancer cells (Heck and Earnshaw, 1986; Chow and Ross, 1987; Heck *et al.*, 1988; Hsiang *et al.*, 1988; Woessner *et al.*, 1991; McClendon and Osheroff, 2007). If the Topo II-induced DSBs remain unrepaired as in the case of Topo II poisoning, the accumulated DNA damage induces apoptosis in cancer cells (Errington *et al.*, 1999; Azarova *et al.*, 2007).

It has been shown that Etoposide-treated patients can develop therapy-related secondary leukemia, especially AML, which is associated with chromosomal

translocation of *mixed lineage leukemia* (MLL) gene (for further information see section 1.2.2.1) at chromosome 11q23 (Baldwin and Osheroff, 2005; Felix *et al.*, 2006; Azarova *et al.*, 2007; Bender and Osheroff, 2008; Ezoe, 2012).

As Etoposide does not interfere with DNA double strand breakage mediated by Topo II but prevents the subsequent resealing of the break, it was concluded that the observed MLL translocations are a result of inaccurate DNA repair process after Topo II cleavage (Broeker *et al.*, 1996; Smith *et al.*, 1996). Therefore such chromosomal translocations are attributed to persistent Topo II β-mediated DSBs (Azarova *et al.*, 2007). Thus, it can be concluded that also malfunctioning Topo II can contribute to the hallmarks of cancer (Hanahan and Weinberg, 2011) as it can cause chromosomal instability leading to specific types of leukemia (McClendon and Osheroff, 2007; Deweese and Osheroff, 2009; Vann *et al.*, 2021).

Generally, the hallmarks of cancer comprise „evasion of programmed cell death apoptosis“, „insensitivity to growth-inhibitory signals“, „limitless replicative potential“, „self-sufficiency in growth signals“, „sustained angiogenesis“, „tissue invasion and metastasis“ (Hanahan and Weinberg, 2000), „avoiding immune destruction“, „deregulation of cellular energetics“, „genome instability“, „tumor promoting inflammation“ (Hanahan and Weinberg, 2011), „nonmutational epigenetic reprogramming“, „polymorphic microbiomes“, „senescent cells“ and „unlocking phenotypic plasticity“ (Hanahan, 2022).

1.3.1 HORMONE-INDUCED DNA DOUBLE STRAND BREAKS

Genomic DSBs have long been regarded as unexceptional accidental and disastrous for a cell. But considering that in developmental processes rapid DNA access to inducible genes is essential for transcription and epigenetically modification, DSBs can enable a fast access to the closed chromatin state of transcriptionally repressed genes. Additionally, cells feature many DSB-sensors and repair mechanisms so that DSBs can be quickly detected and repaired by the cell’s DNA damage response (DDR) (Haber, 2000) using two repair pathways: homologous recombination (HR) (Thompson and Schild, 2001) and nonhomologous end joining (NHEJ) (Lieber, 2008).

Indeed, scheduled DSBs have turned out to play an essential role in stimulus-driven transcription: During the last two decades many studies showed that Topo II β induces transient DSBs in regulatory regions of estrogen regulated genes upon corresponding

hormone stimuli (estrogen, androgens, retinoic acid, insulin and glucocorticoids) and that such scheduled DNA breaks in estrogen-responsive promoters and enhancers enable transcription initiation and also transcriptional elongation (Ju *et al.*, 2006; McNamara *et al.*, 2008; Haffner *et al.*, 2010; Bunch *et al.*, 2015; Trotter *et al.*, 2015). In contrast to the sporadic endogenous DNA damage which can occur as a harmful byproduct of replication and transcription, such hormone-induced DSBs in gene promoter regions are scheduled events which are absolutely essential for the activation of certain transcriptional programs (Calderwood, 2016).

In females, estrogens are produced primarily by the granulosa cells of the ovarian follicles (Cui *et al.*, 2013). In all humans, estrogens are also produced by other tissues such as the adipose tissue, adrenal glands, bones, brain, testicles etc. (Nelson and Bulun, 2001; Cui *et al.*, 2013). Synthesis of estrogen starts with the synthesis of androgen from cholesterol, which is further metabolized to testosterone. The conversion of testosterone into 17 β-estradiol (the most potent and prevalent estrogen (Ruggiero and Likis, 2002) is catalyzed by aromatase (Nelson and Bulun, 2001; Cui *et al.*, 2013).

Estrogens belong to the category of sex hormones and are essential for the development and regulation of the female reproductive system and secondary sex characteristics (Delgado and Lopez-Ojeda, 2022). In addition, it was shown that the male reproduction system relies on estrogen in spermatogenesis and fertility (O'Donnell *et al.*, 2001) due to the finding that mice lacking estrogen receptors or aromatase were infertile (Lubahn *et al.*, 1993; Korach, 1994; Hess *et al.*, 1997). Moreover, estrogen is able to initiate genetic programs for differentiation and proliferation (Borellini and Oka, 1989). It was shown that genes coding for anti-apoptotic proteins, different growth factors or cell cycle proteins are generally upregulated upon estrogen stimulus. Important examples for estrogen-regulated cell cycle genes are *cyclin D1* (Sabbah *et al.*, 1999; Cicatiello *et al.*, 2004; Waladali *et al.*, 2009), *cyclin A* (Doisneau-Sixou *et al.*, 2003; Vendrell *et al.*, 2004) and *cyclin E* (Kashima *et al.*, 2009). Furthermore, proto-oncogenes like *FOS* (c-fos) and *MYC* (c-myc) are known to be estrogen-responsive (van der Burg *et al.*, 1989; Szijan *et al.*, 1992; Doisneau-Sixou *et al.*, 2003; Vendrell *et al.*, 2004). In particular, c-myc and cyclin D1 have been assigned to play a central role in estrogen-regulated cell cycle progression by activating cyclin E-CDK2, which finally triggers G1/S phase transition

(Doisneau-Sixou *et al.*, 2003; Yang *et al.*, 2007). Besides this proliferation-promoting effect, estrogen is also able to inhibit anti-proliferative and pro-apoptotic genes (Frasor *et al.*, 2003). The transcription of various receptors is also regulated by estrogen. While the progesterone receptor is upregulated by estrogen (Katzenellenbogen *et al.*, 1987), the proto-oncogene HER2/neu (a biological marker for prognosis and treatment of breast cancer (Burns and Korach, 2012)) exhibited a suppressing effect upon estrogen stimulus (Read *et al.*, 1990; Bortoli *et al.*, 1992; Russell and Hung, 1992). Due to its major impact on proliferation, estrogen is strongly associated with the development and progression of various diseases including different cancer types (breast, ovarian, prostate), endometriosis, obesity and osteoporosis (Deroo and Korach, 2006; Burns and Korach, 2012).

Like other steroid hormones, estrogen enters passively into the cell (Mangelsdorf *et al.*, 1995; Nelson and Bulun, 2001; O'Donnell *et al.*, 2001). After binding and activating the intra cellular steroid hormone receptor ERα, the estrogen-NR complex translocates into the nucleus. ERα belongs to the nuclear receptors (NR), which are ligand-activated transcription factors (Mangelsdorf *et al.*, 1995; Katzenellenbogen, 1996). Within the nucleus, the transcription factor (estrogen-ERα complex) binds to and activates hormone response element (HRE), especially the estrogen responsive element (ERE) within certain gene promoters (Mangelsdorf *et al.*, 1995; Nelson and Bulun, 2001). This leads to the transcription of E2-responsive genes by interacting directly with components of the transcription machinery or indirectly via co-activators or co-repressors (Mangelsdorf *et al.*, 1995; Nelson and Bulun, 2001; O'Donnell *et al.*, 2001; Auger and Jessen, 2009).

New insights revealed that, beside estrogen, also further physiological stimuli (e.g. androgens, insulin, glucocorticoids, retinoic acid and serum) intentionally induce transient Topo II β mediated DSBs within promotors of the respective stimulus-responsive genes (Ju *et al.*, 2006; McNamara *et al.*, 2008; Wong *et al.*, 2009; Haffner *et al.*, 2010; Bunch *et al.*, 2015; Madabhushi *et al.*, 2015; Trotter *et al.*, 2015).

Chromatin-immunoprecipitation (ChIP) experiments in MCF-7 cells showed, that in the uninduced state, Topo II β was located in a repressor complex on the pS2 gene promoter, in association with proteins such as PARP1 (poly (ADP ribose) polymerase 1), Nucleolin (Nuc), nucleophosmin 1 (NPM1), Hsp70 (human heat shock protein 70), HDAC3 (histone deacetylase 3) and the nuclear corepressor N-Cor (Ju *et*

al., 2006) preventing transcriptional elongation by RNA polymerase II (pol II) (Ju *et al.*, 2006; Beneke, 2012).

Upon treatment with 17β-estradiol (E2), estrogen receptor α (ERα), PARP1 and Topo II β were rapidly recruited to the promotor of the estrogen-responsive gene pS2 resulting in the formation of a transient DSB within the promotor, while the other components of the corepressor complex were released (Ju *et al.*, 2006). In contrast, simultaneous inhibition of Topo II β and treatment with estradiol did not result in the formation of DSBs leading to the conclusion that Topo II β is responsible for the DSBs (Ju *et al.*, 2006).

Additionally, various proteins involved in DNA damage and repair machinery are associated with Topo II β like, PARP1, DNA-PK (DNA-dependent kinase) and the regulatory DNA binding subunits Ku70 and Ku86 (Burma and Chen, 2004; Mayeur *et al.*, 2005; Ju *et al.*, 2006). The DSB formation leads to the subsequent recruitment of components of NHEJ demonstrating that Topo II β mediated DSBs are not re-ligated by itself but by NHEJ (Ju *et al.*, 2006). It was further shown that RNA polymerase II (pol II) is released of its paused site due to stimulus driven, Topo II β -generated DSBs (Bunch *et al.*, 2015).

Taken together, the following scenario is conceivable for hormone-induced DSBs and stimulus-induced transcription in general:

As other steroid hormones, E2 is transported across the cell membrane by passive diffusion (Mangelsdorf *et al.*, 1995; Nelson and Bulun, 2001; O'Donnell *et al.*, 2001). In the cytosol it binds to and activates the intracellular steroid hormone receptor ERα, which belongs to the nuclear receptors (NR) that are ligand-dependent transcription factors. The estrogen-ERα complex translocates into the nucleus where it binds to estrogen-responsive elements (EREs) within certain gene promoters (Mangelsdorf *et al.*, 1995; Katzenellenbogen, 1996; Nelson and Bulun, 2001). This leads to the release of the corepressor components Nuc, NPM1, Hsp70, HDAC3 and N-Cor and the recruitment of PARP1 and Topo II β to the promotor of the estrogen-responsive gene. Then Topo II β generates a transient DSB within the promotor (Ju *et al.*, 2006). Via this transient DSB, Topo II β can solve topological barriers in the promoter region such as DNA supercoiling or knots. This finally allows an open chromatin conformation enabling the transcription machinery to gain rapid access for the immediate synthesis

of mRNA. The described recruitment of several components of the DNA damage and repair pathways (PARP, DNA-PK) (Ju and Rosenfeld, 2006) presumably ensures a proper repair of the generated DSBs.

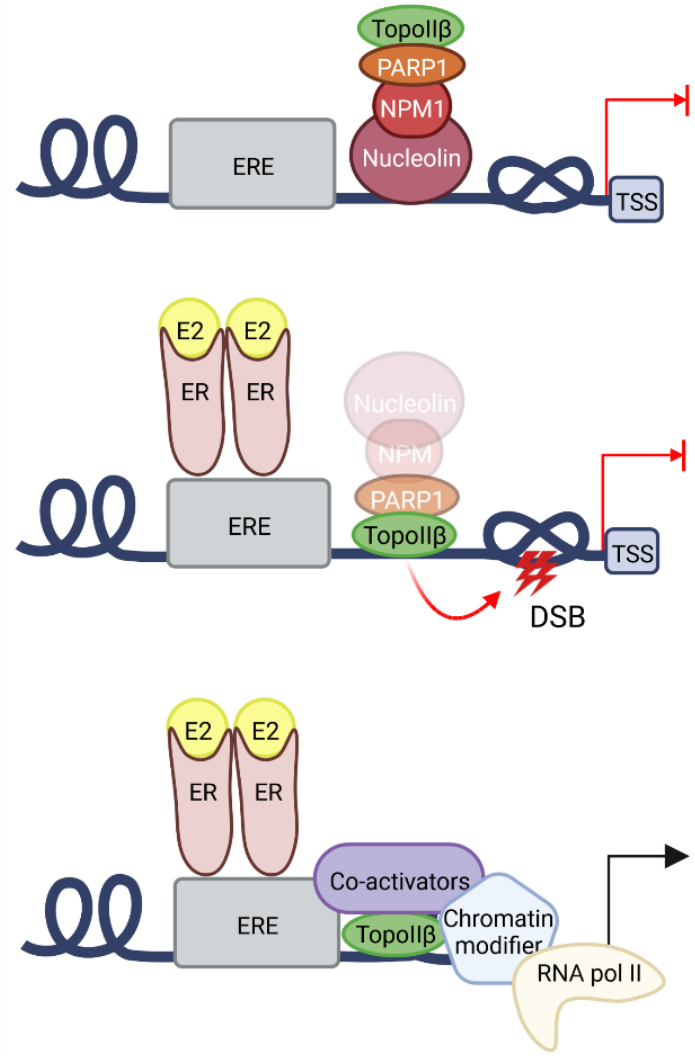

Figure 1.6: Hitherto proposed procedure of estrogen-induced, Topo II β-mediated DNA double strand breaks leading to transcriptional activation of responsive genes.
In an uninduced state, the corepressor complex consisting of Nucleolin, NPM1, PARP1 and Topo II β is bound to hormone-sensitive promotor regions thereby preventing transcriptional initiation. Moreover, transcription is additionally prevented by transcriptional barriers such as DNA supercoils and knots. After estrogen-stimulus, the E2-ER (estrogen receptor) complex binds to and activates the estrogen responsive element (ERE) within the gene promoter leading to the release of the corepressor components Nucleolin and NPM1. PARP1 and Topo II β are recruited to the promotor of the estrogen-responsive gene, where Topo II β generates a transient DSB to solve the topological constraints thereby allowing unhindered access for the transcription machinery. This illustration was created with BioRender.com.

1.4 AIM OF THIS THESIS

An upregulation of the human protease Taspase1 has been described for leukemia, solid tumor types and diverse cancer cell lines. It is classified as a non-oncogene addiction protease because a knockout of Taspase1 leads to an upregulation of CDKIs and a downregulation of cyclins leading to a diminished cell proliferation and an enhanced apoptosis rate. In addition, MEFs lacking Taspase1 are resistant to oncogenic transformation induced by classical oncogene pairs and cancer cell lines with a high level of Taspase1 are addicted to Taspase1 to maintain cell proliferation.

Taspase1´s function is essential for differentiation and embryonic development by processing relevant regulators, such as the leukemia proto-oncogene MLL. It cleaves diverse substrates e.g. MLL, TF2A, USF2 and Myosin1f, which are involved in a broad range of biological processes including transcriptional regulation, cell cycle and apoptosis. Although regulated by the same protease, Taspase1's substrates show no apparent links that could be assigned to a common cellular process, biological pathway or signaling cascade, indicating to an overriding function of Taspase1. Besides its substrates, only a few proteins have been identified as interactors of Taspase1. At the beginning of this project only NPM1 and APP have been known.

Therefore, the aim of this thesis is to gain a better understanding of Taspase1's sphere of activity, by identifying new transient or stable interaction partners of this cancer relevant protease. In consequence, a better defined interactome and the detailed analysis of Taspase1's binding to new interactors may unravel further important details allowing to classify the superordinated function of Taspase1 within a cellular context.

2 MATERIAL AND METHODS

2.1 MATERIAL

2.1.1 EUKARYOTIC CELLS

The eukaryotic cell lines used in this thesis are listed in Table 2.1.

Table 2.1: Eukaryotic cell lines

cell line	origin	property	Research resource identifier
HEK 293T	*Homo sapiens*, embryonic kidney	adherent	CVCL_1926
HeLa Kyoto	*Homo sapiens*, cervical adeno carcinoma	adherent	CVCL_1922
MCF-7	*Homo sapiens*, breast carcinoma	adherent	CVCL_0031

2.1.2 BACTERIAL STRAINS

All bacterial strains used in this work are listed in Table 2.2.

Table 2.2: Bacterial strains

E. coli strain	genotype	supplier
BL21-CodonPlus (DE3)-RIL	*F⁻ ompT hsdS(r_B^- m_B^-) dcm⁺ Tetr gal λ(DE3) endA Hte [argU ileY leuW Cam^r]*	Agilent Technologies
DH5α	*F⁻ endA1 glnV44 thi-1 recA1 relA1 gyrA96 deoR nupG Φ80dlacZΔM15 Δ(lacZYA-argF)U169, hsdR17(r_K^- m_K^+), λ–*	Addgene
NEB 5-alpha	*fhuA2 Δ(argF-lacZ)U169 phoA glnV44 Φ80Δ (lacZ)M15 gyrA96 recA1 relA1 endA1 thi-1 hsdR17*	New England BioLabs GmbH (NEB)
NEB 10-beta	*Δ(ara-leu) 7697 araD139 fhuA ΔlacX74 galK16 galE15 e14-ϕ80dlacZΔM15 recA1 relA1 endA1 nupG rpsL (Str^R) rph spoT1 Δ(mrr-hsdRMS-mcrBC)*	New England BioLabs GmbH
SoluBL21	F⁻ *ompT hsd SB* (r_B^- m_B^-) *gal dcm* (DE3) + further uncharacterized mutations	Genlantis
XL2-Blue	*endA1 supE44 thi-1 hsdR17 recA1 gyrA96 relA1 lac* [F' *proAB lacI^{q}Z$_Δ$M15 Tn10* (TetR) Amy CamR]	Agilent Technologies

2.1.3 PLASMIDS

The plasmids used in this work are listed in Table 2.3.

Table 2.3: Eukaryotic expression plasmids

plasmid	features	reference
pBR322		Thermo Scientific (SD0041)
pc3-USF2-GFP	WT USF2 with C-terminal GFP-tag	(Bier *et al.*, 2011b)
pc3-Taspase1TV-HA	Catalytically inactive mutant (T234V) Taspase1 with C-terminal HA-tag	Christine Heiselmayer, Knauer group, University of Essen
pc3-WTTaspase1-HA	WT Taspase1 with C-terminal HA-tag	Christine Heiselmayer, Knauer group, University of Essen
pc3-WTTaspase1-GFP	WT Taspase1 with C-terminal GFP-tag	(Bier *et al.*, 2011b)
pc3-Taspase1TV-GFP	Catalytically inactive mutant (T234V) Taspase1 with C-terminal GFP-tag	(Bier *et al.*, 2011b)
pc3-GFP	Green fluorescent GFP	Knauer group, University of Essen
pcDNA3.1-N FLAG/Hyg-FLAG-MED4	WT MED4 with N-terminal FLAG-tag	a gift from Joan Conaway & Ronald Conaway (Addgene plasmid # 15425)
pc3-MED4-GFP	WT MED4 with C-terminal GFP-tag	This work
pcDNA3.1(+)	cloning vector with amp^r, neo^r	Invitrogen
pCMV-p16INK4A	WT p16INK4A	a gift from Bob Weinberg (Addgene plasmid # 10916)
pc3-p16INK4A-GFP	WT p16INK4A with C-terminal GFP-tag	This work
pEGFPC1-GFP-Nucleolin	WT Nucleolin with N-terminal GFP-tag	a gift from Michael Kastan (Addgene plasmid # 28176)
pCMV-WTTopoisomerase II α-GFP	WT Topoisomerase II α with C-terminal GFP-tag	(Christensen *et al.*, 2002)
pCMV-Topoisomerase II αQEAA-GFP	Topoisomerase II α cleavage mutant (1251DG1252AA) with C-terminal GFP-tag	This work
pCMV-WTTopoisomerase II β-GFP	WT Topoisomerase II β with C-terminal GFP-tag	(Christensen *et al.*, 2002)

Table 2.4: Prokaryotic expression plasmids

plasmid	features	reference
pET22b-Taspase1-His	WT Taspase1 with C-terminal poly His-tag	Knauer group, University of Essen

2.1.4 ENZYMES

The enzymes used in this work are listed in Table 2.5.

Table 2.5: Enzymes

Enzyme class	Enzyme	supplier
Endonucleases	BamHI-High-Fidelity	New England BioLabs GmbH
	Desoxyribonuclease (DNase) I	Applichem GmbH
	EcoRI-High-Fidelity	New England BioLabs GmbH
	KpnI-High-Fidelity	New England BioLabs GmbH
	NheI-High-Fidelity	New England BioLabs GmbH
	NotI	New England BioLabs GmbH
	XhoI	New England BioLabs GmbH
Isomerases	Topoisomerase II α	Inspiralis
	Topoisomerase II β	Inspiralis
Proteases	Lysozyme	Applichem GmbH
Proteinases	Proteinase K	Roche

2.1.5 OLIGONUCLEOTIDES AND PRIMERS

The used siRNAs are listed in Table 2.5. The indicated single strand (ss) siRNA was pooled and annealed according to manufacturer's protocol.

Table 2.6: siRNA for RNA interference

siRNA	target	reference
siTasp, ss	Taspase1	Sigma-Aldrich SASI_Hs01_00187376
siTasp, ss	Taspase1	Sigma-Aldrich SASI_Hs01_00187378
Negative universal control	Non-targeting	Invitrogen, 46-2001

The synthetically generated DNA primers, listed in Table 2.7 and used for PCR (2.2.1.1), were acquired from Eurofins Genomics. They were dissolved in ultra-pure H_2O and stored as 100 µM stock solutions at -20 °C. The sequencing primers (Table 2.8) were synthesized by Laboratory of the Government Chemist (LGC) Genomics GmbH.

Table 2.7: PCR primers

name	sequence (5'→ 3')
BamHI-p16-fw new	TTTGGATCCACATGGAGCCTTCGGCTGActgg
NheI-p16-rev new	TTTGCTAGCATCGGGGATATCTGAGGGacct
BamHI-MED4_fw	TTTGGATCCACATGGCTGCGTCTTCGAGT
NheI-MED4_rev	TTTGCTAGCATCAGACTCACTACTACT
Topo2alpha_QEAA_F	CCCTCAAGAAGCTGCTGTGGAACTAG
Topo2alpha_QEAA_R	CTTCCTTCAGTATTTTCATTC

Table 2.8: Sequencing primers

name	sequence (5'→ 3')
CMV-F	CGCAAATGGGCGGTAGGCGTG
pcDNA3.1-R	TAGAAGGCACAGTCGAGGCT

2.1.6 DNA AND PROTEIN STANDARDS

All DNA and protein standards used in this work are listed in Table 2.9.

Table 2.9: DNA and protein standards

name	supplier
GeneRuler 1 kb Plus DNA Ladder	Thermo Fisher Scientific
Spectra Multicolor Broad Range Protein Ladder	Thermo Fisher Scientific

2.1.7 ANTIBODIES

The primary (Table 2.10) and secondary antibodies (Table 2.11) were used for western blotting (WB, section 2.2.3.6), immunofluorescence (IF, section 2.2.4.8) or proximity ligation assay (PLA, section 2.2.4.9).

Table 2.10: Primary antibodies

antigen	origin	dilution			manufacturer
		WB	IF	PLA	(order number)
AF9	Rabbit polyclonal	1:5000	-	-	Novus Biologicals (NB100-1566)
CDK9	Rabbit monoclonal	1:5000	-	-	Abcam (ab76320)
Cyclin E	Mouse monoclonal	1:200	-	-	Thermo Fishe (32-1600)
c-myc	Mouse monoclonal	1:250	-	-	Invitrogen (13-2500)
c-fos	Rabbit monoclonal	1:1000	-	-	Abcam (ab134122)
ERα	Rabbit polyclonal	1:250	-	-	Novus Biologicals (NBP1-84827)
ERβ	Rabbit polyclonal	1:1000	-	-	Abcam (ab3576)
GFP	Mouse polyclonal	1:1000	-	-	Santa Cruz (sc-9996)
HA-tag	Rabbit polyclonal	1:4000	-	-	Abcam PLC (AB9110)
HA	Mouse monoclonal	1:1000	-	-	BioLegend (901501)
Histone H3 K4 (trimethylierung)	Rabbit monoclonal	1:1000 (5 % BSA/TBST)	-	-	Cell signaling (9751)
HoxA9	Rabbit monoclonal	1:1000	-	-	Abcam (ab140631)
MED4	Rabbit polyclonal	1:500	-	-	Novus Biologicals (NBP1-84977)
Menin	Mouse monoclonal	1:100	-	-	Santa Cruz (sc-374371)
MLL/KMT2A	Rabbit polyclonal	1:2000	-	-	Novus Biologicals (NB600-248)
NPM1/B23	Mouse monoclonal	1:500	-	-	Santa Cruz (sc-47725)
Nucleolin	Rabbit polyclonal	1:1000	-	-	Abcam (ab22758)
p16/CDKN2A	Mouse monoclonal	1:500	-	-	Biolegend (675602)

antigen	origin	dilution			manufacturer
		WB	IF	PLA	(order number)
p16-INK4A	Rabbit polyclonal	1:750	-	-	Proteintech (10883-1-AP)
p21/CDKN1	Mouse monoclonal	1:250	-	-	Santa Cruz (sc-271610)
p21	Rabbit polyclonal	1:750	-	-	Proteintech (10355-1-AP)
p27 Kip1/CDKN1B	Mouse monoclonal	1:250	-	-	Santa Cruz (sc-1641)
p27 Kip1	Rabbit monoclonal	1:1000	-	-	Cell signaling (3686)
p53	Mouse monoclonal	1:1000	-	-	Santa Cruz (sc-47698)
POLR2A	Mouse monoclonal	1:1000	-	-	Novus Biologicals (NB200-598)
POLR2A S5P	Rabbit polyclonal	1:1000	-	-	Abcam (ab5131)
Rb1	Mouse monoclonal	1:100	-	-	Thermo Fisher (MA5-11387)
SPT5	Rabbit monoclonal	1:1000	-	-	Abcam (ab126592)
Taspase1	Rabbit polyclonal	1:250	-	-	Origene (AP11325PU-N)
Taspase1	Mouse monoclonal	-	-	1:100	Santa Cruz sc-390934
Topoisomerase II α	Mouse monoclonal	1:500	-	-	Santa Cruz (sc-365071)
Topoisomerase II α+β	Rabbit monoclonal	1:10000	1:100	1:200	Abcam (ab109524)
Topoisomerase II β	Mouse monoclonal	1:500	-	-	Santa Cruz (sc-365916)
α-Tubulin	Mouse monoclonal	1:5000	-	-	Sigma-Aldrich (T6074)
γH2AX	Mouse monoclonal	1:5000	-	-	BioLegend (613402)

Table 2.11: Secondary antibodies

antibody	origin	dilution		manufacturer
		WB	IF	(order number)
Anti-rabbit IgG-AF568	Goat	-	1:1000	Life Technologies GmbH (A11011)
Anti-mouse IgG-HRP	Sheep	1:10000	-	GE Healthcare Life Sciences (NXA931)
Anti-rabbit IgG-HRP	Donkey	1:10000	-	GE Healthcare Life Sciences (NA934)

2.1.8 KITS

Kits that were used in this work are listed in Table 2.12.

Table 2.12: Kits

kit	supplier
µMACS™ Epitope Tag Protein Isolation	Miltenyi Biotec
Duolink® In Situ Detection Reagents Orange	Sigma-Aldrich
Duolink® In Situ PLA® Probe Anti-Mouse MINUS and Anti-Rabbit PLUS	Sigma Aldrich
Chromatin Extraction	Abcam
Expand High Fidelity PLUS PCR System	Roche
NucleoBond Xtra Midi	Macherey-Nagel GmbH & Co. KG
NucleoSpin Gel and PCR Clean-up	Macherey-Nagel GmbH & Co. KG
NucleoSpin Plasmid	Macherey-Nagel GmbH & Co. KG
Phusion™ High-Fidelity PCR Kit	Thermo Fisher Scientific
Pierce™ ECL Plus Western Blotting Substrate	Thermo Fisher Scientific
Q5® Site-Directed Mutagenesis Kit	New England BioLabs GmbH
SuperSignal™ West Femto Maximum Sensitivity Substrate	Thermo Fisher Scientific
TaKaRa DNA ligation version 2.1	Clontech

2.1.9 CHEMICALS

Chemicals and reagents were acquired from Applichem GmbH, if not stated otherwise. All other chemicals and reagents used in this thesis are listed in Table 2.13.

Table 2.13: Chemicals and reagents

chemical/reagent	supplier
Antibiotic-Antimycotic	Life Technologies GmbH
Bambanker	NIPPON Genetics EUROPE GmbH
Bio-Rad Protein Assay Dye Reagent (5x)	Bio-Rad Laboratories GmbH
Bortezomib	Sigma Aldrich
Charcoal Stripped Fetal Bovine Serum (FBS)	Life Technologies GmbH
Deoxynucleotide triphosphate (dNTP) Mix	New England BioLabs GmbH
Bradford Reagent (Protein Assay Dye Reagent Concentrate)	BioRad
Dulbecco's Modified Eagle Medium (DMEM), high glucose, GlutaMax supplement	Life Technologies GmbH
Optimized Minimum Essential Medium (Opti-MEM)	Life Technologies GmbH
Dulbecco's Phosphate-Buffered Saline (DPBS)	Life Technologies GmbH
Ethanol	VWR International GmbH
Estradiol (E2)	Sigma Aldrich
Etoposide	Sigma Aldrich
Fetal calf serum (FCS)	Life Technologies GmbH
HCS CellMask™ Deep Red Stain	Life Technologies GmbH
HD Green™ Plus	INTAS Science Imaging Instruments GbmH
Lipofectamine 2000	Life Technologies GmbH
Lipofectamine RNAiMAX	Life Technologies GmbH
Nickel(II) sulfate hexahydrate	Thermo Scientific
Normal goat serum	Dako Deutschland GmbH
Protease Inhibitor cocktail tablets Complete	Roche
Protease Inhibitor Cocktail (1000x)	Abcam
Roti-Histofix 4 %	Carl Roth GmbH & Co. KG
Sodium chloride	Carl Roth GmbH & Co. KG
Sodium dihydrogen phosphate monohydrate	Carl Roth GmbH & Co. KG
TriTrack (6x) DNA Loading Dye	Thermo Scientific
TrypLE Express	Life Technologies GmbH

2.1.10 BUFFERS, SOLUTIONS AND MEDIA

The compositions of buffers, solutions and media used in this work are listed in Table 2.14. Unless stated otherwise, ingredients were dissolved in ultra-pure Milli-Q water (ddH_2O).

Table 2.14: Buffers, solutions and media

buffer/solution/medium	ingredients	final concentration
Binding buffer	Sodium dihydrogen phosphate	50 mM
	Sodium chloride	300 mM
	Imidazol	20 mM
		pH 8.0
Coomassie destaining solution	Acetic acid	10 % (v/v)
	Ethanol	40 % (v/v)
Coomassie staining solution	Acetic acid	10 % (v/v)
	Ethanol	40 % (v/v)
	Coomassie brilliant blue G250	0.1 % (w/v)
Elution buffer (affinity chromatography)	Disodium hydrogen phosphate	50 mM
	Sodium chloride	450 mM
	Imidazol	250 mM
		pH 8.0
Elution buffer (mass spectrometry analysis)	EDTA	1 mM
	SDS	1 %
	DTT	50 mM
	Tris-HCl	50 mM
		pH 6,8
Gel filtration buffer	Disodium hydrogen phosphate	50 mM
	Sodium chloride	450 mM
	DTT	1 mM
		pH 8.0
Growth medium (DMEM++)	Antibiotic-Antimycotic	1x
	FCS (Fetal calf serum)	10 % (v/v)
		in DMEM
HBS (HEPES-Buffered Saline) (2x)	Disodium hydrogen phosphate	2.5 mM
	Sodium chloride	280 mM
	HEPES	50 mM
		pH 7.13

buffer/solution/medium	ingredients	final concentration
Hormone reduced medium	Antibiotic-Antimycotic	1x
	Charcoal Stripped FBS	10 % (v/v)
		in Opti-MEM
IP lysis buffer (co-immunoprecipitation)	Tris	50 mM
	Sodium chloride	150 mM
	EDTA	5 mM
	NP40 (Nonidet P40)	0,5 %
	DTT	1 mM
	PMSF	1 mM
	Protease Inhibitor complete	1x
		pH 8.0
LB agar	Luria-Bertani (LB) agar powder	40 g/l
		pH 7.5
LB medium	LB medium powder	25 g/l
		pH 7.5
NEB antibody dilution buffer	BSA	1 % (w/v)
	Triton X-100	0.3 % (v/v)
		in DPBS
NEB blocking buffer	Normal goat serum	5 % (v/v)
	Triton X-100	0.3 % (v/v)
		in DPBS
PBS (Phosphate-buffered saline)	Disodium hydrogen phosphate	10 mM
	Potassium chloride	2.7 mM
	Potassium dihydrogen phosphate	2 mM
	Sodium chloride	137 mM
		pH 7.4
RIPA (Radioimmunoprecipitation assay buffer)	Tris-HCl	50 mM
	Sodium chloride	150 mM
	EDTA	5 mM
	NP40	1 %
	Natriumdeoxycholat	1 %
	DTT	1 mM
	PMSF	1 mM
	Protease Inhibitor complete	1x
		pH 7.4

buffer/solution/medium	ingredients	final concentration
SDS (Sodium dodecylsulfate) sample buffer (5x)	Bromophenol blue	0.1 % (w/v)
	EDTA	5 mM
	Glycerol	30 % (v/v)
	β-Mercaptoethanol	7.5 % (v/v)
	SDS	15 % (w/v)
	Tris-HCl	60 mM
		pH 6.8
SDS-PAGE running buffer	Glycine	192 mM
	SDS	0.1 % (w/v)
	Tris	25 mM
Separation gel buffer (4x)	SDS	0.8 % (w/v)
	Tris	1.5 M
		pH 8.8
Stacking gel buffer (4x)	SDS	0.8 % (w/v)
	Tris-HCl	0.5 M
		pH 6.8
Stripping buffer	Sodium dihydrogen phosphate	20 mM
	Sodium chloride	500 mM
	EDTA	50 mM
		pH 7.4
TAE (Tris-acetate-EDTA) (10x)	Tris-Acetat	400 mM
	EDTA	10 mM
		pH 8.3
Taspase1 cleavage assay buffer	Sodium dihydrogen phosphate	50 mM
	Saccharose	10 %
	DTT	10 mM
		pH 7.9
Topoisomerase II assay buffer (10x)	Tris-HCl	50 mM
	Sodium chloride	125 mM
	Magnesium chloride	10 mM
	DTT	5 mM
	Albumin	100 µg/ml
		pH 7.5

buffer/solution/medium	ingredients	final concentration
Topoisomerase II dilution buffer	Tris-HCl	50 mM
	Sodium chloride	100 mM
	DTT	1 mM
	EDTA	0.5 mM
	Glycerol	50 % (v/v)
	Albumin	100 µg/ml
		pH 7.5
Tris/HCl	Tris	10 mM
		pH 7.6
Tris-buffered saline (TBS) (1x)	Sodium chloride	150 mM
	Tris-HCl	50 mM
		pH 7.4
Tris-buffered saline and Tween 20 (TBS-T)	TBS	1x
	Tween 20	0.1 % (v/v)
Wash buffer	Disodium hydrogen phosphate	50 mM
	Sodium chloride	450 mM
	Imidazol	10 mM
		pH 8.0
Wet blot buffer	Glycine	192 mM
	Methanol	20 % (v/v)
	SDS	0.01 % (w/v)
	Tris	25 mM
		pH 8.3

2.1.11 INSTRUMENTS

All instruments and devices used in this work are listed in Table 2.15.

Table 2.15: Instruments and devices

instrument	manufacturer
Agarose gel electrophoresis chamber	Peqlab Biotechnologie GmbH
BioPhotometer Plus	Eppendorf AG
Centrifuge 5417 C/R	Eppendorf AG
Centrifuge Heraeus Fresco 21	Thermo Fisher Scientific
Centrifuge ROTINA 380/380 R	Andreas Hettich GmbH & Co. KG
Centrifuge Sorvall™ RC 6 Plus	Thermo Fisher Scientific
ChemiDocTM MP Imaging System	Bio-Rad Laboratories GmbH

instrument	manufacturer
Confocal laser scanning microscope TCS SP8 X Falcon	Leica Microsystems GmbH
Film processor Cawomat 2000 IR	CAWO
Gel caster	Bio-Rad Laboratories GmbH
Gel documentation system E-Box VX2	Vilber Lourmat GmbH
GrantBio 360° vertical multi-function rotator PTR-30	Grant Instruments Ltd
GrantBio orbital shaking platform POS-300	Grant Instruments Ltd
Liquid chromatography (LC) system ÄKTApurifierTM	GE Healthcare Life Sciences
Microscope Primo Vert	Carl Zeiss
peristaltic pump P-1	GE Healthcare Life Sciences
Orbital benchtop shaker MaxQTM 4000	Thermo Fisher Scientific
Orbital shaker POS-300	Grant Instruments Ltd
Orbital tabletop shaker Forma 420 Series	Thermo Fisher Scientific
PAGE chamber Mini-PROTEAN® Tetra Cell	Bio-Rad Laboratories GmbH
PerfectBlueTM tank electro blotter	Peqlab Biotechnologie GmbH
Power supply PeqPower300	Peqlab Biotechnologie GmbH
Power supply PowerPac Basic	Bio-Rad Laboratories GmbH
Rotator PTR-30	Grant Instruments Ltd
Rotator F9S-4x 1000y	Thermo Fisher Scientific
Safety cabinet NuAire NU-437-400E	Integra Biosciences GmbH
Safety cabinets HERAsafe	Thermo Fisher Scientific
Sonopuls HD2200	Bandelin electronic GmbH & Co. KG
Spectrophotometer NanoDropTM 2000c	Thermo Fisher Scientific
Thermocycler TProfessional gradient 96	Biometra GmbH
Trans-Blot® SD Semi-Dry Transfer Cell	Bio-Rad Laboratories GmbH
Ultrasonic homogenizer mini20	Bandelin electronic GmbH & Co. KG
UV Sterilizing PCR Workstation	Peqlab Biotechnologie GmbH
Water purification system Milli-Q®	Merck KGaA

2.1.12 CONSUMABLES

Consumables used in this thesis are listed in Table 2.16.

Table 2.16: Consumables

item	supplier
Affinity chromatography column HisTrap FF	GE Healthcare Life Sciences
Centrifugal Concentrators VivaSpin Turbo 20 (30 K MWCO)	Sartorius AG
Chromatography column size exclusion HiLoad 16/600 Superdex 75 pg	GE Healthcare Life Sciences
Glass bottom dishes (35 mm)	MatTek Corporation
PVDF membrane Amersham Hybond P 0.2	GE Healthcare Life Sciences
µ-Slide 8 well	Ibidi GmbH
µMACS Separator	Miltenyi BioTech

2.1.13 SOFTWARE

The software used in this thesis is listed in Table 2.17.

Table 2.17: Software

software	manufacturer/source
Adobe Illustrator CS4	Adobe Systems GmbH
Canvas 11	ACD Systems International Inc.
Cell Profiler 4.1.3	Carpenter Lab (Broad Institute of Harvard and MIT)
Citavi 6	Swiss Academic Software GmbH
Ciiider, Version 0.9	(Gearing *et al.*, 2019)
Clustal Omega	EMBL-EBI
ExPASy translate	Swiss Institute of Bioinformatics
Gene Construction Kit 3.0	Textco BioSoftware, Inc.
GraphPad Prism 9	GraphPad Software, Inc.
ImageJ/Fiji	U.S. National Institutes of Health
Leica Application Suite X (LAS-X)	Leica Microsystems GmbH
Microsoft Office	Microsoft Corporation
NanoDrop 2000/2000c software	Thermo Fisher Scientific
SnapGene	Insightful Science, available at snapgene.com

2.2 METHODS

2.2.1 MOLECULAR BIOLOGY

2.2.1.1 POLYMERASE CHAIN REACTION

The method of polymerase chain reaction (PCR) is employed to amplify a specific DNA sequence with an exponential rate, using a DNA template, a specific set of primers complementary to the DNA sequence, desoxynucleotide triphosphates (dNTPs) and a DNA polymerase. One PCR cycle composes of three essential steps – denaturation, annealing and elongation – which are repeated 30 to 40 times. First the double stranded DNA (dsDNA) template is denatured at 98 °C together with the sequence-specific primers. After that, the primers anneal to the DNA template at an annealing temperature of 50 – 70 °C. This temperature is 2 °C lower than the melting temperature of the used primer set or can be determined by using the online T_m Calculator (Thermo Fisher Scientific or NEB). At the end, the DNA polymerase elongates the new DNA strand beginning from the primers by integrating free dNTPs. This step requires an optimal working temperature of 72 °C.

In this work the Expand High Fidelity PLUS PCR System (Roche Diagnostics) or PhusionTM High-Fidelity PCR Kit (Thermo Fisher Scientific) was used according to the manufacturer's protocol was used. The used sequence-specific primer pairs are listed in Table 2.7. For a PCR run, a reaction mixture of 50 µl was prepared (Table 2.18) and with a standard PCR program (Table 2.19) the reaction was executed with the Thermocycler TProfessional standard gradient 96 from Biometra. To analyze the efficiency of each PCR, an agarose gel electrophoresis was performed (2.2.1.2).

Table 2.18: PCR reaction mixture

Reagent	Volume
Buffer 2 (5x)	10 µl
each Primer (10 µM)	2 µl
dNTPs (10 mM each)	1 µl
DNA polymerase	0.5 µl
DNA template (20 – 50 ng)	x µl
HPLC H_2O	add to 50 µl

Table 2.19: PCR program

Step	Temperature	Time	
Initial denaturation	98 °C	2 min	
Denaturation	98 °C	30 s	x 30
Annealing	50 – 70 °C	30 s	
Elongation	72 °C	30 – 90 s	
Final elongation	72 °C	5 min	
Storage	15 °C	hold	

2.2.1.2 AGAROSE GEL ELECTROPHORESIS

The agarose gel electrophoresis is used to analyze the results of PCRs (2.2.1.1), restriction digests (2.2.1.6), EMSAs (2.2.1.3) or Topoisomerase II DNA cleavage assays (2.2.1.10). This method separates negatively charged DNA within an electrical field along its size. Smaller DNA fragments move faster through the pores of the agarose gel, in contrast to big fragments, which move much slower. The pore size depends on the used agarose concentration. Via fluorescent DNA-binding dyes the separated DNA was visualized.

0.7 to 1 % (w/v) agarose gels were prepared by solving the respective mass of agarose in 1 x TAE buffer while boiling it. After adding the fluorescent dye HD Green Plus DNA Stain to the mixture in a ratio of 1:10,000, the mixture was inserted into an agarose gel electrophoresis chamber from Peqlab for polymerization. The chamber was filled with 1 x TAE buffer and the samples were loaded on the gel after mixing them with 6x TriTrack DNA Loading Dye. To detect the size of the DNA, a DNA size standard (GeneRuler 1 kb plus DNA ladder from Thermo Scientific) was loaded on the agarose gel, too. The size separation occurred by applying a constant voltage of 90 V with the power supplier PeqPower 300 from Peqlab for 45 – 90 min. For Visualization of the separated DNA bands, the UV light of the gel documentation system E-Box VX2 from Vilber Lourmat or the ChemiDoc™ MP Imaging System from Bio-Rad was used.

2.2.1.3 ELECTROPHORETIC MOBILITY SHIFT ASSAY (EMSA)

Protein-DNA interactions were studied using the electrophoretic mobility shift assay (EMSA). During agarose gel electrophoresis, DNA fragments are separated based on

their size and charge. If a protein is capable of binding to DNA, the DNA band will shift to a higher molecular weight because the protein-DNA complex migrates slower than free linear DNA fragments.

Here, the ability of Taspase1 to bind DNA was investigated. For this, a reaction mix of 10 µl was prepared with different concentrations of recombinant Taspase1-His and 0.5 µg of pBR322 (Thermo Fisher Scientific). The reaction mix was incubated for 15 min at 37 °C and 300 rpm. The samples were immediately mixed with 6x TriTrack DNA Loading Dye to stop the reaction and analyzed via agarose gel electrophoresis (2.2.1.2).

2.2.1.4 PURIFICATION OF DNA FRAGMENTS

The NucleoSpin Gel and PCR Clean-up kit provided by Macherey-Nagel was used to remove contaminations like salts, enzymes, primer or nucleotides from PCR products (2.2.1.1) and to extract and purify DNA fragments from agarose gels (2.2.1.2). The purification procedure was executed according to manufacturer´s protocol. The DNA was bound to a silica membrane and then washed several times and finally the DNA was eluted with respective volumes of ultra-pure H_2O.

2.2.1.5 PHOTOMETRIC DETERMINATION OF DNA CONCENTRATION

Photometric determination of DNA concentration was conducted using the NanoDrop spectrophotometer 2000c (Thermo Scientific) by measuring the absorption at a wavelength of 260 nm. This wavelength corresponds to the absorption maximum of nucleic acid. The DNA concentration was calculated from the observed absorption according to the Lambert-Beer law using an extinction coefficient for dsDNA of 0.02 $(\mu g/ml)^{-1}$ cm^{-1}. Additionally the absorption was measured at 230 nm and 280 nm to examine the purity of the DNA. The ratio of A_{260}/A_{280} provides information about protein or RNA contamination, optimally ranging between 1.8 and 2.0 for pure DNA samples. The ratio of A_{260}/A_{230} determines the contamination with organic substances and should be around 2.0, if the DNA is pure.

2.2.1.6 RESTRICTION DIGEST

The restriction digest was used to introduce double strand breaks at specific sequence locations in plasmids or PCR fragments using restriction enzymes purchased from

New England BioLabs GmbH (Table 2.5). Restriction enzymes belong to type II endonucleases and cut dsDNA by recognizing their recognition site and hydrolyzing the phosphodiester bond of the DNA backbone resulting in cohesive or blunt ends.

Analytical digestions were performed to verify successful cloning using approximate 500 ng DNA and 4 units per restriction enzyme in the recommended digestion buffer at 37 °C for 5 – 15 min. For preparative digestions, 1 – 5 µg DNA were digested with 40 units of each restriction enzyme in a buffer recommended by the manufacturer for 1 – 3 h at 37 °C. To examine the restriction result, digested DNA fragments were analyzed via agarose gel electrophoresis (2.2.1.2). Afterwards, the desired DNA fragments of preparative digestions were extracted from the agarose gel and purified (2.2.1.3) for the following DNA ligation (2.2.1.7).

2.2.1.7 LIGATION

DNA-Ligation is a method of linking adjacent 3' and 5' ends of a dsDNA by enzyme-mediated transesterification of the 5'-OH. This reaction is catalyzed by a T4 DNA ligase, which is able to ligate cohesive or blunt ends. The plasmids and PCR products must be digested with the same restriction enzymes to enable a correct ligation.

The TaKaRa DNA ligation kit (version 2.1) from Clontech was used according to manufacturer's protocol for the ligation of digested and purified vector and insert DNA fragments, which were mixed in a 1:4 ratio with an equivalent amount of TaKaRa Solution I from the kit. The mixture was incubated for 30 min at room temperature (RT) and after that transformed into chemical competent *E. coli* cells (2.2.2.1).

2.2.1.8 SITE-DIRECTED MUTAGENESIS

The Q5 Site-Directed Mutagenesis Kit was used to generate site-specific mutations within a double-stranded plasmid-DNA. After a standard PCR-reaction with specific primers took place, the PCR products are treated with a kinase, a ligase and the restriction enzyme DpnI to circulate the newly generated plasmid and eliminate template DNA. Afterwards, the plasmid is transformed in chemically competent bacterial cells.

Here, a mutation of two amino acids in the potential cleavage motif within a plasmid coding for Topoisomerase II α tagged with GFP should be achieved. The Q5 Site-Directed Mutagenesis was performed according to the manufacturer's protocol.

2.2.1.9 DNA SEQUENCE ANALYSIS

The DNA sequence analysis is necessary to ensure that the plasmids contain the correct coding gene sequences prior to their further use. DNA sequencing was performed by the company LGC Genomics according to the chain termination or Sanger sequencing method (Sanger and Coulson, 1975). The used sequencing primers were provided from the company.

For sequencing, 40 µl plasmid DNA with a concentration of 100 ng/µl were sent to LGC Genomics. The results of the sequence analysis were examined by the online alignment tool Clustal Omega (EMBL-EBI) and ExPASy translate (Swiss Institute of Bioinformatics).

2.2.1.10 TOPOISOMERASE II BETA DNA CLEAVAGE ASSAY

The Topoisomerase II (Topo II) DNA cleavage assay is a plasmid-based system *in vitro* to investigate the cleavage of dsDNA mediated by Topo II. The Topo II activity generates DNA double strand breaks (DSBs) within a plasmid thereby converting supercoiled (sc) DNA into a linear (DSB occurred) or open circle (oc, single strand break occured) form. This assay is based on the protocol from Bandele and Osheroff (Bandele and Osheroff, 2009) and has been adapted accordingly.

First, a 20 µl reaction mix was prepared on ice containing 10x Topo II assay buffer, 1 µg pBR322, different concentration of recombinant Taspase1-His and HPLC H_2O. The reaction was initiated by adding 4 Units Topo II β in Topo II dilution buffer and the samples were incubated for 20 min at 37 °C and 300 rpm. To stop the reaction, 2 µl of 5 % SDS were added. The degradation of Topo II β and Taspase1-His was performed by the addition of Proteinase K to a final concentration of 19 mg/ml and incubation for 30 min at 45 °C and 300 rpm. Afterwards the samples were analyzed via agarose gel electrophoresis (2.2.1.2) regarding the different possible forms of pBR322.

2.2.2 MICROBIOLOGY

2.2.2.1 TRANSFORMATION OF COMPETENT *E. COLI* CELLS

The transformation is used to enable the uptake of exogenous plasmid DNA resulting in genetic alteration of chemically competent bacterial cells. This can be achieved for example by heat shock, through which the cell membrane become transiently permeable.

For heat shock transformation, chemically competent *E. coli* cells (for plasmid amplification: NEB 10-beta, SoluBL21 and XL2-Blue, Table 2.2) were thawed on ice for 10 min. 0.1 – 0.5 µg plasmid DNA or the ligation reaction mix (2.2.1.7) were then incubated with 50 µl of the cell suspension for 30 min on ice. The heat shock took place for 1 min at 42 °C in a water bath followed by an incubation for 2 min on ice. Afterwards the cells were resuspended in 200 µl pre-heated antibiotic-free LB medium and cultivated for 1 – 3 h at 37 °C while shaking at 450 rpm. Finally, 50 µl of the cell suspension were plated on a LB agar plate containing the selective antibiotic and incubated overnight at 37 °C. The type of antibiotic resistance depends on the incorporated plasmid DNA.

The heat shock transformation of the *E. coli* BL21-CodonPlus (DE3)-RIL from Agilent Technologies was carried out according to manufacturer´s protocol. This strain enables an efficient production of heterologous proteins, which is limited to the availability of tRNAs.

2.2.2.2 LONG-TERM STORAGE OF TRANSFORMED *E. COLI* CELLS

To ensure a long-term storage of transformed *E. coli* cells (2.2.2.1), the cells were frozen in glycerin. Glycerin prevents the building of ice crystals, which would otherwise perforate the cells. For this purpose, 800 µl of an overnight bacterial cell suspension were mixed with 200 µl 87 % glycerin in cryogenic vials and stored at -80 °C after shock freezing in liquid nitrogen.

2.2.2.3 PLASMID ISOLATION FROM *E. COLI* CELLS

A mini or midi preparation was performed to isolate plasmid DNA depending on the required DNA amount. The plasmid isolation kits used are based on the principle of alkaline lysis with a subsequent affinity purification.

The NucleoSpin Plasmid kit from Macherey-Nagel was used for mini preparations according to manufacturer´s protocol. For this, a small bacterial culture was grown by inoculating 7 – 10 ml LB medium containing the respective antibiotic (100 µg/ml carbenicillin or 50 µg/ml kanamycin) with one bacterial colony from a LB agar plate. After an overnight incubation at 37 °C under shaking of 200 rpm, 6 ml of the bacterial culture were harvested. The isolated plasmid DNA was eluted in elution buffer or ultra-pure H_2O. For midi preparations, the NucleoBond Xtra Midi kit from Macherey-Nagel was executed according to manufacturer´s protocol. A culture with 200 ml LB medium including the respective antibiotic and a sample from a bacterial glycerin stock (2.2.2.2) or 20 µl of a mini culture was incubated overnight by 37 °C and 120 rpm. Then, the cells were harvested and the plasmids were isolated. The isolated plasmid DNA was precipitated with isopropanol, desalted in 70 % ethanol and afterwards dried and resuspended in ultra-pure H_2O. The plasmid concentration was determined photometrical (2.2.1.5).

2.2.2.4 HETEROLOGOUS EXPRESSION OF RECOMBINANT HIS FUSION PROTEINS

Heterologous expression of recombinant proteins in *E. coli* offers a fast protein production with high yields. Therefore, the used expression system consisting of an expression vector and a suitable *E. coli* host strain is crucial. The most commonly used expression system is based on the bacteriophage T7. The gene of interest is cloned downstream of the T7 promotor into the expression vector. For its transcription the T7 RNA polymerase is necessary, which is expressed by the host strain that contains the corresponding gene. The expression of the T7 RNA polymerase is controlled by the lac operon. By adding an inductor, e.g. isopropyl b-D-1-thiogalactopyranoside (IPTG), which binds the lac repressor, the lac promotor is released and allows the expression of the T7 RNA polymerase. This expression enables the transcription of the gene of interest resulting in the expression of the target protein.

In this thesis, the expression system was composed of a pET22b vector and the *E. coli* BL21-CodonPlus (DE3)-RIL strain. After transforming the plasmid DNA into the bacterial strain (2.2.2.1), 200 ml LB medium supplemented with 100 µg/ml carbenicillin were inoculated with one bacterial colony from the agar plate (2.2.2.1) or a sample from a bacterial glycerin stock (2.2.2.2) (pre-culture) and incubated overnight at 37 °C and 120 rpm. 25 ml of the pre-culture were used to inoculate the main culture

consisting of 1 l LB medium with the respective antibiotic. The protein expression was induced at an OD_{600} of 0.6–0.8 (2.2.2.5) by adding IPTG to a final concentration of 0.2 mM, while shaking the main culture in a 2 l Erlenmeyer flask with chicane at 37 °C and 120 rpm. The protein expression took place for 6 h at 30 °C and 120 rpm. The bacterial cells were harvested by centrifugation for 20 min at 4 °C and 7000 rpm. The pellet was resuspended in 20 ml wash buffer and shock frozen in liquid nitrogen. Until the purification of recombinant proteins (2.2.3.1) the cell suspension was stored at -80 °C.

2.2.2.5 PHOTOMETRIC DETERMINATION OF THE OPTICAL DENSITY

The optical density (OD) was photometrically determined at a wavelength of 600 nm (OD_{600}) using the program “OD600” of the BioPhotometer plus from Eppendorf to monitor the growth progress of bacterial cultures. Therefore 100 µl of the bacterial cell suspension were mixed with 900 µl Milli-Q H_2O in an UV cuvette and measured. Fresh LB medium served as a reference.

2.2.3 BIOCHEMISTRY

2.2.3.1 PURIFICATION OF RECOMBINANT HIS FUSION PROTEINS

The purification of recombinant His-tag fusion proteins is necessary to get access to the target protein. Bacterial cell parts that surround and contain the target protein have to be broken up and removed by several steps including bacterial cell lysis, affinity chromatography and subsequent gel filtration.

2.2.3.1.1 BACTERIAL CELL LYSIS

Bacterial cell lysis is necessary to destroy cell walls and membranes, thereby gaining access to the target protein. Disruption of the cells can be conducted using various procedures based on mechanical, enzymatical, physical or chemical methods. Here, a combination of enzymatic cell lysis by lysozyme and mechanic sonication was used.

The stored cell suspension (2.2.2.4) was thawed on ice before adding lysozyme to a final concentration of 50 µg/ml and 1 mM PMSF in ethanol. Lysozyme hydrolysis glycosidic bonds within peptidoglycans in the bacterial cell wall resulting in cell lysis and the PMSF inhibits released proteases. After stirring the suspension for 1 h at 4 °C

and 100 rpm, it was sonicated three times each 30 s using the Sonopuls HD2200 from Bandelin with an amplitude of 60 %. The sonication took place on ice with intervals of 1 min to avoid excessive heat. To remove cell debris and insoluble proteins, the whole cell lysate was ultra-centrifuged for 90 min at 4 °C and 3900 x g and the supernatant was filtrated through a 0.22 µm filter. After that, an affinity chromatography (2.2.3.1.2) was performed. 10 µl sample were taken from the whole cell lysate and the supernatant and mixed with 20 µl wash buffer for further analysis by SDS-PAGE (2.2.3.4) and Coomassie-staining (2.2.3.5).

2.2.3.1.2 AFFINITY CHROMATOGRAPHY

To isolate the recombinant His-tagged fusion proteins from the bacterial lysate an affinity chromatography was performed using the high affinity of histidine for nickel ions. The poly histidine-tagged proteins were immobilized on the nickel-containing matrix (nickel Sepharose) of a HisTrap FF column (5 ml) from GE Healthcare, while unbound proteins and contaminations were washed away.

The following steps were carried out at 4 °C. Before the supernatant was loaded on the HisTrap FF column, the column was equilibrated with 15 ml Milli-Q H_2O and 25 ml wash buffer using the peristaltic pump P-1 from GE Healthcare with a flow rate of 3 ml/min. The supernatant was loaded on the column with a flow rate of 1.5 ml/min, while the flow through was collected. After washing the column with 50 ml wash buffer using the Äkta-FPLC system from GE Healthcare with a flow rate of 1.2 ml/min, the protein was eluted with a linear gradient of imidazole with concentrations up to 250 mM and a flow rate of 0.5 ml/min. The elution of the recombinant His fusion protein is based on the exchange of the histidine residues by the competitive agent imidazole. 10 µl of the collected fractions mixed with 20 µl wash buffer were analyzed by SDS-PAGE (2.2.3.4) and Coomassie-staining (2.2.3.5). All fractions containing the target protein were united and the protein solution was concentrated using VivaSpin Turbo 30 K MWCO 20 ml by centrifuging for 15 min at 4000 x g until the volume was reduced to less than 3 ml. The eluate was purified via gel filtration (2.2.3.1.3).

2.2.3.1.3 GEL FILTRATION

To separate the concentrated proteins according to their molecular weight, a subsequent gel filtration was performed. The proteins move through a matrix of porous

beads: smaller proteins can diffuse into the beads, while larger ones cannot. Therefore, the larger proteins move faster through the matrix and elute earlier than smaller proteins.

All steps during gel filtration were performed at 4 °C using the Äkta-FPLC system with a flow rate of 1.0 ml/min. First, the Superdex 16/600 gel filtration column (75 pg, 20 ml, GE Healthcare) was equilibrated with 40 ml Milli-Q H_2O and 130 ml gel filtration buffer. The protein solution was loaded on the column and the flow through was collected in 3.5 ml fractions until 130 ml gel filtration buffer have passed through the column. 10 µl of the collected protein-containing fractions were mixed with 20 µl wash buffer and analyzed via SDS-PAGE (2.2.3.4) and Coomassie-staining (2.2.3.5) to determine the fraction with the highest protein amount and the least impurities. All fractions containing the target protein were mixed and the protein solution was concentrated using VivaSpin Turbo 30 K MWCO 20 ml by centrifuging for 15 min at 4000 x g until a concentration of at least 10 mg/ml was reached. 50 µl aliquots of the concentrated protein solution were shock frozen in liquid nitrogen and stored at -80 °C, whereas 2.5 µl were mixed with 27.5 µl wash buffer for the analysis via SDS-PAGE (2.2.3.4) and Coomassie-staining (2.2.3.5).

2.2.3.2 PHOTOMETRIC DETERMINATION OF PROTEIN CONCENTRATION

2.2.3.2.1 BRADFORD ASSAY

The colorimetric Bradford assay is based on the binding of Coomassie Brilliant Blue G-250 to proteins in an acidic environment. This binding causes a shift of the absorption maximum of the dye from 470 nm in the unbound state to 595 nm in the bound state.

For the determination of the protein concentration, 1 µl of lysate was mixed with 800 µl Milli-Q H_2O and 200 µl 5 x Bradford reagent (Bio-Rad) in a UV cuvette. After 5 min incubation at RT, the absorbance at 595 nm was measured using the program “Bradford micro” of the BioPhotometer plus from Eppendorf. Lysis buffer served as a reference. To calculate the protein concentration, a standard calibration curve of defined BSA concentrations (1 – 25 µg/ml) was used.

2.2.3.2.2 ABSORBANCE AT 280 NM

This measurement is based on the absorbance maximum of proteins at 280 nm due to the aromatic amino acids tyrosine and tryptophan. To calculate the protein concentration, the extinction coefficient and the molecular weight of the protein were used.

The protein concentration was measured with the NanoDropTM 2000 c spectrophotometer from Thermo Scientific using 2 µl of the protein solution. The respective buffer served as a reference.

2.2.3.3 SEMI IN VITRO TASPASE1 SUBSTRATE CLEAVAGE ASSAY

A semi *in vitro* Taspase1 substrate cleavage assay (short cleavage assay) was established to investigate the inhibitory effects of potential ligands on substrate cleavage by Taspase1 (Höing *et al.*, 2022). This assay was adapted to verify new Taspase1 substrates. A potential Taspase1 substrate is overexpressed in 293T cells and the whole cell lysate is prepared. After incubation of lysate fractions with or without recombinant Taspase1-His a potential substrate cleavage can be analyzed by SDS-PAGE and Western blot.

In detail, 293T cells were seeded in a 10 cm dish and transfected with plasmid coding for the potential Taspase1 substrate in fusion with a GFP-tag. 24 h after transfection, whole cell lysates were prepared (2.2.4.5) by sonicating the cells in Taspase1 cleavage assay buffer for at least four times. 100 µl cell lysate were mixed with 3x Protease Inhibitor Cocktail (Abcam), 13 µM recombinant Taspase1-His and incubated at 37 °C. As control, cell lysates without recombinant Taspase1-His were used. 50 µl samples were taken after specific time intervals and further analyzed by SDS-PAGE (2.2.3.4) and Western blot (2.2.3.6).

2.2.3.4 SDS-POLYACRYLAMIDE GEL ELECTROPHORESIS

Sodium dodecyl sulfate-polyacrylamide gel electrophoresis (SDS-PAGE) is a method to separate proteins along their molecular mass within an electrical field. The proteins become completely unfolded and negatively charged proportional to their molecular mass by using SDS as a detergent, which attaches to the amino acids of the protein thereby destroying all non-covalent bonds. Due to their negative charge, the proteins

are separated along their molecular mass while moving towards the anode. Small proteins move faster through the pores of the polyacrylamide gel than large ones. The separation properties of the gel depends on the gel´s pore size, which is determined by the used polyacrylamide concentration.

In this work, the discontinuous system consisting of a 7.5 %, 10 % or 12.5 % separation gel and a 4 % stacking gel with a thickness of 1.5 mm (Table 2.20) was used. First, the components of the separation gel were mixed and cast in a BioRad casting module. After polymerization of the separation gel, the stacking gel was cast on the top of the separation gel and a comb was applied to generate wells. The gel was placed to an electrophoresis chamber filled with SDS-PAGE running puffer. Protein samples were mixed with 5 x SDS sample buffer and denatured at 95 °C for 5 – 10 min. The molecular weight marker (Spectra Multicolor Broad Range protein ladder from Thermo Scientific) as well as the protein samples were loaded on the gel and the electrophoresis was performed at 120 V for 60 – 90 min. Next, the polyacrylamide gels were stained with Coomassie (2.2.3.5) or used for further analysis by Western blotting (2.2.3.6).

Table 2.20: Composition of SDS-polyacrylamid gels with a thickness of 1.5 mm

Component	**separation gel**			**stacking gel**
	7.5 %	10 %	12.5 %	4 %
Milli-Q H_2O (ml)	4.3	3.6	2.9	2.5
4 x separation gel buffer (ml)	2.4	2.4	2.4	-
4 x stacking gel buffer (ml)	-	-	-	1.35
30 % acrylamide (ml)	2.3	3.0	4.4	0.65
10 % APS (w/v) (µl)	96	96	96	50
TEMED (µl)	10	10	10	5

2.2.3.5 COOMASSIE-STAINING OF POLYACRYLAMIDE GELS

Coomassie-staining is used to visualize proteins after electrophoretic separation by SDS-PAGE (2.2.3.4). This unspecific protein staining is based on triphenylmethane of Coomassie brilliant blue G-250, which binds to basic amino acids under acidic conditions.

The staining of polyacrylamide gels occurred for 30 min at RT under shaking in Coomassie staining solution, after boiling it. The gels were washed two times with Coomassie destaining solution for 30 min at RT under shaking. The gels were incubated under shaking in Milli-Q H_2O over night at RT to remove background staining and to get clear protein bands.

2.2.3.6 WESTERN BLOTTING

Western blotting is an analytical method to detect proteins with specific antibodies. The negatively charged proteins separated by SDS-PAGE (2.2.3.4) are transferred from the polyacrylamide gel onto a suitable membrane by applying an electrical field. Due to hydrophobic and electrostatic interactions, the proteins are immobilized on the membrane and can be detected by antigen-antibody interactions. For the visualization of the antigen-antibody complex, a secondary antibody is labeled with an enzyme catalyzing a chemiluminescent reaction.

For Western blotting the tank blot technique was applied. After activating the Amersham Hybond P 0.2 or 0.45 PVDF membrane in 100 % methanol for 1 min, the membrane, the polyacrylamide gel and four pieces blotting paper from Carl Roth were equilibrated for 10 min in wet blot buffer. The blot sandwich was amounted within a blot cassette with pads on each side from the anode to the cathode consisting of two pieces blotting paper, the PVDF membrane, the polyacrylamide gel and again two pieces blotting paper and subsequently inserted into the PerfectBlue™ tank electro blotter from Peqlab filled with wet blot buffer. Using the power supplier PeqPower 300 from Peqlab a constant amperage of 120 mA overnight or 360 mA for 90 min was applied at 4 °C. Following protein transfer, the membrane was blocked with blocking solution (5 % non-fat dried milk powder or BSA in TBS-T) compatible with the primary antibody for 45 min while gently shaking at RT to saturate unspecific binding sites. The incubation with the appropriate primary antibody diluted according to Table 2.10 took place for 90 min at RT or overnight at 4 °C with gentle agitation. After three washing steps with TBS-T, each for 5 min while shaking, the membrane was incubated with the horseradish peroxidase (HRP)-conjugated secondary antibody (Table 2.11) diluted in 5 % non-fat dried milk powder in TBS-T for 1 h at RT with gentle shanking. Afterwards, the membrane was again washed thrice with TBS-T and once with TBS before the detection took place by using the Pierce™ ECL Plus Western Blotting Substrate or

SuperSignal™ West Femto Maximum Sensitivity Substrate from Thermo Scientific according to the manufacturer's instructions and the ChemiDoc™ MP Imaging System (Bio-Rad).

2.2.4 CELL BIOLOGY

2.2.4.1 CULTIVATION OF EUKARYOTIC CELLS

During proliferation, eukaryotic cells consume nutrients present in the growth medium and occupy the surface of the cell culture flask. Therefore, it is necessary to subculture them into a new flask with fresh growth medium, when they reach a confluency of about 70 – 90 %. Eukaryotic cell lines were cultivated at 37 °C and 5 % CO_2 in approximately 90 % relative humidity. For the purpose of preventing contaminations like bacteria, fungi and viruses, cell cultivation took place under sterile conditions.

The adherent eukaryotic cell lines used (Table 2.1) were cultivated in DMEM supplemented with 1x Antibiotic-Antimycotic and 10 %FCS (growth medium) according to the manufacturer's protocol and were passaged twice a week. For this purpose, the old growth medium was removed and the cells were washed with 5 ml DPBS. To detach the adherent cells from the cell culture flask T-75 (Sarstedt), 2 ml TrypLE Express (Life Technologies) were added and the cells were incubated on a heating plate at 37 °C until they were detached. To stop the enzymatic reaction, 8 ml new growth medium was added and the cells were resuspended. The cell suspension was diluted in an appropriate ratio of 1:10 to 1:20 with fresh growth medium in a total volume of 10 ml and transferred to a new cell culture flask T-75. For experiments different dell culture dishes or flasks were used and the volumes of cell suspension and growth medium were adjusted respectively.

2.2.4.2 FREEZING AND THAWING OF CELL LINES

For cryoconservation, cells were centrifuged for 5 min at RT and 300 x g and the supernatant was discarded. The cell pellet was resuspended in Bambanker medium at a cell density of about 2 x 10^6 cells / ml and aliquots of 1 ml aliquots were filled into a cryo vial. Aliquots were frozen overnight at -80 °C. Finally, the cryo vials were preserved in a liquid nitrogen tank for long-term storage.

Cryoconserved cells were thawed in a water bath at 37 °C and immediately mixed with 10 ml of preheated growth medium. The cell suspension was transferred in a cell culture flask T-75 and cultivated at 37 °C and 5 % CO_2 in approximately 90 % relative humidity (2.2.4.1).

2.2.4.3 TREATMENT WITH ESTRADIOL

To study the influence of estrogen on protein expression level, the cells were treated with Estradiol (E2). Therefore, cells were seeded in a 6 cm or 10 cm cell culture dish and after 24 h the growth medium was exchanged to hormone reduced medium for 4 h and within this time the cells were treated with 50 nm E2 at certain times.

2.2.4.4 TRANSFECTION OF EUKARYOTIC CELLS

The introduction of foreign DNA into eukaryotic cells is defined as transfection. The term ’stable transfection’ describes a long-term introduction of foreign DNA in which the cells have integrated this DNA in their genome due to antibiotic selection, whereas transiently transfected cells have not genomically integrated the foreign DNA but only harbor the transfected DNA for a limited time. In both cases, plasmid DNA must passage the cell membrane and the nucleus to be transcribed, which can be achieved by different transfection methods based on reagents, instruments or viruses. In this work, two different reagents were used, namely Lipofectamine and calcium phosphate. Lipofectamine forms liposomes, which built complexes with the negatively charged DNA allowing to merge with the cell membrane. By using calcium phosphate a precipitate is formed, which is taken up by cells via endocytosis.

For transfection with calcium phosphate, cells were seeded 24 h prior to transfection. The transfection reagents were mixed as shown in Table 2.21. First, Tris/HCl was mixed with the respective amount of $CaCl_2$ and the plasmid DNA was added to the mixture. Carefully the 2x HBS was added while pulling the pipet from the bottom to the top of the tube. After an incubation of 10 min at RT, the indicated volume of the mixture was added to the cells, which were subsequently incubated for other 24 h at 37 °C and 5 % CO_2 under H_2O saturated atmosphere before they were used for further experiments.

Table 2.21: Pipetting scheme for $CaPO_4$ transfection

Volume of used components	Dish / well size		
	15 cm (152 cm²)	10 cm (57,6 cm²)	3,5 cm (9,6 cm²)
Growth medium (ml)	20	10	2
10 mM Tris/HCl pH 7.6 (µl)	990 - x	495 - x	114 - x
DNA (µl)	x (corresponding to 28 µg DNA)	x (corresponding to 14 µg DNA)	x (corresponding to 3 µg DNA)
2 M $CaCl_2$ (µl)	110	55	11
2x HBS (µl)	1100	550	125
Add to cells (µl)	2000	1000	200

For transfection with Lipofectamine 2000, cells were seeded in a 6-well plate (9.5 cm²) in 3 ml growth medium. Transfection was executed after 24 h incubation of the cells. Therefore, two transfection solutions were prepared: solution A contained 3 µl Lipofectamine 2000 in 100 µl Opti-MEM and solution B comprised 1 – 3 µg DNA in 100 µl Opti-MEM. Both solutions were rigorously vortexed and subsequently mixed followed by an incubation of 5 min at RT allowing complex formation. The transfection mix was added to the cells which were incubated for 24 h. For some experiments different cell culture dishes were used and the volumes of growth medium and transfection reagents were adjusted respectively.

To transfect siRNA, the Lipofectamine RNAiMAX Reagent was used according to the manufacturer´s protocol.

2.2.4.5 PREPARATION OF CELL LYSATES AND CHROMATIN FRACTIONS FROM EUKARYOTIC CELLS

For co-immunoprecipitation experiments whole cell lysates and chromatin bound fractions were prepared. First, transiently transfected cells (2.2.4.4) were detached from a 10 cm cell culture with a cell scraper. The cell suspension was centrifuged for 5 min at 300 x g and 4 °C and the cell pellet was washed with 1 ml PBS. For cell lysis and chromatin extraction, the Chromatin Extraction kit from Abcam was used

according to manufacturer´s protocol. The received chromatin extract was used for co-immunoprecipitation (2.2.4.6).

To prepare whole cell lysates, the received cell pellet was subsequently resuspended in 500 µl IP lysis buffer followed by an incubation for 30 min on ice allowing the cells to be lyzed. Afterwards, the cell lysate was sonicated for at least three times with a Sonopuls mini20 ultrasonic homogenizer using the ultrasonic probe MS 1.5 from Bandelin for 20 s and an amplitude of 90 %.

To analyze protein levels of treated cells, whole cell lysates were prepared with RIPA lysis. The culture medium was discarded and the cells were incubated with 150 µl RIPA buffer for 1 min. The cells were detached from a 6 cm cell culture dish with a cell scraper and the cell suspension was immediately shock frozen in liquid nitrogen. After thawing on ice, the RIPA cell lysates were sonicated for two times with a Sonopuls mini20 ultrasonic homogenizer using the ultrasonic probe MS 1.5 from Bandelin for 30 s and with an amplitude of 90 %.

To remove cell debris, whole cell lysate or RIPA cell lysates were centrifuged for 20 min at 4 °C and 14000 rpm and the supernatant was transferred into a new reaction tube. The protein concentration was determined (2.2.3.2.1) and the cell lysate was stored at -80 °C after shock freezing in liquid nitrogen or subsequently used for further experiments.

2.2.4.6 CO-IMMUNOPRECIPITATION

Immunoprecipitation (IP) is used for the isolation of a protein and its associated binding partners from cell lysates. A specific antibody against the target protein is coupled to an immobilized matrix (e.g. magnetic beads) and built a complex with the target, which is precipitated on the immobilized matrix. After washing non-specifically bound proteins away, the target protein is eluted. The investigation of secondary targets (interacting proteins) bounded to the primary target protein enables the study of protein-protein interactions, called co-IP.

Here, the µMACS^{TM} Epitope Tag Protein Isolation kits from Miltenyi Biotec were used, which are based on anti-epitope tag antibody-coated magnetic beads. The precipitation took place by applying a magnetic field. First, whole cell lysates or chromatin extracts (2.2.4.5) from eukaryotic cells transiently transfected (2.2.4.4) with

a plasmid coding for the tagged target protein were prepared. 60 µl input sample were taken from the chromatin extract and cell lysate, while the remaining cell lysate was mixed with 500 µl IP lysis buffer. After adding 50 µl anti-epitope tag antibody-coated magnetic beads to the samples, the µMACS^{TM} Epitope Tag Protein Isolation kit was performed according to manufacturer´s protocol. Instead of the Lysis Buffer from the kit, a self-prepared IP lysis buffer was used. Additionally, the washing steps were changed: the column was washed once with 200 µl Wash Buffer 1 (kit), thrice with IP lysis buffer each 200 µl and in the end once with 100 µl Wash Buffer 2 (kit). For the elution step, the Elution Buffer (Kit) was used, except for mass spectrometry sample preparation, where a self-prepared elution buffer was utilized. The eluates were collected and analyzed together with the input samples by SDS-PAGE (2.2.3.4) and Western Blot (2.2.3.6) or by tandem mass spectrometry, which was conducted in cooperation with the Analytics Core Facility Essen (ACE) (University Duisburg-Essen).

2.2.4.7 CONFOCAL FLUORESCENCE MICROSCOPY

Fluorescence microscopy uses fluorophores, which adsorb light of a particular wavelength to enter an excited state followed by subsequent emission of light with a longer wavelength. The emitted light is detected by different detectors. A special form of fluorescence microscopy is the confocal microscopy, which increases accuracy and information of an image by focusing the observed light on a single layer resulting in high resolution and precise localization information.

Confocal fluorescence microscopy was performed with the laser scanning microscope SP8X Falcon from Leica Microsystems. This microscope is equipped with different lasers (SP8X Falcon: Diode: 405 nm; Argon, 458/476/488/496/514 nm; WLL E: 470 – 670 nm; UVA: 355 nm) and various detectors (PMT confocal imaging detectors and sensitive imaging hybrid detector). The samples were imaged with HC PL APO 63x/1.2 W motCORR CS2 using the visualization software Leica Application Suite X (LAS X) from Leica Microsystems by sequential scans with a scan speed of 200 – 400 Hz and a resolution of 1024 x1024 pixels.

2.2.4.8 IMMUNOFLUORESCENCE STAINING

Proteins can be visualized in cells using immunofluorescence (IF) staining to investigate their cellular localization or intermolecular interactions. Here, the indirect IF

staining took place with two different antibodies: first, a target specific primary antibody and second, a fluorophore-conjugated secondary antibody.

Cells were seeded in µ-Slide 8-Well ibiTreat (Ibidi GmbH) or in 35 mm glass bottom dishes (MatTek). PBS was used for all washing steps. Prior IF staining, the cells were fixed with 4 % Roti-Histofix (Roth) for 20 min at RT. Following three washing steps, the cells were permeabilized and unspecific binding sites were blocked with 0.3 % Triton-X-100, 5 % goat serum in DPBS (NEB blocking buffer) for 30 min at RT and incubated afterwards with the respective primary antibody (Table 2.10) diluted in 0.3 % Triton-X-100, 1 % BSA in DPBS (NEB antibody dilution buffer). The incubation with the primary antibody was carried out in a humidified chamber overnight at 4 °C. To get rid of the primary antibody, the cells were washed three times and incubated with the secondary antibody diluted in NEB antibody dilution buffer for 1 – 2 h at RT. Afterwards, the cells were again washed three times and, if necessary, stained with 10 µg/ml Hoechst33342 and 2 µg/ml HCS CellMask™ Deep Red Stain (Thermo Scientific) in PBS for 30 min at RT. After three final washing steps, the samples were stored at 4 °C in 0.1 % (w/v) sodium azide in PBS and analyzed via confocal fluorescence microscope (2.2.4.7),.

2.2.4.9 PROXIMITY LIGATION ASSAY

The *in situ* proximity ligation assay (PLA) allows the detection of direct protein-protein interactions. Two protein target specific primary antibodies are recognized by two secondary antibodies conjugated with oligonucleotides (PLA probes). If the two protein targets are in close proximity (< 40 nm), indicating a direct interaction, connector oligonucleotides join the PLA probes and a ligase forms a closed circle DNA template that is required for rolling-circle amplification. Using fluorescently labeled oligonucleotides during the amplification step, the PLA signals become visible as a well-defined fluorescent dots (PLA foci) and are analyzed by fluorescence microscopy (Figure 2.1).

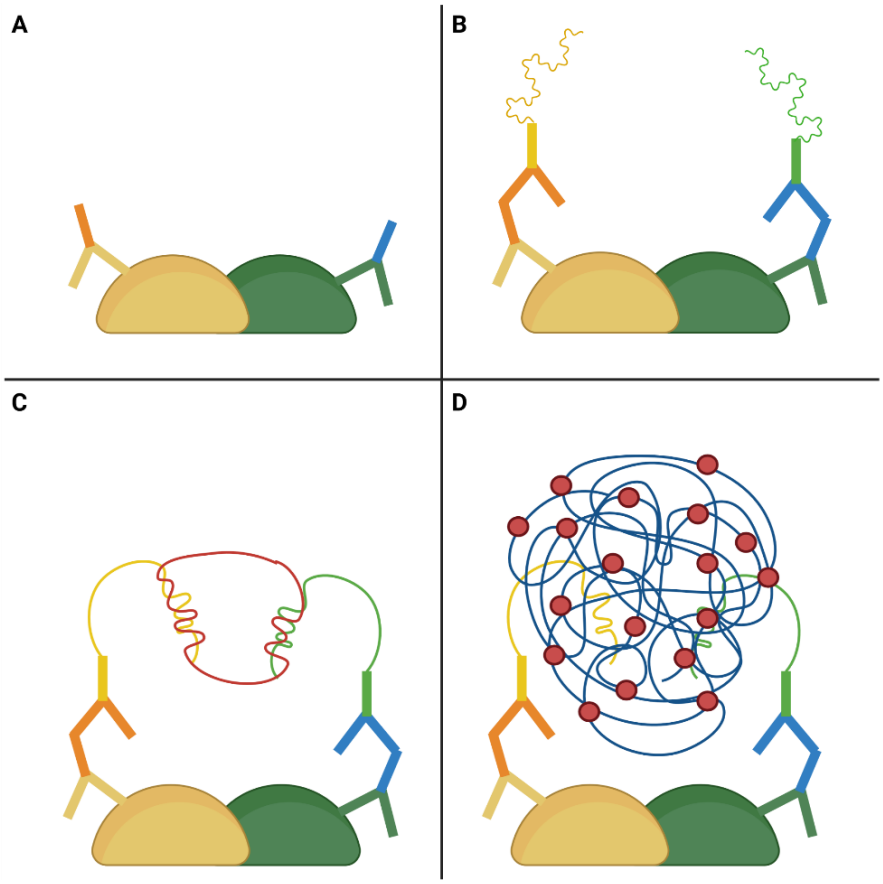

Figure 2.1: Investigation of protein-protein interactions by PLA.
The potentially interacting target proteins are recognized by their specific primary antibodies (A). Secondary antibodies conjugated with oligonucleotides (PLA probes) bind the respective primary antibody (B). If the target proteins interact with each other, they are in close proximity (>40 nm), thereby allowing connector oligonucleotides to hybridize with both PLA probes and a closed circle DNA template is formed by ligation (C). These circular structures are amplified using fluorescently labeled oligonucleotides to gain well-defined fluorescent dots (PLA foci) (D). This illustration was created with BioRender.com.

Cells were seeded in 35 mm glass bottom dishes (MatTek) and the same steps as for IF (2.2.4.8) were executed for fixation, blocking, permeabilization and incubation with primary antibodies. Afterwards, the PLA staining was performed with the Duolink® In-Situ-Detection Reagents Orange, Duolink® In Situ PLA® Probe Anti-Mouse MINUS and Anti-Rabbit PLUS from Sigma-Aldrich according to manufacturer's Duolink® PLA Fluorescence Protocol. All washing steps were performed with PBS. A staining step with 10 µg/ml Hoechst33342 and 1:5000 diluted HCS CellMask™ Deep Red Stain (Thermo Scientific) in PBS for 30 min at RT was performed. The cells were stored at 4 °C in 0.1 % (w/v) sodium azide in PBS until they were analyzed by fluorescence microscopy (2.2.4.7). For quantification of the PLA signals, maximum projection images of z-stacks were taken and analyzed with the cell image analysis software Cell

Profiler 4.1.3 (Figure 2.2). This software recognizes defined primary objects, namely the Hoechst-stained nuclei, and secondary objects, in this case the whole cell defined by plasma membrane staining with HCS CellMask™ Deep Red Stain. Afterwards, PLA foci were analyzed and assigned to the defined objects.

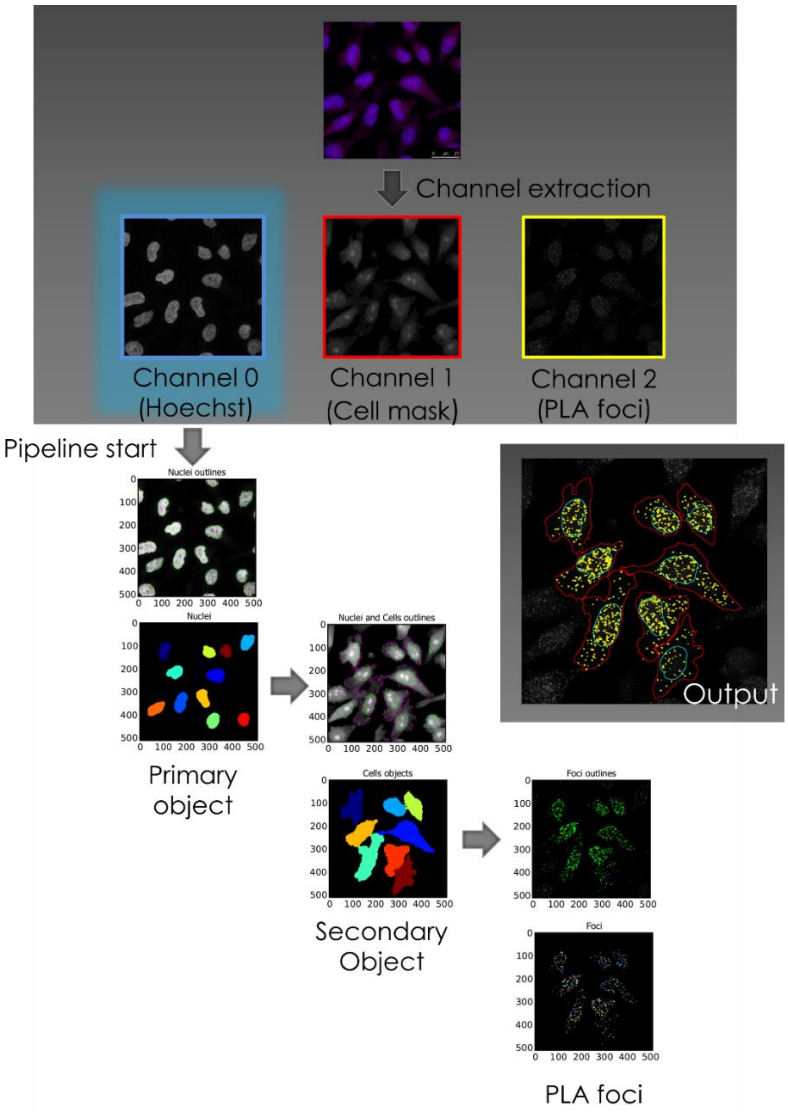

Figure 2.2: Image analysis of PLA foci was performed by Cell Profiler.

PLA foci were quantified with the cell image analysis software Cell Profiler 4.1.3. The software used the Hoechst-stained nuclei to define the primary objects (blue) and the staining of the plasma membrane with HCS CellMask™ Deep Red for the definition of the secondary objects (red). Afterwards, PLA foci (yellow) were counted and assigned to the cellular compartments (Dannheisig, 2016).

3 RESULTS

Taspase1 is overexpressed in leukemia, solid tumor types and diverse human cancer cell lines (Takeda *et al.*, 2006; Chen *et al.*, 2010; Bier *et al.*, 2011a; Bier *et al.*, 2012a). Considering the fact that genetic depletion of Taspase1 in adult mice causes no apparent deficiencies (Takeda *et al.*, 2006) but specifically cancer cells are dependent on Taspase1 expression to sustain cell proliferation (Takeda *et al.*, 2006; Chen *et al.*, 2010), this protease represents a promising therapeutic target for anti-cancer therapy. Apart from Taspase1's influence on development and cell differentiation through cleavage of its substrates, such as the MLL (Mixed lineage leukemia) protein (Hsieh *et al.*, 2003b; Hsieh *et al.*, 2003a; Takeda *et al.*, 2006), there is still much to explore about Taspase1's degradome and interaction network. Mostly high-throughput methods have identified new possible interaction partners and substrates, but only a few were verified, so that a more precise classification of Taspase1 function in the cellular context remains open. Taspase1 with its multiple targets and its involvement in cell cycle progression is likely to form transient interactions with hitherto unknown binding partners. Consequently, it is worthwhile to focus on Taspase1's interaction network, which might help to decipher the complete functionality of this protease.

3.1 IDENTIFICATION OF NOVEL INTERACTION PARTNERS

For a better understanding of Taspase1's sphere of activity, co-immunoprecipitation experiments (co-IPs) were performed (2.2.4.6) to identify novel interaction partners of this cancer-relevant protease. Co-IPs were carried out with 293T cell lysates with ectopically expressed GFP-tagged constructs and anti-GFP antibody-coated magnetic beads. Two versions of immunoprecipitated Taspase1-GFP fusion proteins, namely the wild type (WT) and a catalytic inactive mutant (Taspase1^{T234V}) (as well as the GFP control approach) were analyzed for the presence of co-precipitated endogenous interaction partners. Lysates (input) and immunoprecipitates (eluates) were separated via SDS-PAGE (2.2.3.4) and transferred to a PVDF-membrane followed by immunodetection using diverse antibodies (Western blotting 2.2.3.6). The selection of antibodies for the Taspase1 interaction partner screening was not chosen at random but based on rational considerations resulting from intensive literature research.

Due to Taspase1´s involvement in cancer (Takeda *et al.*, 2006; Chen *et al.*, 2010; Bier *et al.*, 2011a; Bier *et al.*, 2012a) and cell cycle progression (Takeda *et al.*, 2006; Chen *et al.*, 2010; Dong *et al.*, 2014; Takeda *et al.*, 2015), the Taspase1 interaction network was examined in a first approach focusing on cell cycle proteins that also function as tumor suppressor proteins. Therefore, specific antibodies were utilized to investigate if Menin (Yokoyama *et al.*, 2005; La *et al.*, 2006), p16 (Liggett and Sidransky, 1998; Wang *et al.*, 2001; Sasaki *et al.*, 2003), p21 (Wang *et al.*, 2001), p27 (Sasaki *et al.*, 2003; Kossatz and Malek, 2007), p53 (Wang *et al.*, 2001; Sasaki *et al.*, 2003) and Rb1 (retinoblastoma-associated protein 1) (Sasaki *et al.*, 2003; Vélez-Cruz and Johnson, 2017) are possible components of the isolated Taspase1 complexes.

The input samples of GFP, WT Taspase1-GFP and Taspase1^{T234V}-GFP did not allow the detection of p21 and p27, but this could be due to the fact that the respective proteins were more diluted in these samples than in the immunoprecipitates. Co-IPs revealed a significant co-isolation of Menin, p16, p21, p27 and p53 with WT Taspase1 and Taspase1^{T234V}, indicating a transient interaction of these proteins with Taspase1, whereas Rb1 could not be detected in the eluate fractions (Figure 3.1). Nevertheless, low amounts of p16, p21, p27 and p53 were also found in the GFP control approach indicating unspecific binding (Figure 3.1).

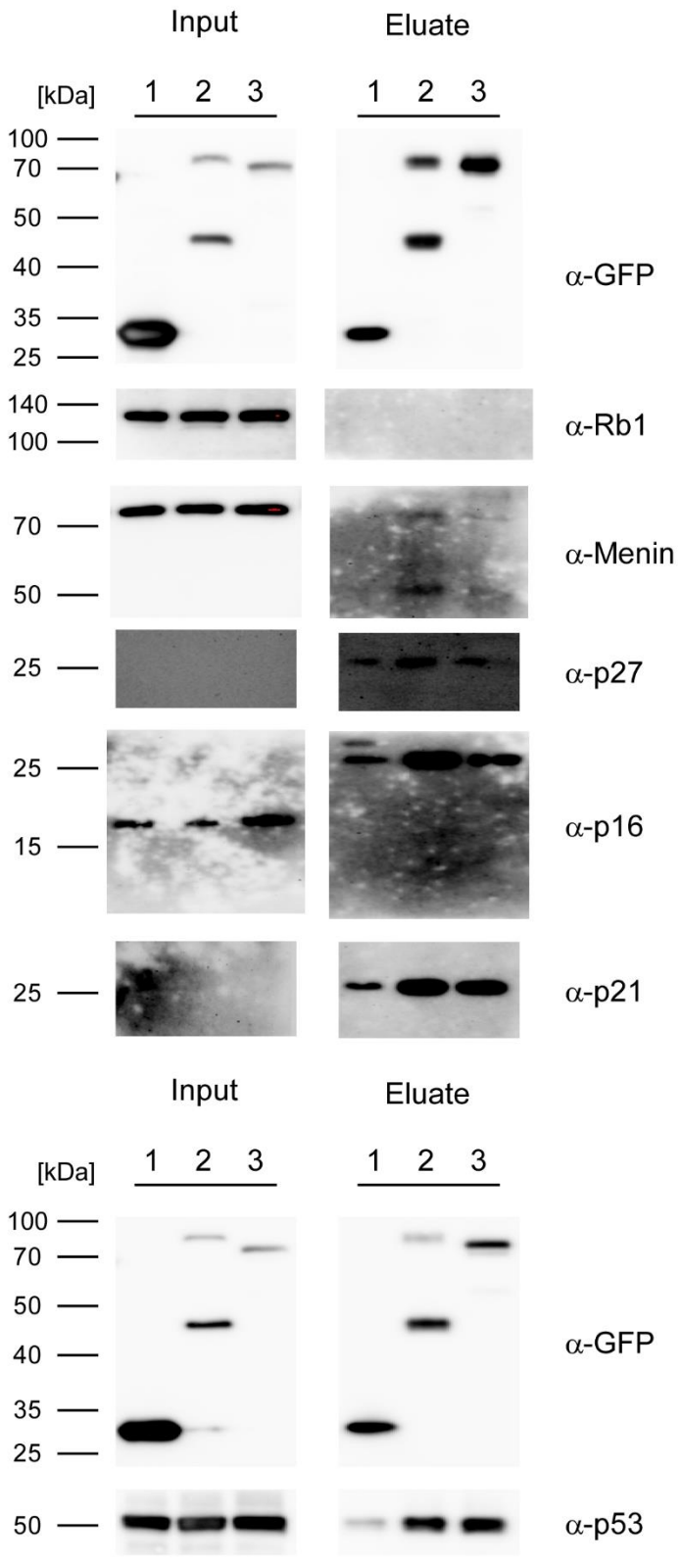

Figure 3.1: Taspase1 interacts with cell cycle proteins that are known as tumor suppressors. 293T cells were transiently transfected with the indicated GFP fusion constructs. The respective cell lysates were incubated with anti-GFP antibody-coated magnetic beads. Lysates (Input) and immunoprecipitates (Eluate) were analyzed for the presence of co-precipitated endogenous interaction partners via SDS-PAGE and Western blotting. Representative immunoblots are shown.

To verify those results, the co-IPs were repeated in an inversed manner by immunoprecipitation of plasmid-encoded, GFP-fused p16, p21, p27 and p53 proteins that were either present in the Knauer group or were successfully cloned using PCR (2.2.1.1). The respective precipitates from 293T cell lysates were analyzed for the presence of co-precipitated, ectopically expressed Taspase1-HA or Taspase1^{T234V}-HA. Uncleaved Taspase1 (WT and mutant) could be co-isolated in significant amounts with p16-, p21- and p53-GFP, but not in the GFP control approach (Figure 3.2) reinforcing the evidence that p16, p21 and p53 are interaction partners of Taspase1. The HA-tagged β-subunit of Taspase1 was not detected in the eluates, meaning that either these interactions are restricted to uncleaved Taspase1 or that the interactions are mediated by Taspase1´s α-subunit, which is not recognized by the used HA antibody.

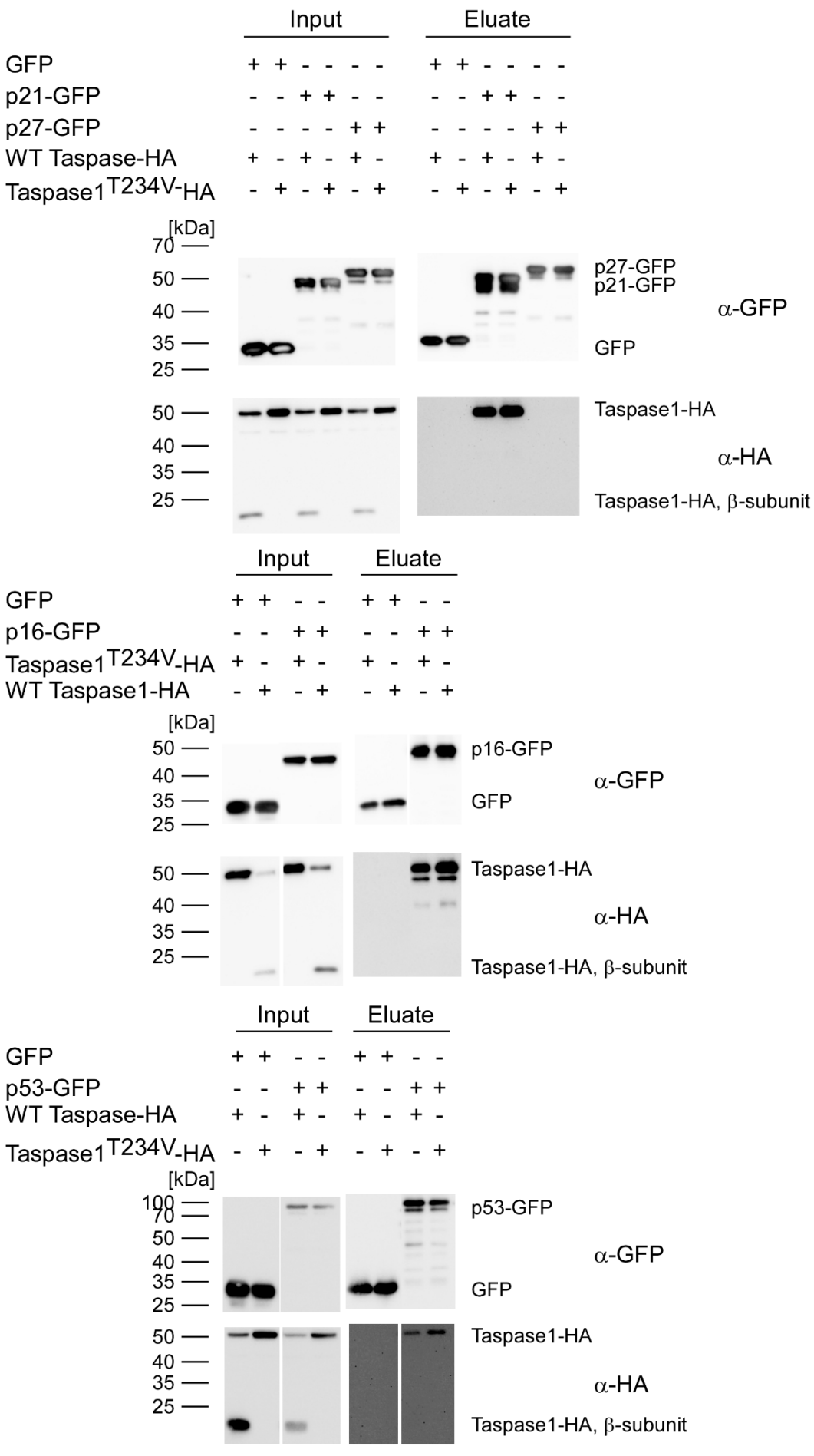
Input
Eluate
GFP + + - - - - + + - - - -
p21-GFP - - + + - - - - + + - -
p27-GFP - - - - + + - - - - + +
WT Taspase-HA + - + - + - + - + - + -
Taspase1T234V-HA - + - + - + - + - + - +
[kDa]
70
50
40
35
25
p27-GFP
p21-GFP
α-GFP
GFP
50
40
35
25
Taspase1-HA
α-HA
Taspase1-HA, β-subunit
Input
Eluate
GFP + + - - + + - -
p16-GFP - - + + - - + +
Taspase1T234V-HA + - + - + - + -
WT Taspase1-HA - + - + - + - +
[kDa]
50
40
35
25
p16-GFP
α-GFP
GFP
50
40
35
25
Taspase1-HA
α-HA
Taspase1-HA, β-subunit
Input
Eluate
GFP + + - - + + - -
p53-GFP - - + + - - + +
WT Taspase-HA + - + - + - + -
Taspase1T234V-HA - + - + - + - +
[kDa]
100
70
50
40
35
25
p53-GFP
α-GFP
GFP
50
40
35
25
Taspase1-HA
α-HA
Taspase1-HA, β-subunit

Figure 3.2: The reciprocal co-IP confirms the tumor suppressor proteins p16, p21 and p53 as interaction partners of Taspase1.

293T cells were transiently transfected with the indicated GFP fusion constructs and additionally with wild type Taspase1-HA or Taspase1^{T234V}-HA. The respective cell lysates were incubated with anti-GFP antibody-coated magnetic beads. Lysates (Input) and immunoprecipitates (Eluate) were analyzed for the association of co-expressed wild type (WT) or catalytic inactive (Taspase1^{T234V}) Taspase1-HA via SDS-PAGE and Western blotting. Representative immunoblots are shown.

A further assumption was the potential involvement of Taspase1 in transcriptional elongation, which takes place after RNA polymerase II (pol II) pausing near promoters. Indications for this guess were the participation of MLL and MLL fusion proteins in this process of RNA pol II pause release and transcription elongation (Milne *et al.*, 2005a; Mueller *et al.*, 2009; Basu *et al.*, 2020). Therefore, the following key players in transcriptional elongation of RNA pol II-dependent genes were investigated as potential interaction partners of Taspase1: MED4 (mediator complex subunit 4) (Myers and Kornberg, 2000), AF9 (ALL1-fused gene from chromosome 9 protein) (Strissel *et al.*, 2000), CDK9 (cyclin-dependent kinase 9) (Cojocaru *et al.*, 2011), transcription elongation factor SPT5 (Yamaguchi *et al.*, 1999) or POL2RA (DNA-directed RNA polymerase II subunit RPB1) and its paused form (Liu *et al.*, 2015), which displays an enrichment of phosphorylation at Serine 5 (S5P).

All input samples of GFP, WT Taspase1-GFP and Taspase1^{T234V}-GFP allowed the detection of proteins investigated. Analysis of Taspase1 (WT and mutant) complexes displayed a co-isolation of AF9, POLR2A, POLR2A S5P and SPT5, but not CDK9 (Figure 3.3). POLR2A and POLR2A S5P were also detected in low amounts in the GFP control approach (Figure 3.3), indicating a nonspecific binding to matrix surface or GFP antibody. However, the MED4, AF9 and SPT5 detected bands of the input samples are not fully consistent with the bands of the immunoprecipitates (Figure 3.3). Additionally, it must be taken into account that the immunoprecipitated SPT5 shows several bands, which do not correspond to the size of the detected lysate bands. Normally, the antibody against SPT5 recognizes a band at 160 kDa, but the predicted molecular weight of SPT5 is around 120 kDa. The detected bands between these sizes are probably degradation products of a post-translationally modified SPT5 species as post-translational modifications are known for this protein. Nevertheless, small amounts of SPT5 could be detected in Taspase1-GFP isolated complexes, which indicate an interaction between these proteins (Figure 3.3).

AF9 could be detected in immunoprecipitates of WT Taspase1 and Taspase1^{T234V}, but the associated AF9 forms have different molecular weights (Figure 3.3). Whereas the identified band of approx. 50 kDa in the eluate sample of WT Taspase1 complexes corresponds to the lower, less pronounced AF9-antibody signals in the input samples, the detected signal appeared at a higher molecular weight of ca. 70 kDa in case of the isolated Taspase1^{T234V}complexes, presumably depicting the unprocessed AF9, which has a predicted molecular weight of 63 kDa. It can be assumed that the 50 kDa band represents an AF9 degradation product and it is a notable finding that WT Taspase1 associates significantly with this shortened AF9 version but not with the full-length protein, which instead is co-precipitated with the Taspase1 cleavage-inactive mutant. But in this case, no distinct conclusion was possible as the eluate of GFP control also shows the presence of full-length AF9.

MED4, which was co-isolated with Taspase1^{T234V}, displayed with 70 kDa a much higher molecular weight than the detected MED4-antibody signal at approx. 50 kDa in the input samples. MED4 has a calculated molecular weight of approx. 30 kDa, but is commonly observed at around 36 kDa. Therefore, the higher migrating forms of MED4 presumably represent different post-translational modified variants. An interesting observation is that none of the described MED4-species could be found associated with WT Taspase1-GFP, once again indicating differences in the complexes of wild type and cleavage deficient Taspase1.

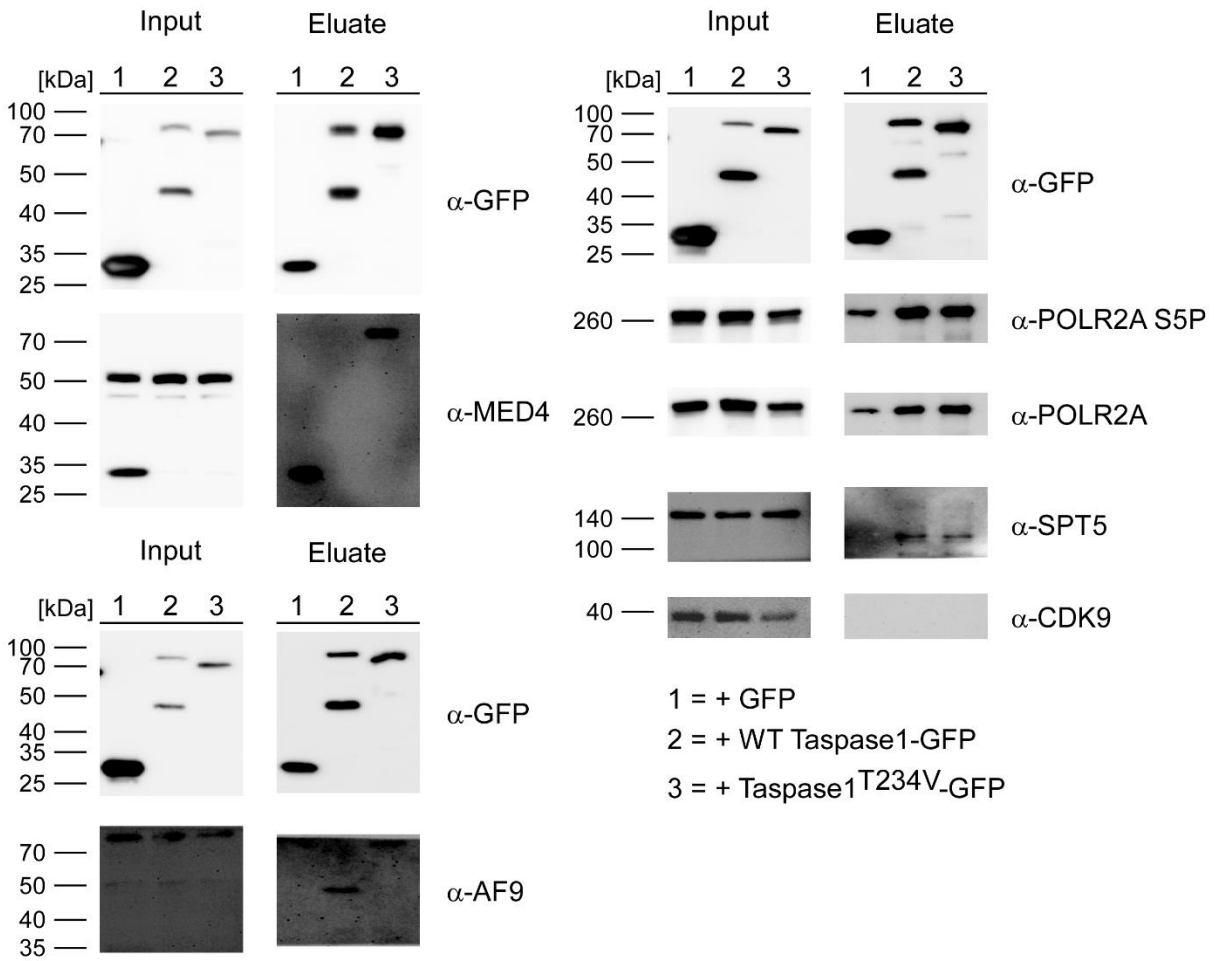

Figure 3.3: Taspase1 interacts with different proteins that are involved in transcriptional elongation.

293T cells were transiently transfected with the indicated GFP fusion constructs. The respective cell lysates were incubated with anti-GFP antibody-coated magnetic beads. Lysates (Input) and immunoprecipitates (Eluate) were analyzed for the presence of co-precipitated endogenous interaction partners via SDS-PAGE and Western blotting. Representative immunoblots are shown.

The cloning of a GFP-tagged MED4 by PCR (2.2.1.1) enabled the performance of co-IPs in an inversed manner to monitor the possible interaction of MED4 with Tapase1 in more detail. The respective precipitates from 293T cell lysates expressing MED4-GFP were checked for the presence of co-precipitated, ectopically expressed WT Taspase1-HA or Taspase1^{T234V}-HA by SDS-PAGE (2.2.3.4) and Western blotting (2.2.3.6).

The immunoblot-analysis showed that Taspase1-HA (WT and mutant) could be detected in the isolated MED4-GFP complexes, but not in the control approach with GFP alone (Figure 3.4). The amount of co-isolated WT Taspase1-HA was significantly enriched compared to the cleavage-inactive Taspase1. In addition, no HA-tagged

β-subunit of Taspase1 could be detected suggesting that this interaction is due to a binding particularly with the α-subunit of Taspase1.

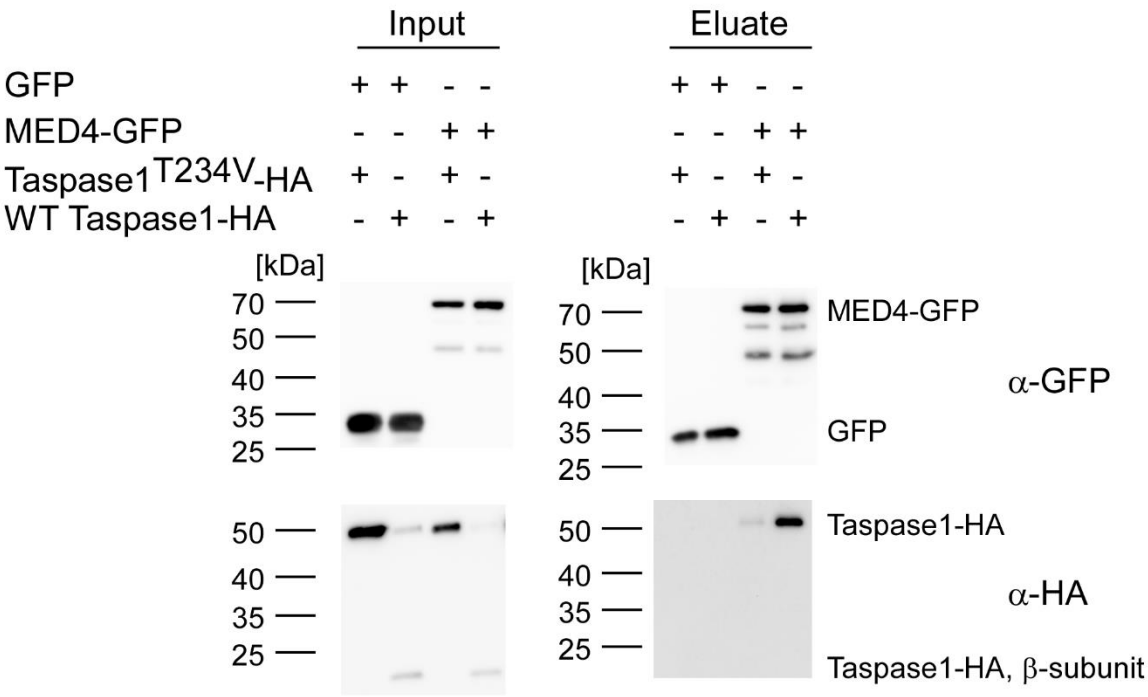

Figure 3.4: The reciprocal co-IP confirms MED4 as an interaction partner of Taspase1.
293T cells were transiently transfected with the indicated GFP fusion constructs and additionally with wild type Taspase1-HA or Taspase1T234V-HA. The respective cell lysates were incubated with anti-GFP antibody-coated magnetic beads. Lysates (Input) and immunoprecipitates (Eluate) were analyzed for the association of co-expressed wild type (WT) or catalytic inactive (Taspase1T234V) Taspase1-HA via SDS-PAGE and Western blotting. Representative immunoblots are shown.

Taspase1's most prominent targets, the MLL proteins (Hsieh et al 2003), are known to be involved in estrogen-mediated regulation of estrogen (E2) responsive genes (Dreijerink *et al.*, 2006; Ansari *et al.*, 2009; Ansari *et al.*, 2011). Interestingly, the Taspase1 targets TFIIA and USF2 were recently discovered to be transcribed in an estrogen-responsive manner (The UniProt Consortium, 2021). In addition, the proven interaction partner NPM1 is upregulated after E2 induction in specific cancer cells (Skaar *et al.*, 1998; Zhu *et al.*, 2006; Chao *et al.*, 2013; Zhou *et al.*, 2014) and is also known as a component of the co-repressor complex located at estrogen-dependent gene promotors in the uninduced state (Ju *et al.*, 2006; Beneke, 2012). Further hints for a possible contribution of Taspase1 in the estrogen response are the recent identification of estrogen receptor (ER) α as an interaction partner of Taspase1 through a screening (The UniProt Consortium, 2021) and the fact that estrogen triggers G1/S phase transition (Doisneau-Sixou *et al.*, 2003; Yang *et al.*, 2007), in which

Taspase1 is also involved (Takeda *et al.*, 2006). Therefore, Taspase1 complexes were investigated with respect to co-isolated proteins that participate in the estrogen response and hormone-driven DNA double-strand breaks (DSBs) like ERα, ERβ, MLL, NPM1, Nucleolin, Topoisomerase (Topo) II α, Topo II β and phosphorylated histone H2AX (γH2AX) as an indicator of DSBs (Ju *et al.*, 2006).

The lysates of GFP, WT Taspase1-GFP and Taspase1^{T234V}-GFP contained all examined proteins (Figure 3.5). Input samples that detected ERα, ERβ, Nucleolin and Topo II α+β showed several bands of the respective proteins, which were present in all samples. Compared to the GFP control, the proteins ERα, ERβ, NPM1, Nucleolin, Topo II α+β and γH2AX were only detected in co-isolated complexes of Taspase1-GFP (WT and mutant) highlighting the specific interaction between Taspase1 and the previously mentioned proteins (Figure 3.5). Just the MLL protein was additionally detected in the immunoprecipitates of the GFP control approach. However, MLL has already been identified and verified as an interactor and substrate of Taspase1, so the amounts of co-isolated MLL might vary due to certain conditions within the cell and also small amounts can bind non-specifically to the matrix surface or GFP antibodies. Moreover, eluate samples of isolated WT Taspase1-GFP- and Taspase1^{T234V}-GFP-complexes displayed several bands of the detected proteins ERα, ERβ, MLL, Nucleolin and Topo II α+β just like in the input samples, except for the input sample detecting MLL, which exhibited only one prominent band for MLL (Figure 3.5). These bands presumably represent degradation products or post-translationally modified proteins. The comparison of the co-isolated proteins of WT Taspase1-GFP and Taspase1^{T234V}-GFP indicates that the protein levels of MLL, NPM1 and Nucleolin are noticeably higher in WT Taspase1 complexes, whereas the amounts of ERα, ERβ, Topo II α+β and γH2AX are about the same (Figure 3.5). In sum, besides the known interaction partners MLL and NPM1, also Nucleolin, Topo II α+β, ERα, ERβ and γH2AX could be co-isolated in significant amounts with Taspase1 WT and the cleavage mutant, but not with the isolated sole GFP-tag (Figure 3.5).

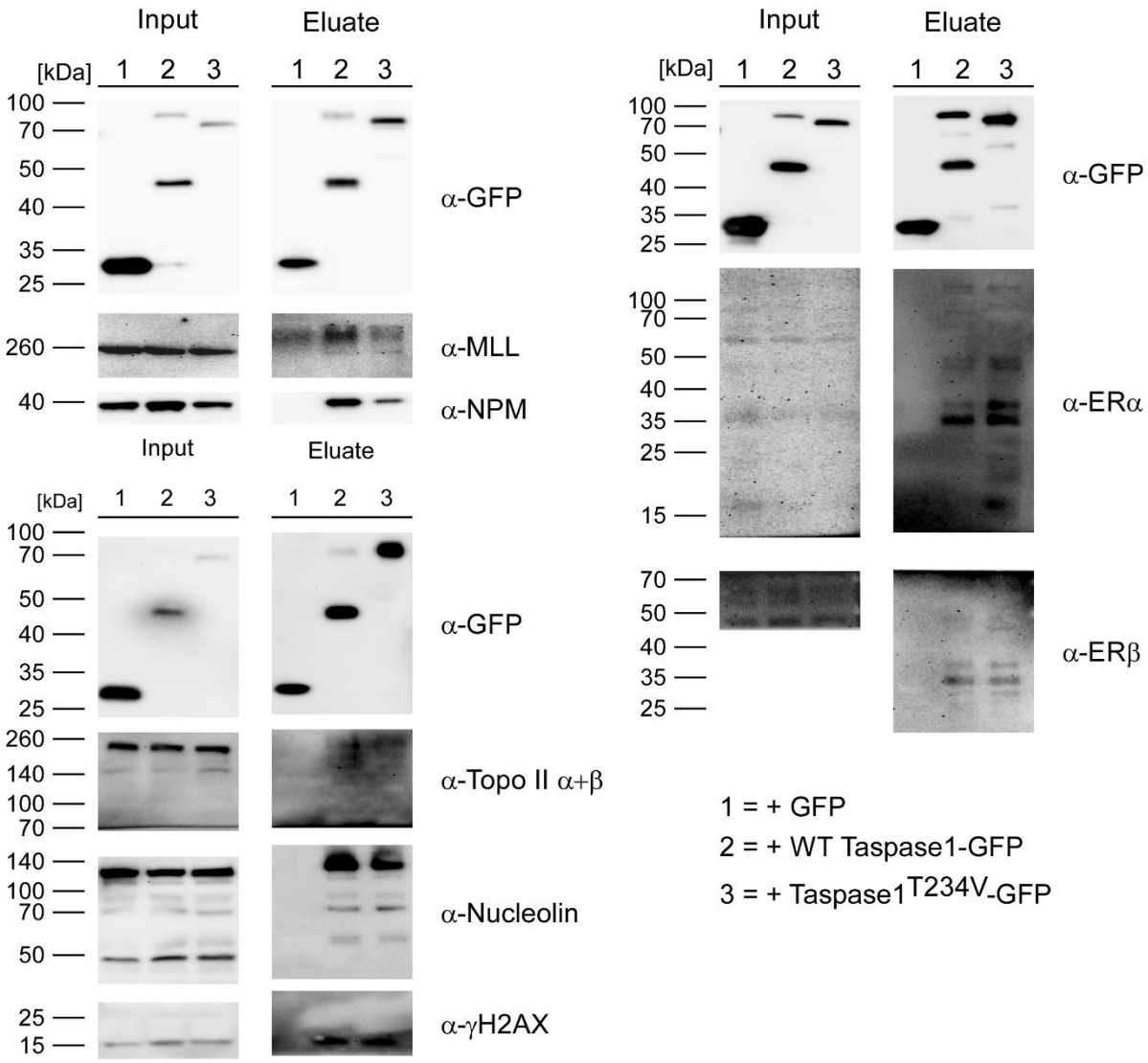

Figure 3.5: Taspase1 interacts with different proteins that are involved in the cellular estrogen response.

293T cells were transiently transfected with the indicated GFP fusion constructs. The respective cell lysates were incubated with anti-GFP antibody-coated magnetic beads. Lysates (Input) and immunoprecipitates (Eluate) were analyzed for the presence of co-precipitated endogenous interaction partners (via SDS-PAGE and Western blotting. Representative immunoblots are shown.

The reciprocal co-IP with Nucleolin-GFP and co-expressed Taspase1-HA showed that WT Taspase1- and Taspase1^{T234V}-HA were co-isolated in significant amounts with Nucleolin-GFP (Figure 3.6) suggesting that Nucleolin is an interaction partner of Taspase1. Besides the uncleaved Taspase1 proenzyme, also the HA-tagged β-subunit of Taspase1, which is recognized by the used HA antibody, was detected in the eluate, indicating an interaction of Nucleolin also with the activated Taspase1.

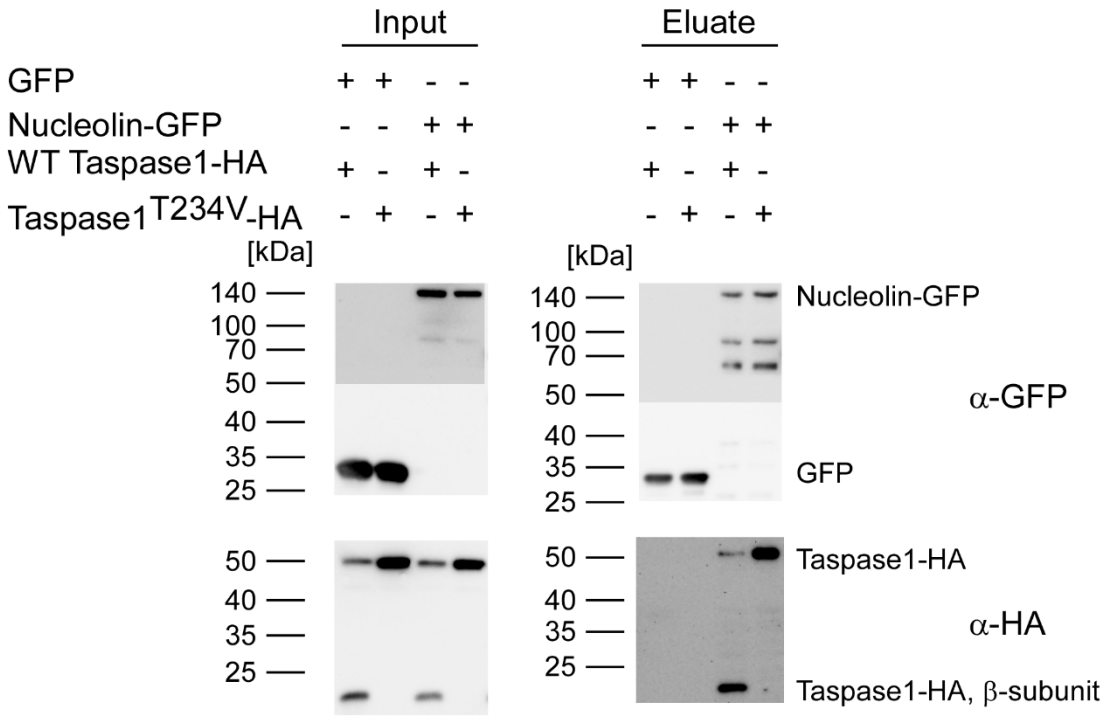

Figure 3.6: The reciprocal co-IP confirms Nucleolin as an interaction partner of Taspase1.
293T cells were transiently transfected with the indicated GFP fusion constructs and additionally with wild type Taspase1-HA or Taspase1^{T234V}-HA. The respective cell lysates were incubated with anti-GFP antibody-coated magnetic beads. Lysates (Input) and immunoprecipitates (Eluate) were analyzed for the association of co-expressed wild type (WT) or catalytic inactive (Taspase1^{T234V}) Taspase1-HA via SDS-PAGE and Western blotting. Representative immunoblots are shown.

To confirm the identified interaction partners and to reveal further associated proteins, isolated Taspase1 complexes (2.2.4.6) were analyzed by tandem mass spectrometry (MS) in cooperation with the Analytics Core Facility Essen (ACE) (University Duisburg-Essen).

MS-data analysis revealed that isolated Taspase1 complexes are composed of approximately 300 proteins (Table 6.1), e.g. general transcription factors required for RNA polymerase III-mediated transcription, diverse nucleolar proteins, mediator complex proteins of RNA pol II transcription and ribosomal proteins, which functions in various cellular processes. However, the MS analysis verified that NPM1, Nucleolin, Topo II α and Topo II β are part of the co-isolated Taspase1 complexes (Figure 3.7) indicating a link between Taspase1 and estrogen driven transcription.

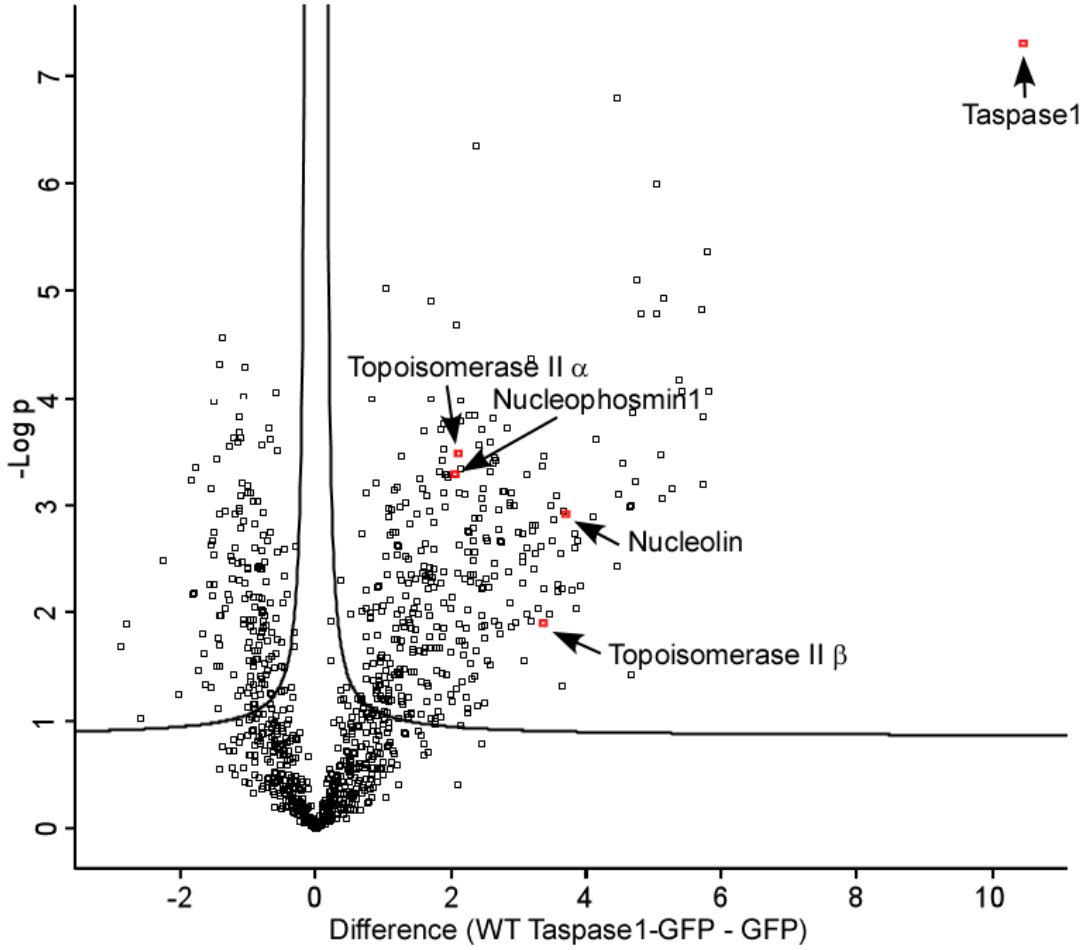

Figure 3.7: Volcano plot depicting protein enrichment in WT Taspase1-GFP complexes according to mass spectrometry analysis.

293T cells were transiently transfected with plasmids coding for WT Taspase1-GFP or GFP alone. Respective cell lysates were incubated with anti-GFP antibody-coated magnetic beads. Immunoprecipitates (eluates) were analyzed via mass spectrometry. The volcano plot shows the enrichment of identified proteins in the Taspase1-GFP eluate (x-axis, difference WT Taspase1-GFP – GFP) plotted against the -log p-value (y-axis), which is a measure for the reproducibility of respective protein enrichment. The relevant proteins are highlighted in red.

3.2 TASPASE1 AND THE ESTROGEN RESPONSE

A potential role of Taspase1 in estrogen driven transcription was initially indicated by the following findings: First, the Taspase1 substrates TFIIA and USF2 are estrogen-regulated genes (The UniProt Consortium, 2021), and MLL proteins are known to interact with estrogen receptors and coordinate estrogen-dependent gene regulation. (Dreijerink *et al.*, 2006; Ansari *et al.*, 2009; Ansari *et al.*, 2011). Second, NPM1, Nucleolin and Topo II β were identified as components of a co-repressor complex, which is present on promoters of estrogen-responsive genes but disappears there

rapidly after E2 treatment (Ju *et al.*, 2006; Beneke, 2012). The expression of the Taspase1 interactor NPM1 was also shown to be up-regulated by estrogen in specific cancer cells (Skaar *et al.*, 1998; Zhu *et al.*, 2006; Chao *et al.*, 2013; Zhou *et al.*, 2014). So far, the results of this thesis identified additional Taspase1 interactors such as Nucleolin and Topo II β that are key players in hormone-driven transcription.

To check if the expression of Taspase1 itself and of its newly identified interaction partners are estrogen-inducible, 293T as well as MCF-7 cells were treated with 50 nM E2 (2.2.4.3) for different time periods and the subsequently prepared cell lysates (2.2.4.5) were investigated with respect to changing protein expression levels after estradiol stimulus via SDS-PAGE (2.2.3.4) and Western blotting (2.2.3.6).

After estrogen stimulation, the expression pattern of Taspase1, Topo II α, Topo II β, ERα, histone H3 lysine 4 methylation (H3K4me), HoxA9 (a MLL target gene) and γH2AX displayed a cyclic upregulation and all of them reached a peak within 30 min in 293T cells (Figure 3.8 A) and within 40 min in MCF-7 cells (Figure 3.8 B). 293T cells, that represent a cell line with low amounts of Taspase1 in an uninduced state (Hsieh *et al.*, 2003a), Topo II α- and Topo II β-concentrations showed a first peak after 30 min and 20 min and a second peak after 120 min and 60 min, respectively. Interestingly, the expression profiles of Taspase1, γH2AX, HoxA9 and Cyclin E displayed also two peaks that are comparable to that of Topo II β, whereas the expression profile of ERα revealed only one prominent peak at 30 min in 293T cells. In MCF-7 cells, both Topo II isoforms were expressed in a similar pattern with two peaks after 40 min and 90 min following estrogen treatment. A comparable expression profile was detected for HoxA9, H3K4 methylation and γH2AX, while Cyclin E only showed one peak after 40 min estrogen exposure. Uninduced MCF-7 cells displayed a high expression level of Taspase1 (Coezy *et al.*, 1982), followed by a reduction and subsequently gained a peak after 30 min. Thereafter, the Taspase1 level decreased and increased again, so that a second maximum was reached after 180 min estrogen exposition. The expression level of ERα exhibited only one peak after 30 min estrogen stimulus.

Taken together, the immunoblot analysis of the time course showed cyclically elevated expression levels of Taspase1, Topo II α, Topo II β, ERα, H3K4 methylation, HoxA9 and γH2AX. The increased Taspase1 expression after estrogen treatment implies that Taspase1 itself is E2-inducible.

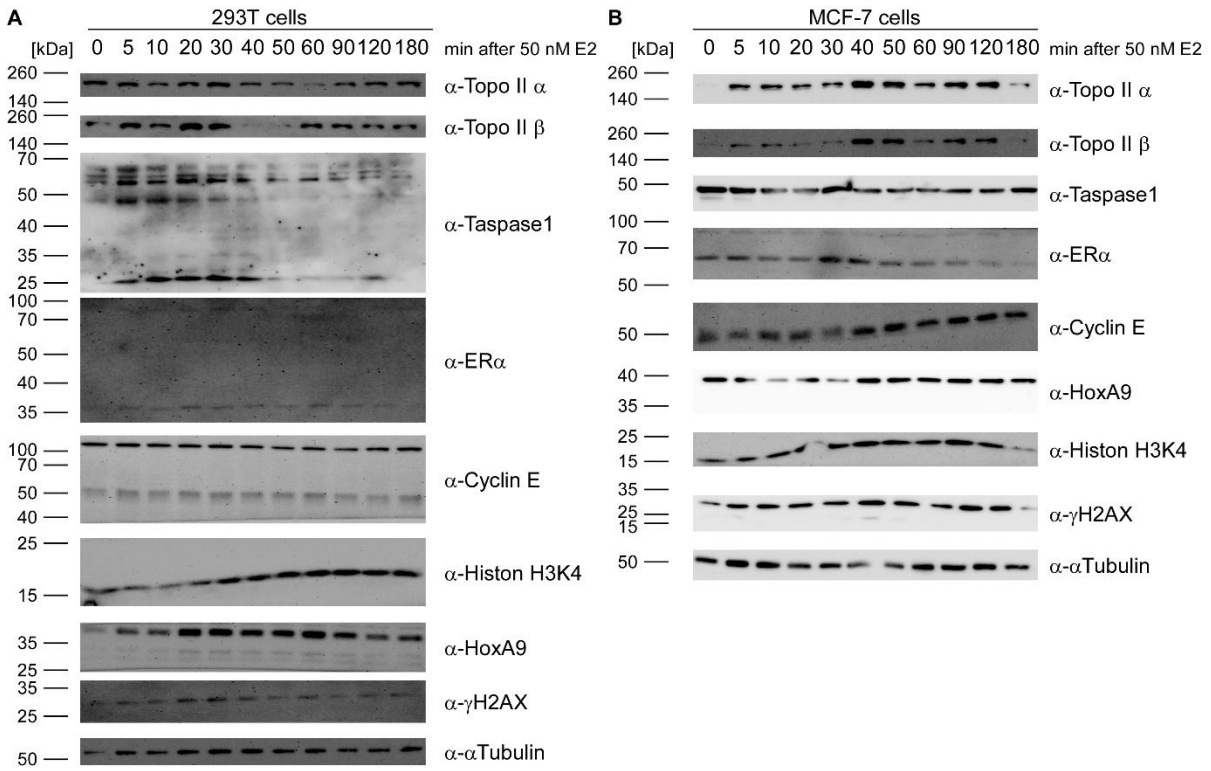

Figure 3.8: *TASP1* is an estrogen-responsive gene.

293T- (A) and MCF-7 (B) cells were treated with 50 nM E2 in hormone-free culture medium for distinct time periods. RIPA cell lysates were prepared and the samples of the time course were analyzed with respect to protein expression levels via SDS-PAGE and Western blotting. Representative immunoblots are shown.

In addition, ERα was identified as a Taspase1 interaction partner (The UniProt Consortium, 2021). The experimentally detected estrogen inducibility of the *TASP1* gene was complemented by the finding that the regulatory region of the *TASP1* gene contains an estrogen response element (ERE). This ERE was bioinformatically predicted with the software Ciiider (Gearing *et al.*, 2019), which uses the MATCH algorithm (Kel *et al.*, 2003) for the prediction of transcription binding sites. The SnapGene software was used by Paul Stahl to identify the location of an ERE 7.8 kbp upstream of the *TASP1* promotor (Figure 3.9). The sequence of this predicted ERE was proven to be high responsive to the activated estrogen-ER complex and seems to be a functional ERE (Klinge, 2001).

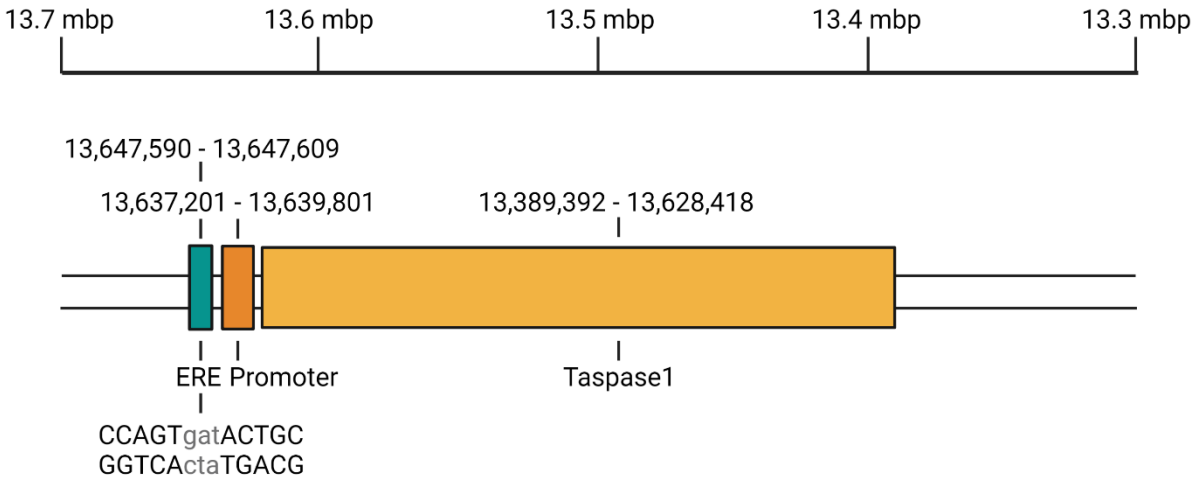

Figure 3.9: *TASP1* harbors a functional estrogen-responsive element.

Visual representation of the predicted estrogen-responsive element (ERE), which is located about 7.8 kbp upstream of the *TASP1* promoter. The MATCH algorithm (Kel *et al.*, 2003) in the Ciiider software (Gearing *et al.*, 2019) was used to predict the ERE within *TASP1* gene, which was identified by Paul Stahl using the SnapGene software.

It was speculated that *TASP1* is not simply an estrogen target gene but that Taspase1 has a direct function within the process that takes place at E2-responsive genes shortly after hormone exposure. To investigate this hypothesis changes in Taspase1 complex composition shortly after E2 incubation were analyzed. Therefore, co-IPs (2.2.4.6) from chromatin fractions of 293T cells (2.2.4.5) overexpressing GFP tagged proteins either treated with 50 nM E2 or mock-treated for 1 h were executed.

The analysis of chromatin-associated Taspase1-GFP (WT and cleavage mutant) as well as chromatin-associated NPM1-GFP complexes regarding co-isolated proteins displayed a massive increase of Taspase1-associated NPM1, Nucleolin, ERα, Topo II and γH2AX after one hour treatment with E2 compared to untreated immunoprecipitates (Figure 3.10). In addition, the GFP control approach showed no co-isolation of these proteins and therefore confirmed a specific interaction of Topo II, Nucleolin, NPM1, ERα and γH2AX with Taspase1 and NPM1 at chromatin level (Figure 3.10). The changing amounts of the respective complex components upon hormone stimulus indicate that the observed Taspase1 interactions are not stable but transient protein-protein interactions. This strengthens the hypothesis of a direct involvement of Taspase1 in the transcriptional regulation of estrogen-induced genes.

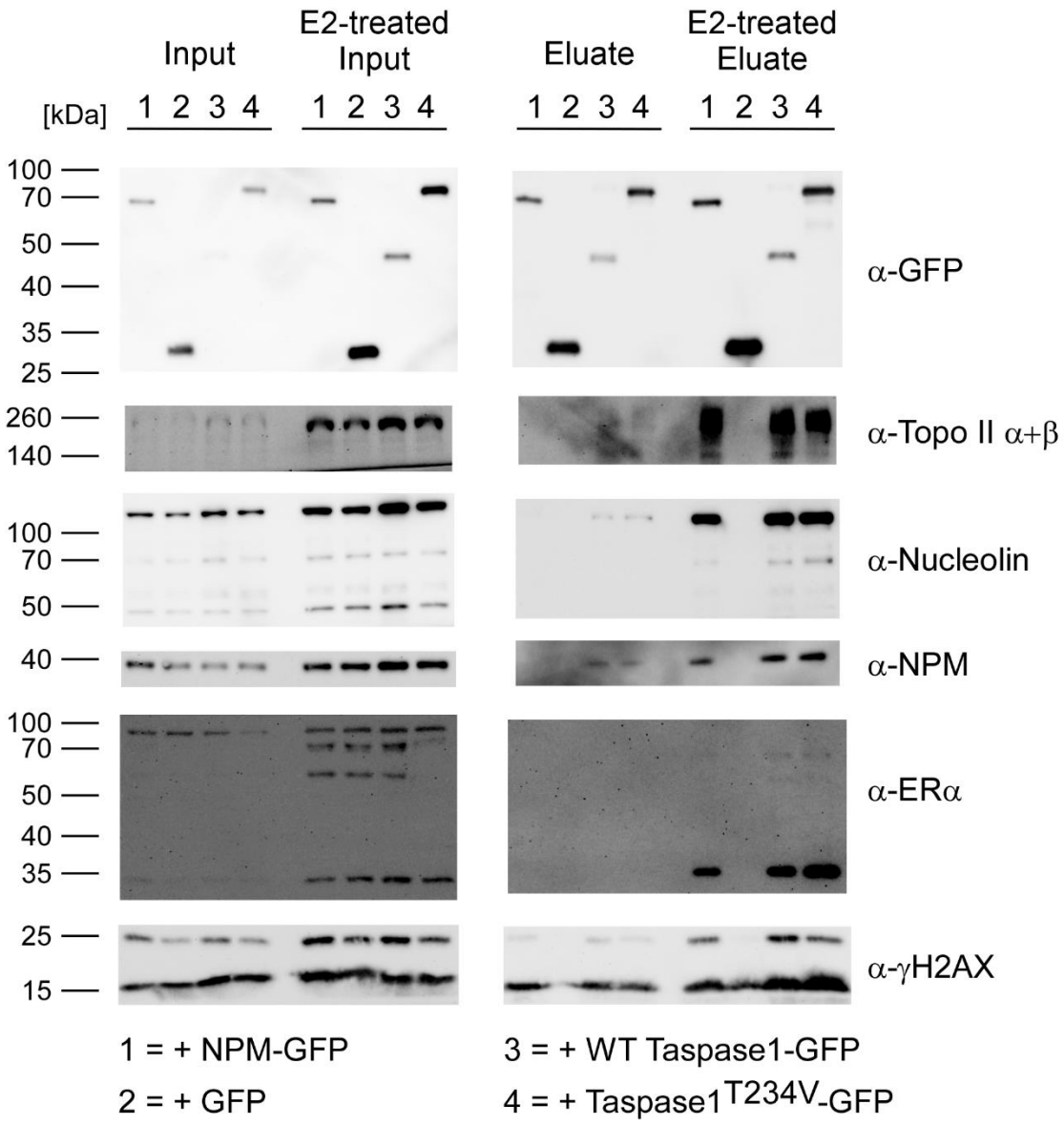

Figure 3.10: Taspase1 has a direct function within transcriptional activation of estrogen responsive genes.

293T cells were transiently transfected with indicated GFP fusion constructs and after 24 h either treated with 50 nM E2 or mock-treated for 1 h. Chromatin fractions were prepared and incubated with anti-GFP antibody-coated magnetic beads. Lysates (Input) and immunoprecipitates (Eluate) were analyzed via SDS-PAGE and Western blotting for the presence of co-precipitated endogenous interaction partners. Representative immunoblots are shown.

3.3 TOPOISOMERASE II – A NEW INTERACTION PARTNER OF TASPASE1

As Topo II was identified as an estrogen-dependent component of immunoprecipitated Taspase1-GFP complexes, the potential interplay between Taspase1 and Topo II was further analyzed. The identification of a simple Taspase1 cleavage site $Q^3X^2D^1/G^{1'}$ (Hsieh *et al.*, 2003b) within Topo II α sequence at aa ^{1249}QEDG^{1252} indicated that Topo II α might be a possible Taspase1 substrate. Cleavage would result in a N-terminal fragment with 1251 amino acids and a molecular mass of approximately 140 kDa and a C-terminal fragment comprising 280 amino acids and a molecular mass of about 30 kDa.

A potential cleavage of Topo II α was investigated by co-IPs with cell lysates of 293T cells co-expressing Topo II α-GFP and WT Taspase1-HA or the enzymatically inactive Taspase1^{T234V}-HA mutant (2.2.4.6). To prevent 26S-mediated proteasomal degradation of possible cleavage products, the cells were treated with 50 nM Bortezomib for 6 h beforehand. The known threonine protease inhibitor Bortezomib (Adams and Kauffman, 2004; Chen *et al.*, 2011) has no inhibitory influence on Taspase1 activity (Chen *et al.*, 2012). The immunoprecipitates were analyzed for the presence of potential Topo II α cleavage products and immunodetection with specific Topo II antibodies and the GFP antibody indeed revealed fragments that correspond to the calculated molecular weight of Topo II α full length, as well as to the predicted N- and C-terminal cleavage products (Figure 3.11). Regarding the treatment with Bortezomib or with the co-expression of WT Taspase1 or its cleavage-inactive variant, no differences could be determined. However, a difference was expected at least in case of the wild type Taspase1 co-expression compared to the approach with co-expression of the Taspase1^{T234V} mutant since the cleavage-inactive Taspase1 variant is not able to cleave its substrates. But as none of the lower molecular Topo II α signals disappear in the respective lane of immunoblot, it is not possible to assign the observed Topo II α degradation fragments to a proteolytic cleavage conducted specifically by Taspase1-His.

Moreover, a precise assignment of the bands to possible Topo II cleavage products is made more difficult due to two basic problems with the significance of this experiment. On the one hand, it is known that GFP degradation products, detected by GFP-antibody, can occur in co-IP experiments (Landgraf *et al.*, 2008; Bicknell *et al.*,

2010). On the other hand, the analysis of various antibodies, recognizing either both Topo II isoforms or specifically one of them, showed that the Topo II α+β-antibody as well as the isoform specific antibody Topo II β detected multiple bands in cell lysates with overexpressed Topo II α-GFP and Topo II β-GFP. However, the isoform specific antibody Topo II α only recognized two specific bands (Figure 3.12). Therefore, the results of the aforementioned co-IP are difficult to evaluate which is the reason why a different methodical approach was required.

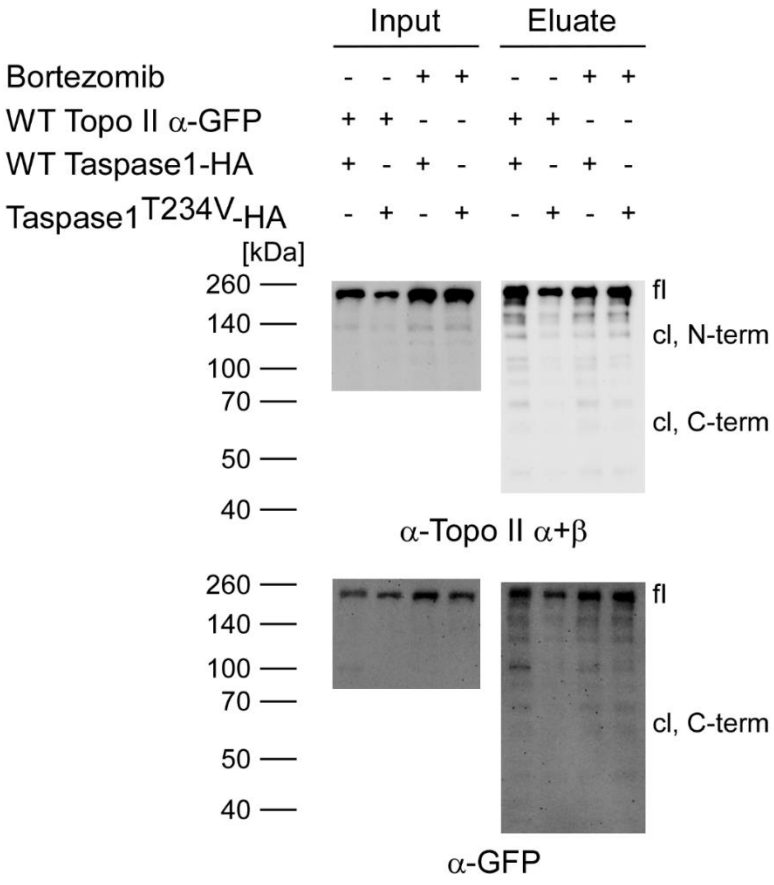

Figure 3.11: Topo II α is not cleaved by Taspase1 *in vivo*.

293T cells were transiently co-transfected with plasmids coding for Topoisomerase II α-GFP and WT Taspase1- or the enzymatically inactive mutant Taspase1^{T234V}-HA and after 18 h they were either treated with 50 nM Bortezomib or mock-treated for 6 h. Whole cell lysates were incubated with anti-GFP antibody-coated magnetic beads. Lysates (Input) and immunoprecipitates (Eluate) were analyzed via SDS-PAGE and Western blotting for the presence of potential cleavage products of Topo IIα. Representative immunoblots are shown. fl: full length; cl, C-term: C-terminal cleavage product; cl, N-term: N-terminal cleavage product.

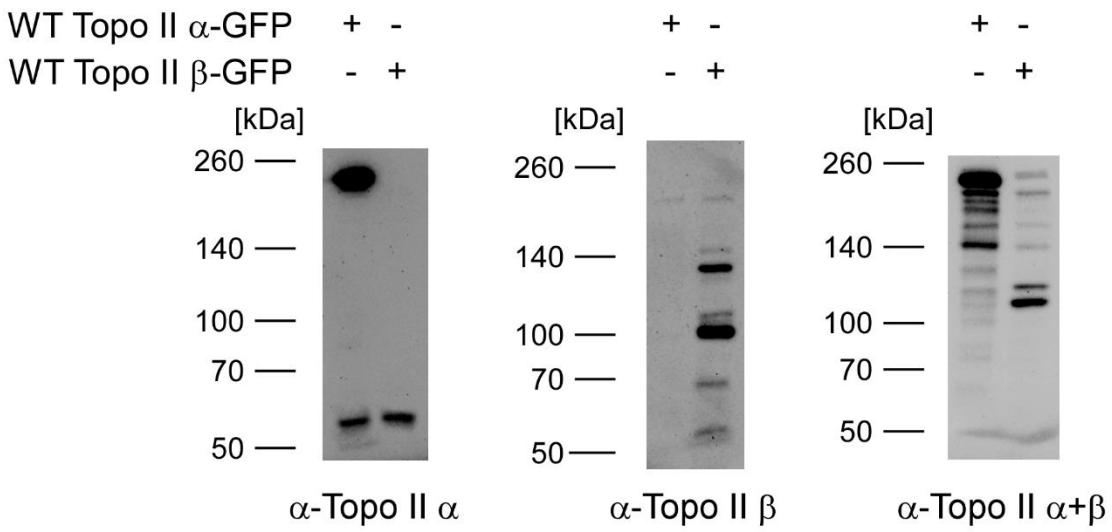

Figure 3.12: Immunoblot analysis of different antibodies directed against Topo II.
293T cells were transfected with plasmids coding for wild type Topo II α or Topo II β tagged with a GFP. After 24 h, RIPA cell lysates were prepared and analyzed via SDS-PAGE and Western blotting using specific antibodies against Topo II α, Topo II β or an antibody recognizing both isoforms Topo II α+β.

Since the co-IP did not permit any clear conclusion regarding a suspected Topo II α cleavage, the aspartic acid and the glycine (aa ^{1251}DG^{1252}) within the predicted Taspase1 cleavage site of Topo II α were mutated to alanine by site-directed mutagenesis (2.2.1.8) generating an uncleavable double mutant (Topo II α^{mut}). Then the semi *in vitro* Taspase1 substrate cleavage assay (abbreviated 'cleavage assay'), which was developed in this thesis to investigate the inhibitory effects of potential ligands on substrate cleavage by Taspase1 (Höing *et al.*, 2022), was adapted to verify new Taspase1 substrates (2.2.3.3). Therefore, lysates of 293T cells overexpressing WT Topo II α-GFP or Topo II α^{mut}-GFP were incubated with a protease-inhibitor-mix and recombinant Taspase1-His. Samples were taken after different time points and analyzed for the presence of possible Topo II α cleavage fragments. If Topo II α is a Taspase1 substrate, the addition of recombinant Taspase1-His is expected to increase substrate cleavage products over time compared to the samples without Taspase1.

The resulting immunoblot bands reflecting potential N- and C-terminal cleavage products were comparable in both approaches, regardless whether the cleavage assay was conducted with WT Topo II α or its uncleavable mutant Topo II α^{mut} (Figure 3.13). As clearly no Taspase1-dependent Topo II α-GFP degradation products were detectable in case of the potentially cleavable Topo II α, it seems that Topo II α is not cleaved by Taspase1 and thus, Topo II α could not be classified as a new Taspase1

substrate. Nevertheless, it cannot be completely excluded that under specific circumstances, other than in the performed cleavage assay, Topo II α might be processed by Taspase1.

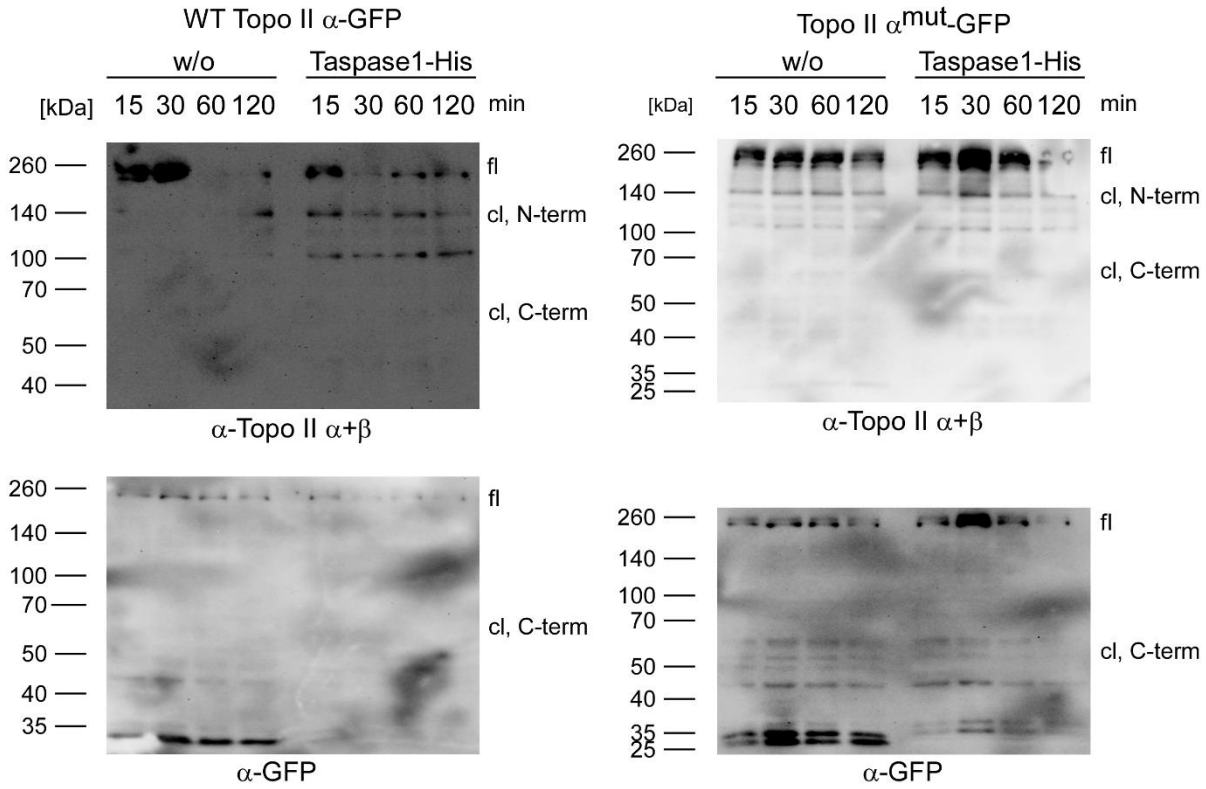

Figure 3.13: A semi *in vitro* Taspase1 substrate cleavage assay could not verify Topo II α as a Taspase1 substrate.

293T cells were transiently transfected with plasmids encoding WT Topo II α-GFP and Topo II α^{mut}-GFP. After 24 h, whole cell lysates were prepared and incubated with proteasome-inhibitor mix (Abcam) and 13 µM recombinant Taspase1-His at 37 °C, 300 rpm for indicated time points. The samples were subsequently analyzed via SDS-PAGE and Western blotting for the presence of possible Topo II α cleavage products. The antibody signals that fit to the calculated molecular weights of the full length Topo II α-GFP (fl) and its putative Taspase1 cleavage products (cl, N-term and cl, C-term) are indicated. Representative immunoblots are shown.

Since Topo II α could not be identified as a new Taspase1 substrate, but as a significant estrogen-dependent component of Taspase1-GFP complexes, the interaction of Taspase1 and Topo II was further investigated with localization studies As 293T cells usually do not express high Taspase1 levels, WT Taspase1-GFP was overexpressed in 293T cells as well as in HeLa cells. Afterwards, the cells were fixed, immunostained (2.2.4.8) and microscopically analyzed (2.2.4.7). Both proteins, Taspase1 and Topo II, are expected to localize within the nucleus and show

accumulation in the nucleoli (Heck *et al.*, 1988; Austin and Marsh, 1998; Bakshi *et al.*, 2001; Christensen *et al.*, 2002; Wang, 2002; Bier *et al.*, 2011a; Pommier *et al.*, 2016).

Localization studies in 293T cells via fluorescence microscopy demonstrated that ectopically expressed Taspase1-GFP localizes predominantly to the nucleus with an accumulation at the nucleoli (Figure 3.14, top row). Using immunostaining with a specific antibody, Topo II α+β was also detected in the nucleus, but not within the nucleoli (Figure 3.14, middle row). 293T cells that were both, transfected with a Taspase1-GFP encoding plasmid and immunostained for Topo II α+β, exhibited a partial nuclear co-localization of Taspase1 and Topo II α+β (Figure 3.14, bottom row).

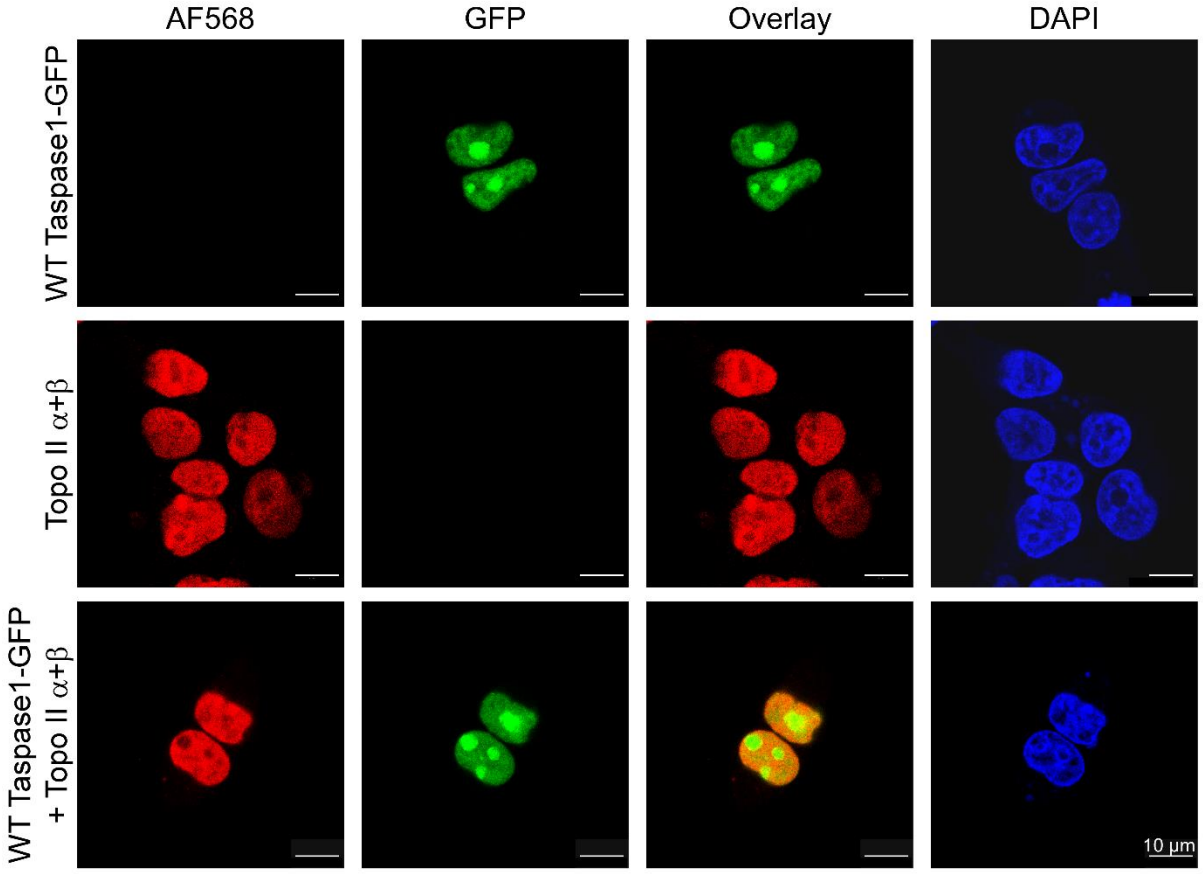

Figure 3.14: Taspase1 and Topo II partially co-localize at the nucleus in 293T cells.
293T cells overexpressing WT Taspase1-GFP or untransfected cells were fixed and an immunofluorescence staining with a Topo II α+β antibody, a secondary goat anti-rabbit IgG-AF568 antibody and DAPI was performed. Cells were microscopically analyzed with the laser scanning microscope SP8X Falcon from Leica Microsystems. Taspase1-GFP is shown in green, Topo II α+β in red and DNA in blue. Representative images are shown. Scale bar: 10 µM.

A nuclear and nucleolar localization in HeLa cells was shown for both, cells overexpressing Taspase1-GFP (Figure 3.15, top row) and cells immunostained for

endogenous Topo II α+β (Figure 3.15, middle row). Simultaneously transfected and immunostained HeLa cells exhibited a co-localization of Taspase1 and Topo II α+β in the nucleus and the nucleoli (Figure 3.15, bottom row).

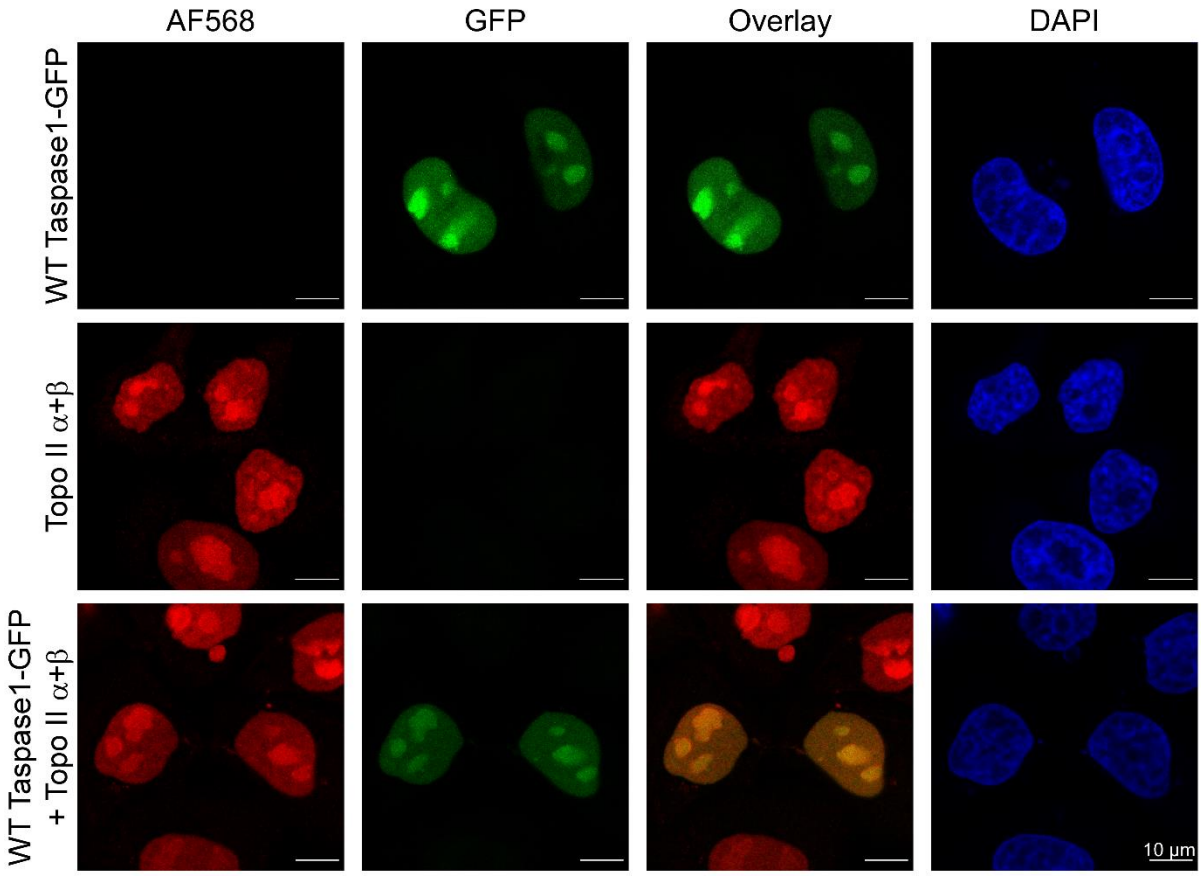

Figure 3.15: Taspase1 and Topo II co-localize at the nucleus and nucleoli in HeLa cells.
HeLa cells overexpressing WT Taspase1-GFP or untransfected cells were fixed and an immunofluorescence staining with a Topo II α+β antibody, a secondary goat anti-rabbit IgG-AF568 antibody and DAPI was performed. Cells were microscopically analyzed with the laser scanning microscope SP8X Falcon from Leica Microsystems. Taspase1-GFP is shown in green, Topo II α+β in red and DNA in blue. Representative images are shown. Scale bar: 10 µM.

Proximity ligation assays (PLAs) were performed (2.2.4.9) to examine whether the interaction of Taspase1 and Topo II α+β is possibly direct on an endogenous level or mediated by other proteins. Here, fixed HeLa cells were incubated over night with primary antibodies against both Taspase1 and Topo II α+β. Afterwards an incubation with the PLA probe MINUS and PLUS, followed by a ligation and an amplification took place. Negative controls were carried out by incubating the cells with only one primary antibody, but with both PLA probes. Only when the PLA probes are in close proximity (< 40 nm), a distinct fluorescent spot becomes visible, which can be captured by

fluorescence microscopy (2.2.4.7). For quantification, the cell image analysis software Cell Profiler was used with a pipeline provided from Imaging Center Campus Essen (ICCE) (University Duisburg-Essen), which counts all PLA foci within the nucleus and cytoplasm.

The negative control incubated with a specific antibody directed against Taspase1 showed only low level of background signals (median of about two PLA foci per nucleus) in contrast to the negative control of Topo II α+β, which demonstrated higher background signals (median of round about nine PLA foci per nucleus) (Figure 3.16 A and B). The higher rate of unspecific binding might be due to an excessively high concentration of the primary antibody leading to non-specific signals. Nevertheless, with a median of about 45 foci in the interaction sample (Taspase1 + Topo II α+β), a significant increase of PLA foci was revealed compared to the control samples (Figure 3.16 A and B.), indicating a presumable direct protein-protein interaction of Taspase1 and Topo II α+β.

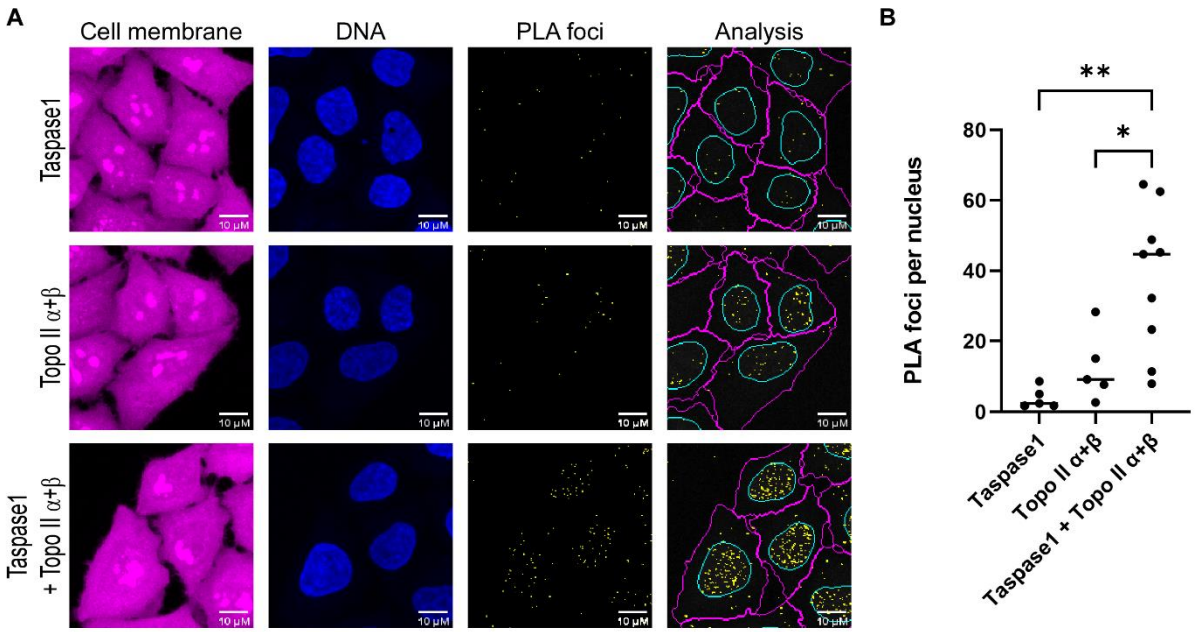

Figure 3.16: The Taspase1-Topo II α/β interaction is presumably a direct protein-protein interaction.

(A) HeLa cells were seeded and fixed after 24 h. An overnight incubation with primary antibodies against both Taspase1 and Topo II α+β or control approaches with only one of the respective antibodies, was subsequently followed by an incubation with both PLA probes, MINUS and PLUS. Afterwards, a ligation as well as an amplification step were performed and the cells were microscopically analyzed with the laser scanning microscope SP8X Falcon from Leica Microsystems. Whole cells were stained with HCS CellMask Deep Red (illustrated in magenta), DNA was stained with Hoechst (represented in blue) and

PLA foci are depicted in yellow. The analysis of PLA foci was performed with the cell image analysis software Cell Profiler 4.1.3. Representative images are shown. Scale bar: 10 µM. (B) A quantitative analysis of five independently performed PLAs was applied. The graph shows the number of PLA foci per nucleus and the indicated median. Each dot represents an individual PLA sample, for which at least 150 cells were counted. The data were analyzed by one-way ANOVA (analysis of variance). One asterisk (*) indicates a $p < 0.05$ and two asterisks (**) indicate a $p < 0.01$.

3.4 TASPASE1 AND TOPOISOMERASE II INTERPLAY

After Topo II has now demonstrated to be a probable direct interaction partner of Taspase1, a molecular insight in the Taspase1-Topo II interplay was required. Since Topo II β plays a critical role in hormone-induced DNA double strand breaks (DSBs) at hormone-regulated promotors (Ju *et al.*, 2006), Taspase1 function within this context was examined *in vivo*. Consequently, 293T cells expressing one of the two Topo II isoforms alone or in combination with WT Taspase1-HA, as well as a GFP control approach were either treated with 50 nM Etoposide or mock-treated for 1 h. Thereafter, cell lysates were prepared (2.2.4.5) and investigated with respect to resulting DNA DSBs via SDS-PAGE (2.2.3.4) and Western blotting (2.2.3.6). If Taspase1 has an influence on the formation of DNA DSBs, there should be an increase in the amount of the DSB indicator γH2AX in those samples, where Taspase1 and Topo II are overexpressed in combination. This experiment was performed by Dr. Astrid Hensel. The Topo II inhibitor Etoposide causes permanent DNA DSBs by arresting Topo II within the enzyme-DNA intermediate upon DNA cleavage (Fortune and Osheroff, 2000; Baldwin and Osheroff, 2005; Deweese and Osheroff, 2009; Vann *et al.*, 2021). Hence, a change in resulting DNA DSBs is expected compared to the controls.

As expected, the lowest amount of DNA DSBs was found in the GFP control (Figure 3.17). Elevated γH2AX signals could be observed in the cells with WT Taspase1-HA, Topo II α-GFP or Topo II β-GFP overexpression (Figure 3.17). The increase of DSBs was most evident in the lysate samples of cells co-expressing WT Taspase1-HA and Topo II-GFP, especially the isoform Topo II β (Figure 3.17). The Etoposide-treated samples revealed the same trend, albeit to an even more pronounced degree, since the DNA DSBs cannot be repaired resulting in general higher levels of γH2AX, especially in presence of Topo II β together with WT Taspase1-HA (Figure 3.17). These results implicate that the presence of Taspase1 enhances the formation of Topo II β-mediated DNA DSBs, which are

essential for estrogen-responsive gene transcription (Ju *et al.*, 2006). Thus, a functional role in estrogen-inducible transcription can be assigned to Taspase1.

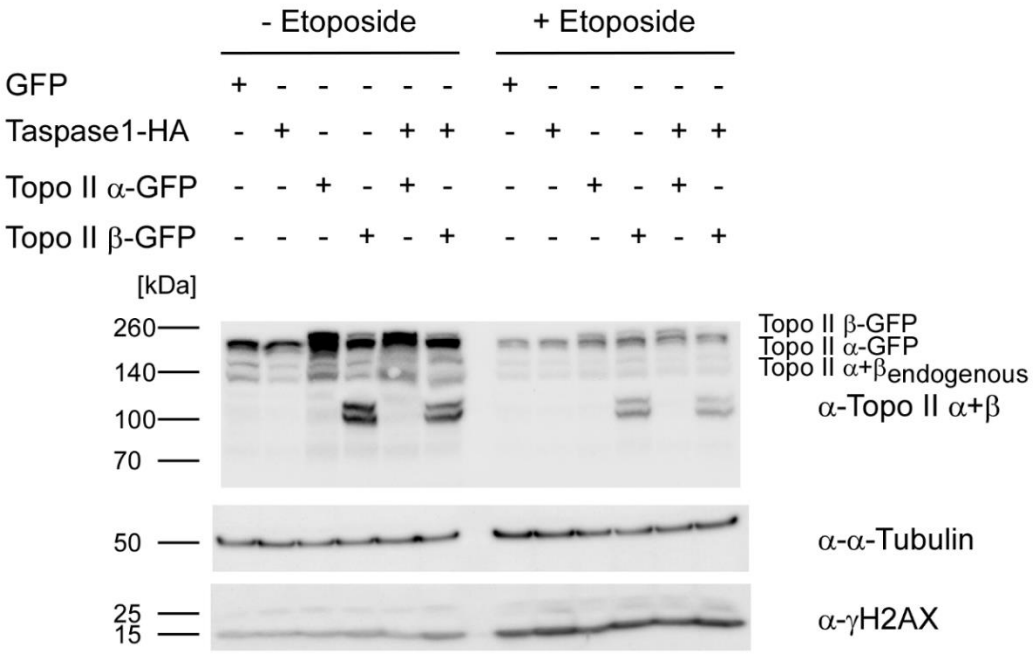

Figure 3.17 Taspase1 promotes formation of DNA double strand breaks mediated by Topo II β. 293T cells were transiently transfected with GFP, Topo II α-GFP, Topo II β-GFP or WT Taspase1-HA alone or co-transfected with WT Taspase1-HA and each Topo II isoform in combination. After the treatment with 50 nM Etoposide for 1 h, whole cell lysates were prepared, analyzed by SDS-PAGE and Western blotting and evaluated with regard to occurring DNA double strand breaks represented by γH2AX. This experiment was performed by Dr. Astrid Hensel. A representative immunoblot is shown.

To subsequently clarify whether the influence of Taspase1 on Topo II β-mediated DNA DSBs is direct or indirect, a Topo II β DNA cleavage assay (2.2.1.10) was performed. Here, the plasmid pBR322 was incubated with Topo II β and increasing concentrations of recombinant Taspase1-His. The samples were analyzed by agarose gel electrophoresis (2.2.1.2). The activity of Topo II β generates a linear (DSB occurred) or open circle (oc, single strand break occurred) form of the supercoiled (sc) plasmid.

The Topo II β DNA cleavage assay showed that pBR322 occurs primarily in its supercoiled (sc) form (Figure 3.18, Lane 2), which is partially linearized in the presence of 4 Units Topo II β (Figure 3.18, Lane 3). It could be observed, that with rising concentrations of recombinant Taspase1-His, the level of pBR322´s sc form decreases whereas the amount of linearized forms as well the oc form increase (Figure 3.18, Lane 4 – 8). This leads to the conclusion that Taspase1 directly facilitates Topo II β-mediated DNA DSBs.

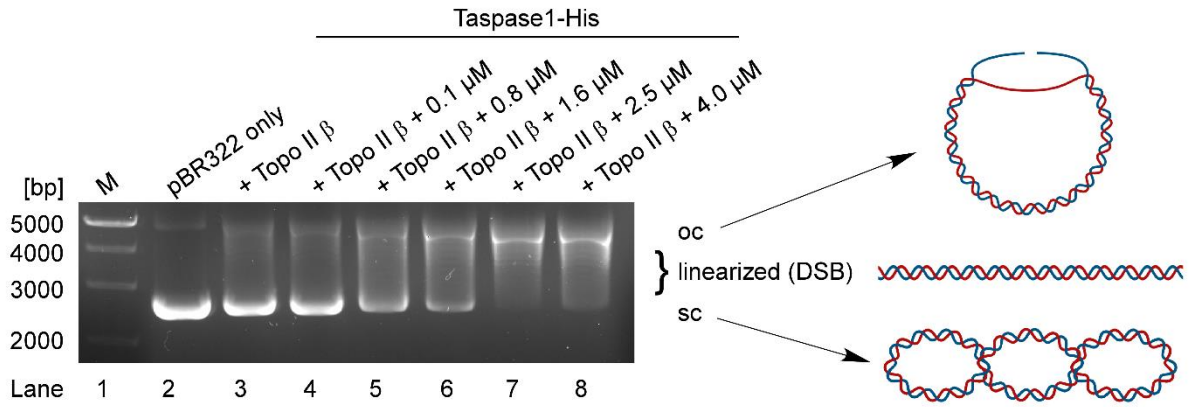

Figure 3.18: Taspase1 significantly enhances Topo II β-mediated DNA double strand breaks in a dose-dependent manner.

A Topo II β DNA cleavage assay was performed by incubating 1 µg of the plasmid pBR322 with 4 units recombinant Topo II β and increasing concentrations of recombinant Taspase1-His for 20 min at 37 °C and 300 rpm. After stopping the reaction and digesting the proteins with proteinase K, the samples were analyzed with an agarose gel electrophoresis. A representative image is shown. oc: open circle; sc: supercoiled; M: Marker.

As previously demonstrated, Taspase1 participates in Topo II β-mediated estrogen-regulated transcription. The results described above suggest that Taspase1 contributes through a direct enhancement of Topo II β activity to this process. A mechanistic explanation how Taspase1 facilitates Topo II β-mediated DNA DSBs might be a direct binding of DNA by the protease. Thus, electrophoretic mobility shift assays (EMSAs) were performed with pBR322 and different concentrations of recombinant Taspase1-His (2.2.1.3) and the collected samples were investigated by agarose gel electrophoresis (2.2.1.2). When Taspase1 is indeed capable of binding DNA, pBR322 should move slower due to the resulting protein-DNA complex, as the electrophoretic mobility of such a complex is typically lower than that of pBR322 alone.

Indeed, the EMSA revealed a gradual shift of supercoiled pBR322 with increasing concentrations of recombinant Taspase1-His (Figure 3.19, Lane 3 – 7) and reached a maximal shift of Taspase1-pBR322 complexes with a Taspase1-His concentration of 2.5 µM (Figure 3.19, Lane 7). Higher concentrations of Taspase1-His did not result in a further reduced mobility of pBR322 (Figure 3.19, Lane 8 – 9), indicating a saturation of plasmid DNA with bound Taspase1-His. The slower electrophoretic mobility of the plasmid pBR322 upon addition of recombinant Taspase1-His indicates a complex formation of Taspase1 and pBR322 and leads to the conclusion that Taspase1 is able to bind DNA.

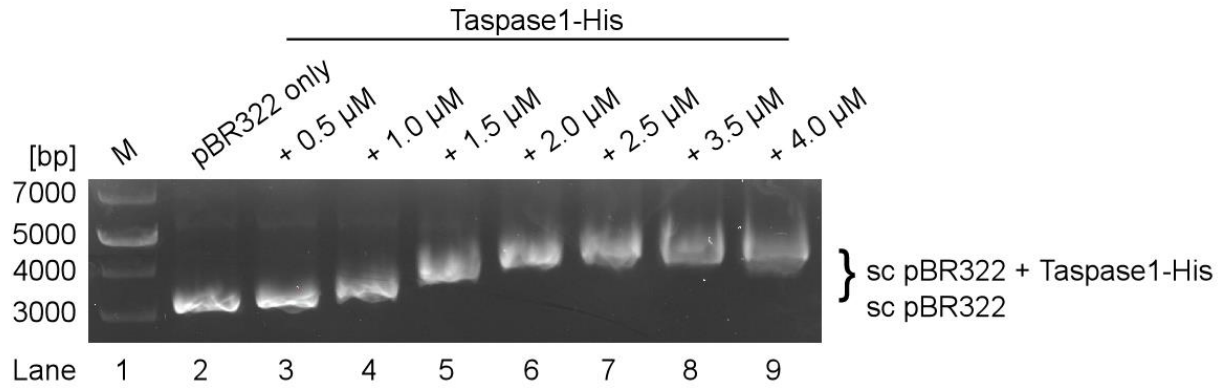

Figure 3.19: Taspase1 is a DNA binding protein.

An electrophoretic mobility shift assay was performed. Therefore 0.5 µg pBR322 was incubated with different concentrations of recombinant Taspase1-His for 15 min at 37 °C and 300 rpm and afterwards samples were analyzed by agarose gel electrophoresis. A representative image is shown. M: Marker; sc: supercoiled.

The results described above propose a crucial role for Taspase1 in Topo II β-mediated transcriptional activation of estrogen-responsive genes. To validate this, Taspase1-depletion studies were performed. 293T cells were transfected with siRNA (small interfering RNA) for 24 h and 48 h (2.2.4.4) to silence Taspase1 expression. In a parallel approach, control siRNA with a nonsense sequence was used. To assess if the intensity of cellular estrogen response is modulated by Taspase1 depletion, the expression of c-myc and c-fos, two genes that are experimentally proven to be up-regulated by estrogen (van der Burg *et al.*, 1989; Szijan *et al.*, 1992; Doisneau-Sixou *et al.*, 2003; Vendrell *et al.*, 2004), was determined. Following RIPA-lysis (2.2.4.5), the expression levels of the aforementioned estrogen-regulated genes were investigated with SDS-PAGE (2.2.3.4) and Western blotting (2.2.3.6).

The Taspase1 expression level was successfully reduced upon treatment with *TASP1* siRNA compared to the control approach demonstrating the efficiency of the *TASP1* siRNA used. Indeed, the expression levels of c-myc and c-fos were reduced upon *TASP1* siRNA transfection compared to the approach with control siRNA (Figure 3.20). The immunoblot of c-myc revealed three different bands: one above 50 kDa, a second at 40 kDa and a band below 40 kDa. The band above 50 kDa was primarily considered, as this size reflects the theoretical molecular weight of c-myc. The diminution of c-myc was more evident 48 h after *TASP1* depletion compared to the 24 h sample (Figure 3.20). In addition, a decreased γH2AX concentration was observed upon *TASP1* siRNA transfection (Figure 3.20).

At least after 24 h, control siRNA treatment does not substantially influence Topo II β expression level as compared to the untreated cells, whereas *TASP1* siRNA treated 293T cells exhibited an increased expression level of Topo II β after 24 h (Figure 3.20). It must be taken into account that the loading control (α-Tubulin) revealed no equal protein loading between the samples, so that the expression levels of the various proteins can only be assessed with consideration of the loading control concentration. But in general, these observations also hint towards an essential role of Taspase1 in estrogen-driven transcription.

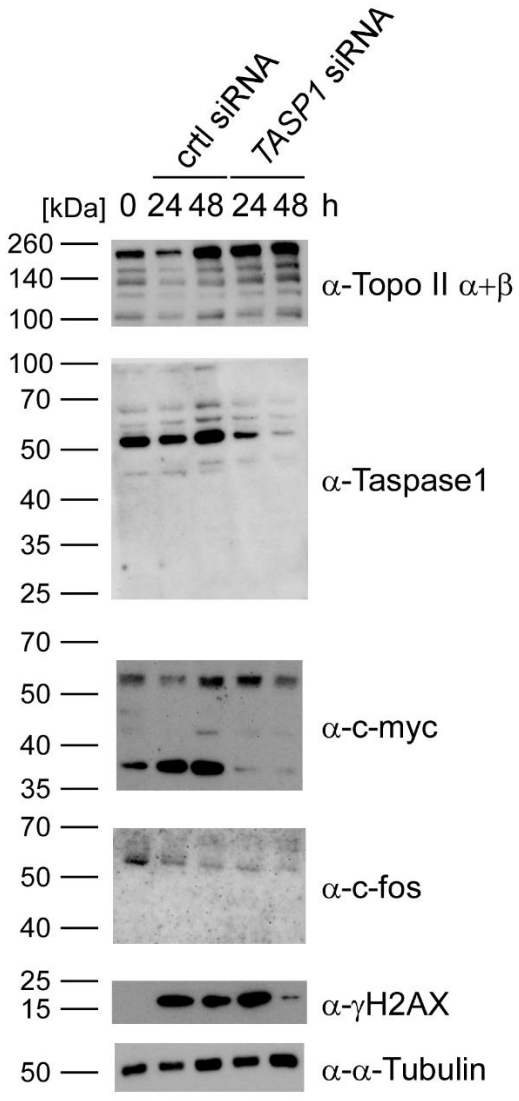

Figure 3.20: Taspase1 plays an essential role in estrogen-driven response.

293T cells were either left untreated, treated with *TASP1* siRNA or a nonsense sequence siRNA as control. RIPA cell lysates were prepared after 24 h and 48 h. The respective samples were analyzed with respect to protein expression levels of estrogen-responsive genes by using SDS-PAGE and Western blotting. Representative immunoblots are shown.

4 DISCUSSION

The human protease Taspase1 (Threonine aspartase 1) plays a critical role in leukemia and solid tumors of different origins including breast, colon, head and neck cancer or glioblastoma (Takeda *et al.*, 2006; Chen *et al.*, 2010; Bier *et al.*, 2011a; Bier *et al.*, 2012a). The finding that mouse embryonic fibroblasts (MEFs) lacking Taspase1 are resistant to oncogenic transformation further underlines Taspase1´s role in tumorigenesis (Takeda *et al.*, 2006). In addition, a Taspase1 knockout results in a disrupted cell cycle and reduced proliferation as well as an increased apoptosis rate (Takeda *et al.*, 2006; Chen *et al.*, 2010; Dong *et al.*, 2014; Takeda *et al.*, 2015). Its fundamental function in development and differentiation has been attributed to its enzymatic activity of cleaving key regulators in *trans* (Hsieh *et al.*, 2003a), such as the proto-oncogene MLL (Mixed lineage leukemia) (Hsieh *et al.*, 2003b; Hsieh *et al.*, 2003a; Takeda *et al.*, 2006). Classified as a non-oncogene addiction protease, Taspase1 serves as a promising therapeutic target for cancer therapy (Chen *et al.*, 2010).

A bioinformatic screening had identified 27 potential Taspase1 substrates, but so far only a few have been verified including MLL (Hsieh *et al.*, 2003b; Hsieh *et al.*, 2003a; Takeda *et al.*, 2006), TFIIA (transcription factor IIA) (Zhou *et al.*, 2006), USF2 (upstream stimulatory factor 2) (Bier *et al.*, 2011b; Heiselmayer, 2018), Myosin1f (Hensel *et al.*, 2022), ALF (TFIIA like factor) (Høiby *et al.*, 2004) and REV3L (Protein reversionless 3-like) (Wang *et al.*, 2020). At the beginning of this project, protein-protein interactions of Taspase1 annotated in BioGRID protein databases (Oughtred *et al.*, 2021) were limited to MLL (Hsieh *et al.*, 2003b) and the amyloid precursor protein (APP) (Oláh *et al.*, 2011). However, those data are based on high-throughput approaches, rendering it difficult to detect all functionally relevant protein-protein interactions as with these methods in particular context-dependent, transient interactions are often overlooked. With this lack of knowledge on the entirety of the Taspase1 interactome, it has not yet been possible to assign Taspase1 to a superior signal pathway and to unravel its full range of functions.

Accordingly, this thesis focusses on the identification of new interaction partners of Taspase1 as the determination of a common cellular field of activity amongst the interactors may help to assess Taspase’1s superordinated role within the cell.

4.1 IDENTIFICATION OF NOVEL INTERACTION PARTNERS

Initially, the interaction of Taspase1 with potential binding partners was investigated at an endogenous level by analyzing the complex composition of immunoprecipitated Taspase1-GFP fusion proteins (wild type (WT) or catalytic inactive (Taspase1^{T234V})). The examined proteins in this systematic interaction partner screening were selected on the basis of previous knowledge about Taspase1. Co-IPs were also performed in a reverse manner with the potential interactor fused to a GFP-tag. Here, the isolated proteins were analyzed for the presence of co-expressed WT Taspase1-HA and Taspase1^{T234V}-HA. The constitution of immuno-precipitated Taspase1-GFP complexes was further explored by tandem mass spectrometry in cooperation with the Analytics Core Facility Essen (ACE) (University Duisburg-Essen) to confirm the previously executed co-IPs. An approach with cells expressing solely GFP served as a control (section 3.1).

4.1.1 TASPASE1 INTERACTS WITH CELL CYCLE PROTEINS THAT ARE KNOWN AS TUMOR SUPPRESSORS

Since Taspase1 fulfills a role in carcinogenesis and progression of cell cycle, different proteins that are involved in both processes were investigated (Figure 3.1 and Figure 3.2).

The tumor suppressors Menin, p16, p21, p27 and p53 were co-isolated with Taspase1-GFP in significant amounts compared to the GFP control approach revealing these proteins as potential interaction partners of Taspase1, whereas Rb1 was not a member of the Taspase1-complexes. Reciprocal immunoprecipitations with p16-, p21-, p27- and p53-GFP constructs and co-expressed WT Taspase1-HA as well as Taspase1^{T234V}-HA validated these tumor suppressor proteins as specific binding partners of Tapsase1. However, these results do not provide sufficient basis to determine if the identified interactions are direct protein-protein interactions or mediated by other proteins. Nevertheless, there are some indications that suggest an indirect interaction modus of Taspase1 with Menin, p16, p21, p27 and p53 which is mediated by the MLL protein.

Actually, the confirmed Taspase1 substrate and interaction partner MLL is known to interact with Menin (Hughes *et al.*, 2004; Yokoyama *et al.*, 2004; Milne *et al.*, 2005b;

Krivtsov and Armstrong, 2007), thereby regulating the expression of cyclin-dependent kinase inhibitors (CDKIs) like transcriptional activation of p27 expression (Milne *et al.*, 2005b) and HOX genes (Yokoyama *et al.*, 2004), processes in which Taspase1 is also involved (Ringrose and Paro, 2004; Xia *et al.*, 2005; Takeda *et al.*, 2006; Schuettengruber *et al.*, 2007; Kotake *et al.*, 2009). Besides, it is assumed that the MLL-Menin fusion protein, emerged from chromosomal translocation t(11;19)(q23;p13.1), interacts directly with the tumor suppressor protein and anti-oncogene p53, thereby suppressing its function to maintain leukemogenesis (Maki *et al.*, 1999). It was further shown, that some of the most abundant MLL fusion proteins repress the transcriptional activity of p53 and subsequently the induction of p21 (Wiederschain *et al.*, 2005). During the cell cycle p21 is known to be regulated by the transcription factor E2F (Hiyama *et al.*, 1998), which is involved in transcriptional regulation as a member of the MLL multi-protein complex (Yokoyama *et al.*, 2004; Takeda *et al.*, 2006). Taspase1´s connection to p16 could also be explained by Taspase1-mediated processing of MLL for regulating expression of both, cyclins and CDKIs like p16 (Takeda *et al.*, 2006). These findings and the additional evidence of a specific interaction between Taspase1 and Menin, p16, p21, p27 and p53 indicate that this protein-protein interaction could be indirectly mediated via the MLL protein or the MLL-Menin interplay under certain conditions within the cell.

4.1.2 TASPASE1 INTERACTS WITH DIFFERENT PROTEINS THAT ARE INVOLVED IN TRANSCRIPTIONAL ELONGATION

The confirmed Taspase1 substrates TFIIA (Zhou *et al.*, 2006) and the MLL proteins (Hsieh *et al.*, 2003b; Hsieh *et al.*, 2003a) are known to play major roles in transcriptional regulation and therefore Taspase1 has been assigned a fundamental role in modulating gene expression through substrate cleavage. Taking this into account, proteins, involved in the process of transcriptional elongation were investigated as possible interactors of Taspase1 (Figure 3.3 and Figure 3.4).

Indeed, the transcription elongation factor SPT5, AF9 (ALL1-fused gene from chromosome 9 protein), POL2RA (DNA-directed RNA polymerase II subunit RPB1) and its paused form that displays an enrichment of phosphorylation at Serine 5 (S5P) were co-isolated in significant higher amounts with Taspase1-GFP complexes than with the GFP control approach. However, small amounts of POLR2A and its paused

form were found in the GFP control, which indicate a non-specific binding to the matrix surface or GFP-antibody. The generation of a MED4-GFP construct and the conduction of the reciprocal co-IP with this construct and the HA-tagged Taspase1 variants, allowed the confirmation of an interaction between Taspase1 and MED4. This time, higher amounts of WT Taspase1-HA were co-isolated than Taspase1^{T234V}-HA. These results indicate a possible interaction between Taspase1 and AF9 as well as SPT5, but clearly demonstrate that MED4, POLR2A and its stalled form, POLR2A S5P, are binding partners of Taspase1. In the BioGRID protein databases (Oughtred *et al.*, 2021) is remarked that the Taspase1 target MLL interacts with both proteins, AF9 (Biswas *et al.*, 2011) and SPT5 (Youn *et al.*, 2018). In addition, AF9 is annotated to interact with APP (Oláh *et al.*, 2011), which is also an interactor of Taspase1. This provided further evidence for a possible indirect interaction of these proteins. The observed interactions of Taspase1 with MED4, POLR2A and its stalled form, lead to the suggestion that Taspase1 is more deeply involved in the process of transcriptional elongation, which takes place after pausing of RNA pol II near promoters of RNA pol II-dependent genes.

Thus, this newly discovered interactors of Taspase1, transcription factors and components of transcriptional elongation, at least show that Taspase1 is physically located at transcribed genes thereby reflecting that Taspase1 is involved in some way in the process of DNA transcription.

4.1.3 TASPASE1 INTERACTS WITH DIFFERENT PROTEINS THAT ARE INVOLVED IN ESTROGEN RESPONSE

Tapase1 seemed to be functionally associated with the cellular steroid hormone response pathway, especially facilitated by estrogen, since the Taspase1 targets TFIIA and USF2 are known as estrogen-responsive genes (The UniProt Consortium, 2021) and due to the fact that the most prominent Taspase1-target, the MLL proteins, participate in estrogen-mediated transcription of estrogen-dependent genes (Dreijerink *et al.*, 2006; Ansari *et al.*, 2009; Ansari *et al.*, 2011). Moreover, the previously known interaction partner NPM1 as well as the newly identified interactors Nucleolin and Topo II are components of a co-repressor complex, which is located at promotors of estrogen-responsive genes (Ju *et al.*, 2006; Beneke, 2012). NPM1 is also highly expressed in specific cancer cells after E2-stimulus (Skaar *et al.*, 1998; Zhu *et al.*,

2006; Chao *et al.*, 2013; Zhou *et al.*, 2014). Further indications of Tapase1´s involvement in the estrogen pathway are the newly discovered interaction partner estrogen receptor (ER) α (The UniProt Consortium, 2021) and the interesting connection that both Taspase1 and estrogen stimulation promote the G1/S phase transition (Takeda *et al.*, 2006; Yang *et al.*, 2007). In order to investigate a possible role of Taspase1 in estrogen-induced transcription, the presence of proteins involved in estrogen response and hormone-induced DNA double-strand breaks (DSBs) were analyzed in immunoprecipitated Taspase1 complexes (Figure 3.5 and Figure 3.6).

These experiments demonstrate that besides the known interaction partners MLL and NPM1, also Nucleolin, Topo II α+β, ERα, ERβ and γH2AX were co-isolated in significant amounts with Taspase1 (WT and cleavage inactive mutant), identifying these proteins as new binding partners of Taspase1. Moreover, the previously described interaction partner ERα (The UniProt Consortium, 2021) could be confirmed with this experiment. Immunoprecipitates of Nucleolin-GFP revealed a co-isolation of WT Taspase1-HA and Taspase1^{T234V}-HA confirming Nucleolin as a binding partner of both Taspase1 variants, WT and cleavage-inactive mutant. In summary, all investigated proteins from the estrogen signaling pathway were identified in the isolated Taspase1 complexes, leading to the conclusion that ERα, ERβ, MLL, NPM1, Nucleolin, Topo II α+β and γH2AX are interactors of Taspase1.

The mass spectrometric analysis in cooperation with ACE (University Duisburg-Essen) confirmed the aforementioned new Taspase1 interactors Topo II α, Topo II β, Nucleolin and NPM1 (Figure 3.7) and also revealed many further possible interaction partners (Table 6.1). The results of the MS analysis together with the co-IP clearly indicate a role of Taspase1 in the estrogen response, which was subsequently further investigated.

4.2 TASPASE1 AND THE ESTROGEN RESPONSE

As mentioned above, many indications pointed towards a connection between Taspase1 and the estrogen response, amongst others the newly discovered interaction of Taspase1 with ERα ((The UniProt Consortium, 2021) and Figure 3.5) and NPM1, Nucleolin and Topo II β (Figure 3.5 and Figure 3.7). This link should be explored in more detail.

4.2.1 *TASP1* IS AN ESTROGEN-RESPONSIVE GENE

To further analyze the diccovered connection between Taspase1 and estrogen-driven transcription (section 3.2), the expression patterns of Taspase1, its newly identified interaction partners including ERα, Topo II and γH2AX and other associated proteins like HoxA9 and H3K4 methylation were initially examined following an E2 treatment in 293T- and MCF-7 cells (Figure 3.8).

Taspase1 shows an estrogen-dependent expression profile as the protease is significantly upregulated after E2 stimulation, especially in 293T cells with low Taspase1 concentrations in the uninduced state. A comparable expression pattern was observed for HoxA9, H3K4 methylation and γH2AX. Both cell lines demonstrate a cyclic upregulation of the expression profiles of estrogen-involved proteins. The observation of cyclic upregulation is in line with observations that transcriptional activation via liganded ER binding is a cyclic process for some target genes: initially, the transcription rates of the target genes increase, then they are reduced and subsequently followed by a repeated upregulation of the transcription rate (Shang *et al.*, 2000). Additionally, the increase in DSBs, indicated by rising γH2AX concentrations, demonstrated an expression pattern that is comparable to the Topo II-, especially to the Topo II β expression profile. The rapid and parallel increase of those proteins after estrogen treatment could represent the event of hormone-induced transcriptional activation through Topo II β-mediated DSBs. Taspase1 expression is upregulated within the same time window, which indicates a contribution of Taspase1 within this process.

The aforementioned observations of an increased Taspase1 concentration after E2 treatment together with the bioinformatic identification of an estrogen response element (ERE) 7.8 kbp upstream of the *TASP1* transcription start site (Figure 3.9) proved that the *TASP1* gene is E2-inducible.

4.2.2 TASPASE1 HAS A DIRECT FUNCTION WITHIN TRANSCRIPTIONAL ACTIVATION OF ESTROGEN RESPONSIVE GENES

To assess if estrogen modulates the composition of Taspase1-GFP complexes, 293T cells were incubated with E2 or a mock treatment and a co-IP from corresponding chromatin fractions was performed. Interestingly, not only the Taspase1-GFP and

NPM1-GFP immunoprecipitates revealed a significant rise in Topo II-, Nucleolin-, NPM1-, ERα- and γH2AX-concentration after estrogen treatment, but also the input samples showed a distinct increase of the respective protein concentrations after estrogen stimulus compared to the untreated lysates and immunoprecipitates. This is consistent with the finding that many estrogen-induced proteins are rapidly enriched upon estrogen stimulus (Shang *et al.*, 2000). The increased presence of Topo II and γH2AX in chromatin-bound Taspase1 complexes shortly after estrogen exposure indicates that chromatin-bound Taspase1 is present at chromatin locations directly on-site, where Topo II β-mediated DNA cleavage occurs. This could mean that Taspase1 has already been located at promoters of estrogen inducible genes to where Topo II β is recruited after the estrogen-ER complex is bound.

Taken together, these experiments revealed that Taspase1 itself is regulated in an estrogen-dependent manner and is moreover directly associated with key players in the estrogen response. This strongly suggests that Taspase1 cleavage activity and potential further activities of Taspase1 contribute to the execution of this pathway.

4.3 TOPOISOMERASE II – A NEW INTERACTION PARTNER OF TASPASE1

The performed co-IPs revealed an interaction between Taspase1 and Topo II in an estrogen-dependent manner, thereby indicating that Taspase1 is directly involved in the estrogen response. But so far, no knowledge was provided about the exact type of interaction and its molecular relevance, therefore the interplay between Taspase1 and Topo II was further investigated (section 3.3).

4.3.1 TOPO II ALPHA AS A POSSIBLE TASPASE1 SUBSTRATE

First, it was examined whether Topo II is a possible substrate of Taspase1. This assumption was supported by the identification of a simple Taspase1 cleavage consensus site $Q^{3}X^{2}D^{1}/G^{1'}$ (Hsieh *et al.*, 2003b) within the Topo II α sequence at aa ^{1249}QEDG^{1252} and was investigated by co-IP experiments (Figure 3.11) and by a semi *in vitro* Taspase1 substrate cleavage assay using lysates containing Topo II α-GFP or a non-cleavable variant thereof (Topo II α^{mut}-GFP) and recombinant Taspase1-His (Figure 3.13). Both approaches did not allow to confirm a specific, Taspase1-dependent proteolytic processing of Topo II α-GFP. Nevertheless, it cannot

be excluded that certain conditions could cause a Taspase1-mediated Topo II α cleavage.

4.3.2 TASPASE1 AND TOPO II CO-LOCALIZE AT THE NUCLEUS IN 293T- AND HELA CELLS

To investigate the interaction between Taspase1 and Topo II in more detail, co-localization studies were performed in 293T- (Figure 3.14) and HeLa cells (Figure 3.15). Since 293T cells usually express only hardly detectable amounts of Taspase1, the cells were transfected with GFP-tagged WT Taspase1 and subsequently stained for endogenous Topo II. To ensure comparability, HeLa cells were treated analogously. In both 293T- and HeLa cells expressing WT Taspase1-GFP alone, Taspase1 was found to be localized in the nucleus with a nucleolar accumulation, which is consistent with previous knowledge of Taspase1 (Bier *et al.*, 2011a). Furthermore, a staining for endogenous Topo II showed that Topo II localizes in the nucleus, but only in HeLa cells a nucleolar localization of Topo II could be confirmed. Nevertheless, these results verified the previously described nuclear and nucleolar localization of Topo in HeLa cells (Heck *et al.*, 1988; Christensen *et al.*, 2002). In sum, the observed partial nuclear co-localization of Topo II and Taspase1 is a further indicator for a functional interaction of these proteins.

4.3.3 THE TASPASE1-TOPO II INTERACTION IS PRESUMABLY A DIRECT PROTEIN-PROTEIN INTERACTION

Due to the partial co-localization of Taspase1 and Topo II within the nucleus, the proven interaction of both proteins in co-IP experiments and the involvement of both proteins in the estrogen response, the question arose whether the binding of Taspase1 and Topo II is a direct protein-protein interaction on endogenous level. This question was clarified with PLA studies (Figure 3.16). For PLAs, HeLa cells were used instead of 293T cells, because this cell line expresses only hardly detectable amounts of Taspase1, while HeLa cells show higher level of endogenous Taspase1. Indeed, the PLA revealed a co-localization in close proximity (< 40 nm) between Taspase1 and Topo II indicating a direct physical interaction of Taspase1 and Topo II in HeLa cells.

The catalytically-irrelevant C-terminal domain (CTD) of Topo II α+β is not conserved between the two isoforms and determines the isoform-specific behaviour, whereas the

highly conserved Topo II core enzyme consists of ATPase- and DNA binding domains (Jenkins *et al.*, 1992; Austin *et al.*, 1993; Sng *et al.*, 1999). As the antibody used for Co-IPs and PLAs recognizes the Topo II core enzyme, it was not possible to assign the observed interaction specifically to one Topo II isoform, but it could be concluded that the Taspase1 binding interface is located within the conserved Topo II domain.

4.4 TASPASE1 AND TOPOISOMERASE II INTERPLAY

Since a presumably direct protein-protein interaction between Taspase1 and Topo has been demonstrated, the functional interplay of the proteins was examined in a cellular context (section 3.4).

4.4.1 TASPASE1 ENHANCES THE FORMATION OF DNA DOUBLE STRAND BREAKS MEDIATED BY TOPO II BETA

It is known that Topo II induces DNA DSBs in promoters of hormone-regulated genes (Ju *et al.*, 2006). Therefore, it was first investigated whether Taspase1 exerts an influence on DNA DSB formation through interaction with Topo II. The analysis of lysates generated from cells that either expressed Topo II α-GFP, Topo II β-GFP or Taspase1-HA alone or in combination with each other should provide information about the functional interrelationship of the proteins *in vivo* (Figure 3.17). In addition, the 293T cells were treated with Etoposide, a Topoisomerase II inhibitor that arrests Topo II-DNA cleavage intermediates and thereby generating permanent DSBs. The results of those *in vivo* experiments demonstrated that Taspase1 overexpression enhances Topo II-induced DNA DSBs and that this effect is even more pronounced by co-expression of Taspase1-HA and Topo II β-GFP. So, it could be concluded that Taspase1 has an influence on the formation of Topo II β-mediated DNA DSBs presumably through the newly discovered direct protein-protein interaction between Taspase1 and Topo II.

With Topo II β DNA cleavage assays, the effect of Taspase1 on the formation of DNA DSBs by Topo II β activity was further examined *in vitro* (Figure 3.18) and the results revealed that Taspase1 directly promotes Topo II β-mediated DNA DSBs. Topo II β activity generates DSBs in the supercoiled (sc) plasmid pBR322 converting it either to the linearized form (DSB) or to the open circle (oc) form. With increasing concentrations of recombinant Taspase1-His, the sc form of pBR322 was drastically

reduced and a rise of linearized pBR322 and oc from could be observed. Taken together, the results of the *in vitro* Topo II β cleavage assays showed that Taspase1 directly facilitates Topo II β-catalyzed DNA double-strand breaks by enhancing Topo II β activity.

Via the introduction of DNA DSBs, Topo II can solve topological barriers such as DNA supercoiling or DNA knots (Tsai-Pflugfelder *et al.*, 1988; Chung *et al.*, 1989; Osheroff *et al.*, 1991; Kellner *et al.*, 2000) allowing an open chromatin conformation. In contrast to the sporadic endogenous DNA damage, which can occur as a harmful byproduct of replication and transcription, such hormone-induced DNA DSBs in gene promoter regions are scheduled events, which are absolutely essential for the activation of certain transcriptional programs (Calderwood, 2016). In sum, the Topo II β mediated transient DNA DSBs permit an open chromatin conformation thereby enabling the transcription machinery to gain rapid access for the immediate synthesis of mRNA. The results obtained in this thesis demonstrate that Topo II β is supported by Taspase1 in the generation of such physiologically relevant, transient DNA DSBs that finally lead to transcriptional induction of E2-responsive genes.

4.4.2 TASPASE1 IS A DNA BINDING PROTEIN

Considering that Taspase1 directly enhances Topo II β-mediated DNA DSBs, the question arose how exactly Taspase1 triggers this effect. Eelectrophoretic mobility shift assays (EMSAs) were used to examine Taspase1´s ability to bind DNA (Figure 3.19). After increasing concentrations of recombinant Taspase1-His were added to the plasmid pBR322, a gradual mobility shift of pBR322 was observed. Even low concentrations of recombinant Taspase1-His were sufficient to cause a small mobility shift. The observed shift enlarges in a Taspase1 dose-dependent manner but concentrations higher than 2.5 µM had no further effects suggesting that the plasmid DNA was saturated with Taspase1 molecules. This result classifies Taspase1 as a DNA binding protein. However, Taspase1 is not known to possess a classical DNA binding domain, but contains a bipartite nuclear localization signal (NLS) (Bier *et al.*, 2011a). NLSs are known to be sometimes involved in DNA binding (LaCasse and Lefebvre, 1995; Cokol *et al.*, 2000), e.g. for several transcription factors such as MyoD or NF-κB, the NLS is an elementary part within the DNA binding domain (Henkel *et al.*, 1992; Vandromme *et al.*, 1995). As Taspase1 harbours a bipartite NLS, a DNA binding

via this cluster of basic residues seems possible, particularly because the bipartite NLS is located in the flexible, surface-exposed loop region of Taspase1 (Bier *et al.*, 2011a; van den Boom *et al.*, 2016). The DNA binding can be mediated either by the ionic interactions via the basic amino acids in the bipartite NLS and the negatively charged sugar-phosphate backbone of the DNA or through hydrogen bridge formation with the DNA bases. Therefore it is important to investigate the DNA-binding ability of the Taspase1 loop, which harbors the bipartite NLS, to verify that the DNA binding domain is located within this region.

So far, it could be assumed that Taspase1 recruits Topo II β to promoter regions destined for double-strand breakage triggered transcriptional activation upon E2-stimulus. ChIP-seq assays that combine chromatin immunoprecipitation (ChIP) with DNA sequencing (seq) are necessary to elucidate which conserved or functional DNA motifs are preferentially bound by Taspase1. Promoters as well as origins of replication contain AT-rich regions as AT base pairing shows a lower thermodynamic stability in comparison to GC base pairs (Vinogradov and Anatskaya, 2017), allowing easier DNA helix opening. It remains to be examined whether Taspase1 shows a preferred binding to AT-rich DNA-sequences.

In addition, less is known about how exactly Topo II activity is regulated to generate DSBs, but several Topo II cleavage sites were identified (Muller *et al.*, 1988; Spitzner and Muller, 1988; Andersen *et al.*, 1989). Many of these sequences are found in AT-rich regions (Cockerill and Garrard, 1986), but no general consensus sequence could be established (Osheroff *et al.*, 1991). Although a specific Topo II cleavage site was found *in vivo* at the human Lamin B2 origin of replication, Topo II alone showed no preference for this sequence *in vitro* (Abdurashidova *et al.*, 2007). Under physiological aspects, a Topo II recognition site that is not predominantly determined by a DNA-sequence is reasonable because it is important to exclude a permanently possible cleavage of inducible genes even in absence of a stimulus. Thus, it is more likely that Topo II recognizes special topological structures of DNA instead of depending on a DNA consensus sequence (Osheroff *et al.*, 1991). Bended DNA is AT-rich and could play a role in Topo II recognition, or DNA topological factors could energetically favor a reaction in the first place and thus mediate it indirectly. Another or an additional possibility is that auxiliary proteins are required, which mediate the contact of Topo II and DNA sites destined for estrogen dependent, transient cleavage.

So, maybe the estrogen-inducible Taspase1 operates as an adapter protein between Topo II and the destined DNA target sequences within the regulatory regions of estrogen inducible genes.

4.4.3 TASPASE1 PLAYS AN ESSENTIAL ROLE IN ESTROGEN-DRIVEN RESPONSE

In conclusion, it was investigated with *TASP1* siRNA to which extent the transcriptional estrogen response is Taspase1-dependent (Figure 3.20). First, *TASP1* siRNA showed a successful reduction of Taspase1 expression level in 293T cells 24 h and 48 h after transfection compared to the 293T cells treated with a control siRNA consisting of a nonsense sequence. The reduction of Taspase1 through siRNA caused a diminution of the expression level of estrogen-regulated genes such as c-fos and c-myc (van der Burg *et al.*, 1989; Szijan *et al.*, 1992; Doisneau-Sixou *et al.*, 2003; Vendrell *et al.*, 2004). Interestingly, the amount of Topo II remained the same in *TASP1* siRNA treated 293T cells, while the amount of γH2AX displayed also a decrease over the time. As this work discovered an enhancement of Topo II β-mediated DNA DSBs by Taspase1, it could be assumed, that the reduction of Taspase1 would result in a decrease of DNA DSBs, indicated by reduced γH2AX concentrations. The observed constant level of Topo II can be explained with the fact that cells always try to counteract disturbances in relevant processes by adapting expression levels of certain genes. Maybe, the cell tries to compensate this reduction of Taspase1 concentration by expressing higher levels of Topo II to reach a sufficient level of important DNA DSBs even without the supporting function of Taspase1. Experiments with Topo II-deficient cells or a respective knockout caused cell death due to mitotic failure and could not be rescued by Topo II β expression (Grue *et al.*, 1998). Similar results were obtained with Topo II $\alpha^{-/-}$ mouse embryo studies that demonstrated a termination of the developing embryo at the 4- or 8-cell stage (Akimitsu *et al.*, 2003). In contrast, cells lacking Topo II β displayed no abnormal behaviour apart from being less sensitive to Topo II targeted drugs (Khélifa *et al.*, 1994; Dereuddre *et al.*, 1997; Errington *et al.*, 1999), but Topo II $\beta^{-/-}$ mice die shortly after birth due to abnormal development of respiration system, which is caused due to a lack of connection between motor and sensory neurons (Yang *et al.*, 2000; Lyu and Wang, 2003; Lyu *et al.*, 2006). Although Topo II β does not appear to be essential for cells during embryonic development, it plays an essential role in the regulation of some genes during late neuronal development (Yang *et al.*, 2000; Lyu and Wang, 2003; Lyu *et al.*, 2006). This in line with the finding that

exclusively Topo II β-mediated DSBs are necessary for transcriptional activation of inducible genes (Ju *et al.*, 2006). Together with the recent finding that Taspase1 promotes such Topo II β catalyzed DSBs, this may explain why a decrease in DSBs is achieved by reducing Taspase1, but the expression level of Topo II remains the same.

As Taspase1 itself is estrogen regulated, a self-reinforcing process can take place: low Taspase1 basal protein levels mediate initial Topo II β triggered DSBs leading to transcriptional activation of E2-responsive genes, including the *TASP1* gene itself. This feedback loop mechanistically would result in a prompt signal amplification. A complete *TASP1* knockout should be investigated to resolve the dependency of Taspase1 in transcriptional regulation of estrogen-inducible genes in a more profound way. Here, it would be advantageous to use a conditional knockout mouse model as this avoids the weakened or even deadly phenotype of conventional *TASP1*$^{-/-}$ knockout mice shortly after birth. Then it would be possible to inactivate the *TASP1* gene in a tissue-specific or age-dependent manner.

4.5 CONCLUSION AND OUTLOOK

In this work, co-IP experiments identified new interaction partners of Taspase1. These either belong to cell cycle proteins that are also known as tumor suppressor proteins (Figure 3.1) or proteins that take part in transcriptional elongation of RNA pol II-dependent genes (Figure 3.3). Moreover, observed interactions with ERα, ERβ, MLL, NPM1, Nucleolin, Topo II α, Topo II β and γH2AX (Figure 3.5) hinted towards an involvement of Taspase1 in the estrogen response. Subsequent MS analysis revealed more than 300 proteins as possible Taspase1 binding partners and verified the interaction of Taspase1 with Topo II α, Topo II β, Nucleolin and NPM1 (Figure 3.7), all of them participating in estrogen-driven transcription. It was further demonstrated that Taspase1 and its newly identified binding partners were upregulated after estrogen stimulation (Figure 3.8). Together with the identification of an estrogen response element (ERE) 7.8 kbp upstream of the *TASP1* promotor (Figure 3.9), it was concluded that Taspase1 itself is an estrogen-responsive gene. Further, co-IPs showed that the newly identified interactors were significantly enriched in isolated Taspase1 complexes after estrogen stimulation (Figure 3.10). The combination of those results points to the conclusion that the overall function of Taspase1 can be assigned to the cellular estrogen response.

Furthermore, the results of this thesis revealed that Taspase1 is directly able to promote Topo II β-mediated DNA DSBs (Figure 3.13 and Figure 3.14). In addition, it was found that Taspase1 is a DNA binding protein (Figure 3.15) and that in the absence of Taspase1, the expression levels of estrogen-regulated genes c-fos and c-myc are reduced (Figure 3.16).

4.5.1 TASPASE1 IS AS A CO-ACTIVATOR OF ESTROGEN-DRIVEN TRANSCRIPTION

Thus, it is demonstrated that Topo II β is supported by Taspase1 in the generation of such physiologically relevant, estrogen-induced transient DSBs within estradiol-responsive promoters that finally lead to transcriptional induction of E2-responsive genes.

The following scenario is imaginable: Taspase1 resides at regulatory chromatin regions of hormone-inducible genes. Here it binds, together with Nucleolin and NPM1 to the promoter-associated repressor complex. After E2-stimulation, followed by DNA-binding of ligand-receptor complex and initial chromatin rearrangements, Taspase1 gets in contact with Topo II β and recruits the enzyme to DNA sites destined for cleavage. As Taspase1 also interacts with the NPM1/Nucleolin repressor complex, it is conceivable that Taspase1 facilitates the switch of the repressor complex thereby making way for Topo II β. Finally, the described estrogen-induced interplay between Taspase1 and Topo II β leads to an altered gene expression pattern of responding genes (Figure 4.1). In summary, Taspase1 functions as a co-activator of estrogen-driven transcription.

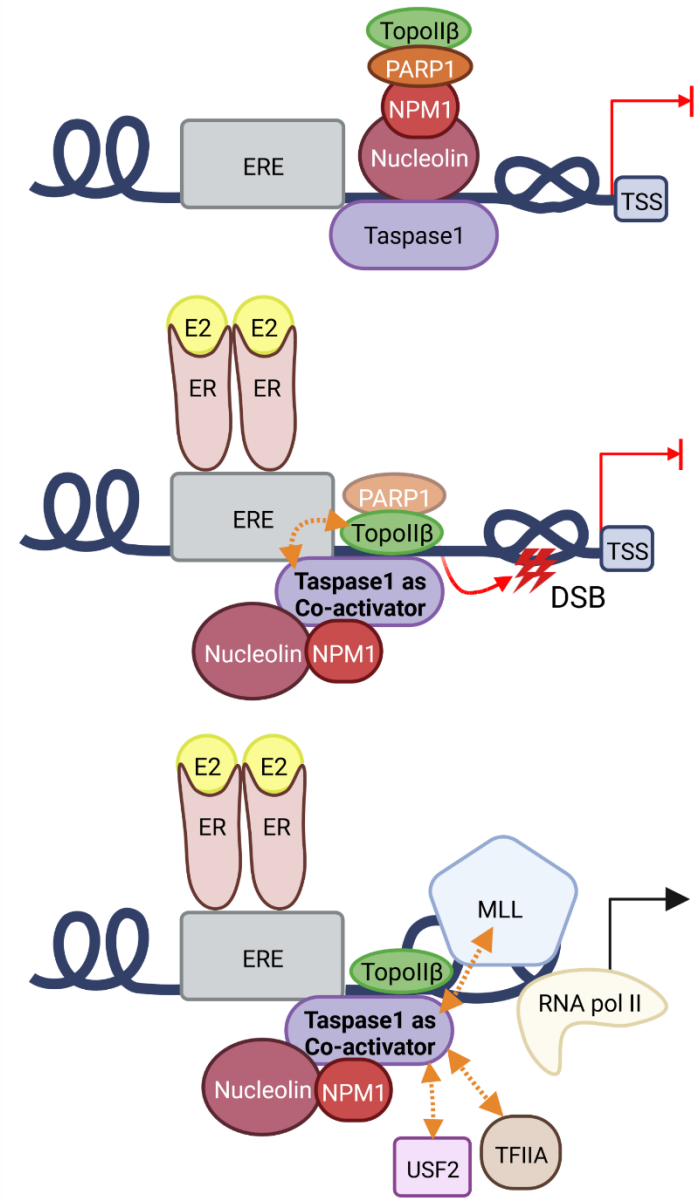

Figure 4.1: The Taspase1-Topo II β interplay and Taspase1-mediated substrate cleavage lead to an altered gene expression pattern of estrogen-induced genes.

In an uninduced state, the co-repressor complex (Nucleolin, NPM1, PARP1 and Topo II β) is bound to hormone-sensitive promotor regions thereby preventing transcriptional initiation. In addition, Taspase1 resides there and binds to Nucleolin and NPM1. Estrogen-stimulation leads to a spatial change of the co-repressor complex and enables Taspase1 to get in contact with Topo II β thereby enhancing a Topo II β-mediated transient DNA DSB. Topological barriers such as DNA knots or DNA supercoiling are solved allowing unhindered access for the transcription machinery. Moreover, Taspase1 cleaves different substrates, e.g. TFIIA and USF2 to adapt their function to changing cellular circumstances. The cleavage of the chromatin modifier MLL enables H3K4me epigenetic labeling. In sum, Taspase1 influences the estrogen response in several ways. This illustration was created with BioRender.com.

4.5.2 TASPASE1 PROMOTES THE ESTROGEN RESPONSE ON SEVERAL LEVELS

The results generated in this thesis strongly suggest that Taspase1 is required for efficient estrogen-stimulated transcription. Besides the direct enhancement of Topo II β-catalyzed DNA cleavage activity, there seem to be further modes of action for Taspase1 to reinforce the cellular estrogen response.

It is well known that steroid hormones such as estrogen initiate genetic differentiation- and developmental programs (Borellini and Oka, 1989). In this respect it makes sense that nuclear steroid hormone receptors are often accompanied by epigenetic writers and modifiers to perpetuate the changed gene expression patterns (Auger and Jessen, 2009). The presented data in this work as well as data from literature show that the MLL1 protein and its family members are also involved in estrogen-driven transcription (Dreijerink *et al.*, 2006; Ansari *et al.*, 2009; Ansari *et al.*, 2011). MLL is a chromatin modifier (Tenney and Shilatifard, 2005) as its C-terminal SET domain has intrinsic histone methyltransferase activity which mediates H3K4me, a specific signature for epigenetic transcriptional activation (Milne *et al.*, 2002; Nakamura *et al.*, 2002). MLL is cleaved by Taspase1 into a 320 kDa N-terminal fragment and a 180 kDa C-terminal fragment (Hsieh *et al.*, 2003b; Hsieh *et al.*, 2003a). The cleavage fragments reassemble into a dimer which is a scaffold for a multi-protein super complex (Nakamura *et al.*, 2002; Hsieh *et al.*, 2003a). The proteolytic processing of the enzyme by Taspase1 is required for a proper histone methyltransferase activity of MLL. As E2 treatment leads to an increased H3K4 signature (Figure 3.10) it can be concluded that Taspase1 is also responsible for the necessary MLL activation by proteolytic cleavage thereby allowing an epigenetic transcriptional activation.

MLL is not the only Taspase1 substrate that can enter the scene of estrogen-stimulated transcriptional initiation. Also TFIIA, a general transcription factor that is part of the transcription preinitiation complex that initiates mRNA synthesis (Orphanides *et al.*, 1996; Thomas and Chiang, 2006; Gupta *et al.*, 2016), is proteolytically cleaved by Taspase1 (Zhou *et al.*, 2006). Uncleaved TFIIA can induce cell cycle-specific transcription, involving the *Cdnk2a* gene locus encoding for the cell cycle regulators p16, p19 and p21, in turn halting cell cycle progression in G1 and S phase (Takeda *et al.*, 2015). But during mouse head formation, a Taspase1-mediated cleavage of TFIIA ensures proper coordination of rapid cell proliferation and morphogenesis by limited

transcription of the negative cell cycle regulators p16 and p19 from the *Cdkn2a* locus (Takeda *et al.*, 2015). Taken together, Taspase1 cleaves TFIIA to allow the initiation of an adapted genetic program. Such a regulation of TFIIA activity presumably occurs upon certain stimuli. As TFIIA also shows an estrogen-dependent gene expression (The UniProt Consortium, 2021), it is likely that the initiation of this proteolytically triggered TFIIA function change is due to hormone stimulus. In general, E2-induced Taspase1 may cleave in a context-dependent manner certain target proteins such as the ubiquitously expressed general transcription factor TFIIA to enable tissue-specific (testis) transcription or developmental-specific transcription.

In sum, Taspase1 is not only a protease that arbitrarily cleaves functionally unconnected substrate proteins. Instead, Taspase1's sphere of action is embedded in a specific signalling cascade, namely the cellular estrogen pathway. At its operation site, the chromatin, Taspase1 contributes to hormone signal forwarding in several ways (Figure 4.1):

1. Taspase1 facilitates estrogen-induced Topo II β mediated transient DNA double-strand breaks that are required for the initiation of stimulus-triggered transcription
2. Taspase1 enables H3K4me epigenetic labelling via cleavage-triggered activation of MLL. The H3K4 methylation epigenetic signature marks transcriptional start sites of active genes and is important for development and cell differentiation.
3. Taspase1 cleaves further transcription factors and other proteins to adapt their function to changing cellular circumstances.

4.5.3 TASPASE1 ASSOCIATION IN LEUKEMIA DEVELOPMENT

The data obtained in this work may give also an explanation for Taspase1's involvement in many leukemia that harbour chromosomal translocations: It was shown that Taspase1 facilitates the Topo II-dependent DSB induction upon hormone stimulation. Usually such DSBs are either religated by Topo II itself (Nitiss, 1998; Champoux, 2001; Wang, 2002; Pommier *et al.*, 2016) or, alternatively, are quickly sensed and repaired by the DNA damage response (DDR) (Haber, 2000) using two partially redundant repair pathways: homologous recombination (HR) (Thompson and Schild, 2001) and classical non-homologous end-joining (C-NHEJ) (Lieber, 2008). But

in case of an over-active or misregulated estrogen signalling cascade, for example caused by overexpressed or malfunctioning proteins in this cascade, there is an increasing risk of unrepaired or misrepaired DSBs, leading to programmed cell death or chromosomal translocations (McClendon and Osheroff, 2007). Here the following scenario is imaginable: genes that are activated at the same time, for example as response to a certain stimulus, are transcribed in parallel and in close proximity to each other in so called transcription factories. If Topo II catalyzed DSBs are generated within regulatory regions of stimulus-induced genes, it may be the case that not the generated fragments from one gene are ligated but that a cross-over with an adjacent, also "broken" gene takes place, resulting in the assembly and ligation of two fragments from different genes on different chromosomes, depicting the phenomenon of chromosomal translocations.

Topo II poisons, which are widely spread in cancer therapy, exploit the hazardous potential of Topo II generated cytotoxic DNA damage, as unrepaired DSBs ideally lead to programmed cell death of cancer cells (McClendon and Osheroff, 2007). Patients treated with the Topo II poison Etoposide develop therapy-related secondary leukemia´s that harbour chromosomal rearrangements (Baldwin and Osheroff, 2005; Felix *et al.*, 2006; Azarova *et al.*, 2007; Bender and Osheroff, 2008; Ezoe, 2012). This underlines once again, that although Topo II catalysed transient DSBs have a high physiological relevance as an initial event for stimulus-provoked transcription, those schedule DNA breaks also represent a great hazard potential if serious disturbances occur in this signalling cascade.

4.5.4 OUTLOOK

This work demonstrated that Taspase1 fulfills a superordinated function in cellular estrogen response where it contributes to hormone signal forwarding on several levels. With this newly acquired knowledge, Taspase1's bona fide substrates as well as the predicted substrates can be revalued with respect to this new context to assess if the respective substrate cleavage and its cellular consequences fit into the hormone-driven, Topo II-mediated gene transcription process. Moreover, the analysis of the interplay between Taspase1 and the newly identified interaction partners should be deepened by further binding studies applying appropriate methods such as SPR

(surface resonance plasmon), PLA or ITC (isothermal titration calorimetry) experiments.

Regarding Taspase1´s newly assigned function as a DNA binder, it is important to investigate which DNA motifs are preferentially bound by Taspase1. Experiments using ChIp-seq would be suitable for this purpose. Furthermore, EMSAs can provide information about whether the DNA binding domains of Taspase1 are really located within the NLS of the Taspase1 loop and whether the catalytically inactive Taspase1 variant is also able to bind DNA and to support Topo II β-mediated DSB formations. Since it is known that stimulus-induced DSBs for the transcriptional regulation of hormone-regulated genes are not only triggered by estrogen but also by other hormones including androgens, retinoic acid, insulin and glucocorticoids (Ju *et al.*, 2006; McNamara *et al.*, 2008; Wong *et al.*, 2009; Haffner *et al.*, 2010; Bunch *et al.*, 2015; Madabhushi *et al.*, 2015; Trotter *et al.*, 2015), it should also be investigated whether Taspase1 plays a role as a co-activator in these hormone responses.

Since Taspase1 promotes the transition from G1 to S phase as is also the case for estrogen, it should be further investigated to what extent Taspase1 plays a role in the cell cycle progression. A cell's progression through G1 phase and the G1/S phase transition is a critical step influenced by many outer signals. For estrogen receptor-positive cells it is known, that estradiol is able to induce proliferation by facilitating G1 to S phase transition (Doisneau-Sixou *et al.*, 2003; Yang *et al.*, 2007). Therefore, it is important to examine if the estrogen-induced transcription activation process, which is mediated (amongst others) by Topo II, Taspase1, Topo II-generated DSBs and MLL, triggers also the G1/S phase transition. If it turns out to be true, that Taspase1-dependent Topo II-mediated transient double-strand breaks are also required for regulated transcription facilitating G1 to S phase transition, it would deliver an explanation for Taspase1's role in cell cycle progression.

5 REFERENCES

Abdurashidova, G., Radulescu, S., Sandoval, O., Zahariev, S., Danailov, M.B., Demidovich, A., *et al.* (2007) Functional interactions of DNA topoisomerases with a human replication origin. *EMBO J* **26** (4): 998–1009.

Adams, J., and Kauffman, M. (2004) Development of the proteasome inhibitor Velcade (Bortezomib). *Cancer Invest* **22** (2): 304–311.

Ahn, J.-Y., Liu, X., Cheng, D., Peng, J., Chan, P.-K., Wade, P.A., and Ye, K. (2005) Nucleophosmin/B23, a nuclear PI(3,4,5)P(3) receptor, mediates the antiapoptotic actions of NGF by inhibiting CAD. *Mol Cell* **18** (4): 435–445.

Akimitsu, N., Adachi, N., Hirai, H., Hossain, M.S., Hamamoto, H., Kobayashi, M., *et al.* (2003) Enforced cytokinesis without complete nuclear division in embryonic cells depleting the activity of DNA topoisomerase IIalpha. *Genes Cells* **8** (4): 393–402.

Andersen, A.H., Christiansen, K., Zechiedrich, E.L., Jensen, P.S., Osheroff, N., and Westergaard, O. (1989) Strand specificity of the topoisomerase II mediated double-stranded DNA cleavage reaction. *Biochemistry* **28** (15): 6237–6244.

Andoh, T., and Ishida, R. (1998) Catalytic inhibitors of DNA topoisomerase II. *Biochimica et Biophysica Acta (BBA) - Gene Structure and Expression* **1400** (1-3): 155–171.

Ansari, K.I., Mishra, B.P., and Mandal, S.S. (2009) MLL histone methylases in gene expression, hormone signaling and cell cycle. *Front Biosci (Landmark Ed)* **14** (9): 3483–3495.

Ansari, K.I., Shrestha, B., Hussain, I., Kasiri, S., and Mandal, S.S. (2011) Histone methylases MLL1 and MLL3 coordinate with estrogen receptors in estrogen-mediated HOXB9 expression. *Biochemistry* **50** (17): 3517–3527.

Auger, A.P., and Jessen, H.M. (2009) Corepressors, nuclear receptors, and epigenetic factors on DNA: a tail of repression. *Psychoneuroendocrinology* **34 Suppl 1:** S39-47.

Austin, C.A., and Fisher, L.M. (1990) DNA topoisomerases: enzymes that change the shape of DNA. *Sci Prog* **74** (294 Pt 2): 147–161.

Austin, C.A., and Marsh, K.L. (1998) Eukaryotic DNA topoisomerase IIβ. *Bioessays* **20** (3): 215–226.

Austin, C.A., Sng, J.-H., Patel, S., and Fisher, L. (1993) Novel HeLa topoisomerase II is the IIβ isoform: complete coding sequence and homology with other type II topoisomerases. *Biochimica et Biophysica Acta (BBA) - Gene Structure and Expression* **1172** (3): 283–291.

Ayton, P.M., and Cleary, M.L. (2001) Molecular mechanisms of leukemogenesis mediated by MLL fusion proteins. *Oncogene* **20** (40): 5695–5707.

Azarova, A.M., Lyu, Y.L., Lin, C.-P., Tsai, Y.-C., Lau, J.Y.-N., Wang, J.C., and Liu, L.F. (2007) Roles of DNA topoisomerase II isozymes in chemotherapy and secondary malignancies. *Proc Natl Acad Sci U S A* **104** (26): 11014–11019.

Bailly, C. (2012) Contemporary challenges in the design of topoisomerase II inhibitors for cancer chemotherapy. *Chem Rev* **112** (7): 3611–3640.

Bakshi, R.P., Galande, S., and Muniyappa, K. (2001) Functional and regulatory characteristics of eukaryotic type II DNA topoisomerase. *Crit Rev Biochem Mol Biol* **36** (1): 1–37.

Baldwin, E.L., and Osheroff, N. (2005) Etoposide, topoisomerase II and cancer. *Curr Med Chem Anticancer Agents* **5** (4): 363–372.

Bandele, O.J., and Osheroff, N. (2009) Cleavage of plasmid DNA by eukaryotic topoisomerase II. *Methods Mol Biol* **582:** 39–47.

Barrett, A.J. (2001) Proteases. *Curr Protoc Protein Sci* **Chapter 21:** Unit 21.1.

Basu, S., Nandy, A., and Biswas, D. (2020) Keeping RNA polymerase II on the run: Functions of MLL fusion partners in transcriptional regulation. *Biochim Biophys Acta Gene Regul Mech* **1863** (8): 194563.

Bender, R.P., and Osheroff, N. (2008) DNA Topoisomerases as Targets for the Chemotherapeutic Treatment of Cancer. In *Checkpoint Responses in Cancer Therapy.* Dai, W. (ed.). Totowa, NJ: Humana Press, pp. 57–91.

Beneke, S. (2012) Regulation of chromatin structure by poly(ADP-ribosyl)ation. *Front Genet* **3:** 169.

Berger, J.M., Fass, D., Wang, J.C., and Harrison, S.C. (1998) Structural similarities between topoisomerases that cleave one or both DNA strands. *Proc Natl Acad Sci U S A* **95** (14): 7876–7881.

Berger, J.M., Gamblin, S.J., Harrison, S.C., and Wang, J.C. (1996) Structure and mechanism of DNA topoisomerase II. *Nature* **379** (6562): 225–232.

Bicknell, A.A., Tourtellotte, J., and Niwa, M. (2010) Late phase of the endoplasmic reticulum stress response pathway is regulated by Hog1 MAP kinase. *J Biol Chem* **285** (23): 17545–17555.

Bier, C., Hecht, R., Kunst, L., Scheiding, S., Wünsch, D., Goesswein, D., *et al.* (2012a) Overexpression of the catalytically impaired Taspase1 T234V or Taspase1 D233A variants does not have a dominant negative effect in T(4;11) leukemia cells. *PLoS ONE* **7** (5): e34142.

Bier, C., Knauer, S.K., Docter, D., Schneider, G., Krämer, O.H., and Stauber, R.H. (2011a) The importin-alpha/nucleophosmin switch controls taspase1 protease function. *Traffic* **12** (6): 703–714.

Bier, C., Knauer, S.K., Klapthor, A., Schweitzer, A., Rekik, A., Krämer, O.H., *et al.* (2011b) Cell-based analysis of structure-function activity of threonine aspartase 1. *J Biol Chem* **286** (4): 3007–3017.

Bier, C., Knauer, S.K., Wünsch, D., Kunst, L., Scheiding, S., Kaiser, M., *et al.* (2012b) Allosteric inhibition of Taspase1's pathobiological activity by enforced dimerization in vivo. *FASEB J* **26** (8): 3421–3429.

Biersack, H., Jensen, S., Gromova, I., Nielsen, I.S., Westergaard, O., and Andersen, A.H. (1996) Active heterodimers are formed from human DNA topoisomerase II alpha and II beta isoforms. // Active heterodimers are formed from human DNA topoisomerase II alpha and II beta isoforms. *Proc Natl Acad Sci U S A* **93** (16): 8288–8293.

Biswas, D., Milne, T.A., Basrur, V., Kim, J., Elenitoba-Johnson, K.S.J., Allis, C.D., and Roeder, R.G. (2011) Function of leukemogenic mixed lineage leukemia 1 (MLL)

fusion proteins through distinct partner protein complexes. *Proc Natl Acad Sci U S A* **108** (38): 15751–15756.

Blais, A., and Dynlacht, B.D. (2004) Hitting their targets: an emerging picture of E2F and cell cycle control. *Current Opinion in Genetics & Development* **14** (5): 527–532.

Bond, J.S. (2019) Proteases: History, discovery, and roles in health and disease. *J Biol Chem* **294** (5): 1643–1651.

Borellini, F., and Oka, T. (1989) Growth control and differentiation in mammary epithelial cells. *Environ Health Perspect* **80:** 85–99.

Borgoño, C.A., and Diamandis, E.P. (2004) The emerging roles of human tissue kallikreins in cancer. *Nat Rev Cancer* **4** (11): 876–890.

Bortoli, M. de, Dati, C., Antoniotti, S., Maggiora, P., and Sapei, M.L. (1992) Hormonal regulation of c-erbB-2 oncogene expression in breast cancer cells. *The Journal of Steroid Biochemistry and Molecular Biology* **43** (1-3): 21–25.

Box, J.K., Paquet, N., Adams, M.N., Boucher, D., Bolderson, E., O'Byrne, K.J., and Richard, D.J. (2016) Nucleophosmin: from structure and function to disease development. *BMC Mol Biol* **17** (1): 19.

Bracken, A.P., Ciro, M., Cocito, A., and Helin, K. (2004) E2F target genes: unraveling the biology. *Trends Biochem Sci* **29** (8): 409–417.

Bunch, H., Lawney, B.P., Lin, Y.-F., Asaithamby, A., Murshid, A., Wang, Y.E., *et al.* (2015) Transcriptional elongation requires DNA break-induced signalling. *Nat Commun* **6:** 10191.

Burma, S., and Chen, D.J. (2004) Role of DNA-PK in the cellular response to DNA double-strand breaks. *DNA Repair (Amst)* **3** (8-9): 909–918.

Burns, K.A., and Korach, K.S. (2012) Estrogen receptors and human disease: an update. *Arch Toxicol* **86** (10): 1491–1504.

Calderwood, S.K. (2016) A critical role for topoisomerase IIb and DNA double strand breaks in transcription. *Transcription* **7** (3): 75–83.

Carcamo, J., Lobos, S., Merino, A., Buckbinder, L., Weinmann, R., Natarajan, V., and Reinberg, D. (1989) Factors involved in specific transcription by mammalian RNA polymerase II. *Journal of Biological Chemistry* **264** (13): 7704–7714.

Cardone, M.H., Roy, N., Stennicke, H.R., Salvesen, G.S., Franke, T.F., Stanbridge, E., *et al.* (1998) Regulation of cell death protease caspase-9 by phosphorylation. *Science* **282** (5392): 1318–1321.

Champoux, J.J. (2001) DNA topoisomerases: structure, function, and mechanism. *Annu Rev Biochem* **70:** 369–413.

Chao, A., Lin, C.-Y., Tsai, C.-L., Hsueh, S., Lin, Y.-Y., Lin, C.-T., *et al.* (2013) Estrogen stimulates the proliferation of human endometrial cancer cells by stabilizing nucleophosmin/B23 (NPM/B23). *J Mol Med (Berl)* **91** (2): 249–259.

Chen, D., Frezza, M., Schmitt, S., Kanwar, J., and Dou, Q.P. (2011) Bortezomib as the first proteasome inhibitor anticancer drug: current status and future perspectives. *Curr Cancer Drug Targets* **11** (3): 239–253.

Chen, D.Y., Lee, Y., van Tine, B.A., Searleman, A.C., Westergard, T.D., Liu, H., *et al.* (2012) A pharmacologic inhibitor of the protease Taspase1 effectively inhibits breast and brain tumor growth. *Cancer Res* **72** (3): 736–746.

Chen, D.Y., Liu, H., Takeda, S., Tu, H.-C., Sasagawa, S., van Tine, B.A., *et al.* (2010) Taspase1 functions as a non-oncogene addiction protease that coordinates cancer cell proliferation and apoptosis. *Cancer Res* **70** (13): 5358–5367.

Chen, N., Szentirmay, M.N., Pawar, S.A., Sirito, M., WANG, J., Wang, Z., *et al.* (2006) Tumor-suppression function of transcription factor USF2 in prostate carcinogenesis. *Oncogene* **25** (4): 579–587.

Chi, T.F., Khoder-Agha, F., Mennerich, D., Kellokumpu, S., Miinalainen, I., Kietzmann, T., and Dimova, E.Y. (2020) Loss of USF2 promotes proliferation, migration and mitophagy in a redox-dependent manner. *Redox Biol* **37:** 101750.

Chow, K.C., and Ross, W.E. (1987) Topoisomerase-specific drug sensitivity in relation to cell cycle progression. *Mol Cell Biol* **7** (9): 3119–3123.

Christensen, M.O., Larsen, M.K., Barthelmes, H.U., Hock, R., Andersen, C.L., Kjeldsen, E., *et al.* (2002) Dynamics of human DNA topoisomerases IIalpha and IIbeta in living cells. *J Cell Biol* **157** (1): 31–44.

Chung, T.D., Drake, F.H., Tan, K.B., Per, S.R., Crooke, S.T., and Mirabelli, C.K. (1989) Characterization and immunological identification of cDNA clones encoding two human DNA topoisomerase II isozymes. *Proc Natl Acad Sci U S A* **86** (23): 9431–9435.

Cicatiello, L., Addeo, R., Sasso, A., Altucci, L., Petrizzi, V.B., Borgo, R., *et al.* (2004) Estrogens and progesterone promote persistent CCND1 gene activation during G1 by inducing transcriptional derepression via c-Jun/c-Fos/estrogen receptor (progesterone receptor) complex assembly to a distal regulatory element and recruitment of cyclin D1 to its own gene promoter. *Mol Cell Biol* **24** (16): 7260–7274.

Clausen, T., Kaiser, M., Huber, R., and Ehrmann, M. (2011) HTRA proteases: regulated proteolysis in protein quality control. *Nat Rev Mol Cell Biol* **12** (3): 152–162.

Cockerill, P.N., and Garrard, W.T. (1986) Chromosomal loop anchorage of the kappa immunoglobulin gene occurs next to the enhancer in a region containing topoisomerase II sites. *Cell* **44** (2): 273–282.

Coezy, E., Borgna, J.L., and Rochefort, H. (1982) Tamoxifen and metabolites in MCF7 cells: correlation between binding to estrogen receptor and inhibition of cell growth. *Cancer Res* **42** (1): 317–323.

Cojocaru, M., Bouchard, A., Cloutier, P., Cooper, J.J., Varzavand, K., Price, D.H., and Coulombe, B. (2011) Transcription factor IIS cooperates with the E3 ligase UBR5 to ubiquitinate the CDK9 subunit of the positive transcription elongation factor B. *J Biol Chem* **286** (7): 5012–5022.

Cokol, M., Nair, R., and Rost, B. (2000) Finding nuclear localization signals. *EMBO Rep* **1** (5): 411–415.

Corre, S., and Galibert, M.-D. (2005) Upstream stimulating factors: highly versatile stress-responsive transcription factors. *Pigment Cell Res* **18** (5): 337–348.

Cowell, I.G., Sondka, Z., Smith, K., Lee, K.C., Manville, C.M., Sidorczuk-Lesthuruge, M., *et al.* (2012) Model for MLL translocations in therapy-related leukemia involving topoisomerase IIβ-mediated DNA strand breaks and gene proximity. *Proc Natl Acad Sci U S A* **109** (23): 8989–8994.

Cui, J., Shen, Y., and Li, R. (2013) Estrogen synthesis and signaling pathways during aging: from periphery to brain. *Trends in Molecular Medicine* **19** (3): 197–209.

Dannheisig, D. (2016) Impact of survivin acetylation on its biological function. *Master's Thesis (University Duisburg-Essen)*.

Daser, A., and Rabbitts, T.H. (2004) Extending the repertoire of the mixed-lineage leukemia gene MLL in leukemogenesis. *Genes Dev* **18** (9): 965–974.

Debernardi, S., Lillington, D.M., Chaplin, T., Tomlinson, S., Amess, J., Rohatiner, A., *et al.* (2003) Genome-wide analysis of acute myeloid leukemia with normal karyotype reveals a unique pattern of homeobox gene expression distinct from those with translocation-mediated fusion events. *Genes Chromosomes Cancer* **37** (2): 149–158.

DeJong, J., and Roeder, R.G. (1993) A single cDNA, hTFIIA/alpha, encodes both the p35 and p19 subunits of human TFIIA. *Genes Dev* **7** (11): 2220–2234.

Delgado, B.J., and Lopez-Ojeda, W. (2022) *StatPearls: Estrogen.* Treasure Island (FL).

Dereuddre, S., Delaporte, C., and Jacquemin-Sablon, A. (1997) Role of topoisomerase II beta in the resistance of 9-OH-ellipticine-resistant Chinese hamster fibroblasts to topoisomerase II inhibitors. *Cancer Res* **57** (19): 4301–4308.

Deroo, B.J., and Korach, K.S. (2006) Estrogen receptors and human disease. *J Clin Invest* **116** (3): 561–570.

Deweese, J.E., and Osheroff, N. (2009) The DNA cleavage reaction of topoisomerase II: wolf in sheep's clothing. *Nucleic Acids Res* **37** (3): 738–748.

Doisneau-Sixou, S.F., Sergio, C.M., Carroll, J.S., Hui, R., Musgrove, E.A., and Sutherland, R.L. (2003) Doisneau-Sixou et al 2003_Estrogen and antiestrogen regulation of cell cycle progression in breast cancer cells. // Estrogen and antiestrogen regulation of cell cycle progression in breast cancer cells. *Endocr Relat Cancer* **10** (2): 179–186.

Dong, Y., van Tine, B.A., Oyama, T., Wang, P.I., Cheng, E.H., and Hsieh, J.J. (2014) Taspase1 cleaves MLL1 to activate cyclin E for HER2/neu breast tumorigenesis. *Cell Res* **24** (11): 1354–1366.

Dou, Y., Milne, T.A., Ruthenburg, A.J., Lee, S., Lee, J.W., Verdine, G.L., *et al.* (2006) Regulation of MLL1 H3K4 methyltransferase activity by its core components. *Nat Struct Mol Biol* **13** (8): 713–719.

Dou, Y., Milne, T.A., Tackett, A.J., Smith, E.R., Fukuda, A., Wysocka, J., *et al.* (2005) Physical association and coordinate function of the H3 K4 methyltransferase MLL1 and the H4 K16 acetyltransferase MOF. *Cell* **121** (6): 873–885.

Doucet, A., and Overall, C.M. (2008) Protease proteomics: revealing protease in vivo functions using systems biology approaches. *Mol Aspects Med* **29** (5): 339–358.

Drabkin, H.A., Parsy, C., Ferguson, K., Guilhot, F., Lacotte, L., Roy, L., *et al.* (2002) Quantitative HOX expression in chromosomally defined subsets of acute myelogenous leukemia. *Leukemia* **16** (2): 186–195.

Drake, F.H., Hofmann, G.A., Bartus, H.F., Mattern, M.R., Crooke, S.T., and Mirabelli, C.K. (1989) Biochemical and pharmacological properties of p170 and p180 forms of topoisomerase II. *Biochemistry* **28** (20): 8154–8160.

Dreijerink, K.M.A., Mulder, K.W., Winkler, G.S., Höppener, J.W.M., Lips, C.J.M., and Timmers, H.T.M. (2006) Menin links estrogen receptor activation to histone H3K4 trimethylation. *Cancer Res* **66** (9): 4929–4935.

Du, H., Roy, A.L., and Roeder, R.G. (1993) Human transcription factor USF stimulates transcription through the initiator elements of the HIV-1 and the Ad-ML promoters. *EMBO J* **12** (2): 501–511.

Egeblad, M., and Werb, Z. (2002) New functions for the matrix metalloproteinases in cancer progression. *Nat Rev Cancer* **2** (3): 161–174.

Ernst, P., Fisher, J.K., Avery, W., Wade, S., Foy, D., and Korsmeyer, S.J. (2004) Definitive Hematopoiesis Requires the Mixed-Lineage Leukemia Gene. *Developmental Cell* **6** (3): 437–443.

Ernst, P., WANG, J., Huang, M., Goodman, R.H., and Korsmeyer, S.J. (2001) MLL and CREB bind cooperatively to the nuclear coactivator CREB-binding protein. *Mol Cell Biol* **21** (7): 2249–2258.

Errington, F., Willmore, E., Tilby, M.J., Li, L., Li, G., Li, W., *et al.* (1999) Murine transgenic cells lacking DNA topoisomerase IIbeta are resistant to acridines and mitoxantrone: analysis of cytotoxicity and cleavable complex formation. *Mol Pharmacol* **56** (6): 1309–1316.

Ezoe, S. (2012) Secondary leukemia associated with the anti-cancer agent, etoposide, a topoisomerase II inhibitor. *Int J Environ Res Public Health* **9** (7): 2444–2453.

Fair, K., Anderson, M., Bulanova, E., Mi, H., Tropschug, M., and Diaz, M.O. (2001) Protein interactions of the MLL PHD fingers modulate MLL target gene regulation in human cells. *Mol Cell Biol* **21** (10): 3589–3597.

Falini, B., Bolli, N., Shan, J., Martelli, M.P., Liso, A., Pucciarini, A., *et al.* (2006) Both carboxy-terminus NES motif and mutated tryptophan(s) are crucial for aberrant nuclear export of nucleophosmin leukemic mutants in NPMc+ AML. *Blood* **107** (11): 4514–4523.

Falini, B., Mecucci, C., Tiacci, E., Alcalay, M., Rosati, R., Pasqualucci, L., *et al.* (2005) *Cytoplasmic nucleophosmin in acute myelogenous leukemia with a normal karyotype*.

Falini, B., Nicoletti, I., Bolli, N., Martelli, M.P., Liso, A., Gorello, P., *et al.* (2007) Translocations and mutations involving the nucleophosmin (NPM1) gene in lymphomas and leukemias. *Haematologica* **92** (4): 519–532.

Felix, C.A., Kolaris, C.P., and Osheroff, N. (2006) Topoisomerase II and the etiology of chromosomal translocations. *DNA Repair (Amst)* **5** (9-10): 1093–1108.

Fortune, J.M., and Osheroff, N. (1998) Merbarone inhibits the catalytic activity of human topoisomerase IIalpha by blocking DNA cleavage. *J Biol Chem* **273** (28): 17643–17650.

Fortune, J.M., and Osheroff, N. (2000) Topoisomerase II as a target for anticancer drugs: When enzymes stop being nice. In *Progress in Nucleic Acid Research and Molecular Biology Volume 64:* Elsevier, pp. 221–253.

Frasor, J., Danes, J.M., Komm, B., Chang, K.C.N., Lyttle, C.R., and Katzenellenbogen, B.S. (2003) Profiling of estrogen up- and down-regulated gene expression in human

breast cancer cells: insights into gene networks and pathways underlying estrogenic control of proliferation and cell phenotype. *Endocrinology* **144** (10): 4562–4574.

Froelich-Ammon, S.J., and Osheroff, N. (1995) Topoisomerase poisons: harnessing the dark side of enzyme mechanism. *J Biol Chem* **270** (37): 21429–21432.

Gearing, L.J., Cumming, H.E., Chapman, R., Finkel, A.M., Woodhouse, I.B., Luu, K., *et al.* (2019) *CiiiDER: a new tool for predicting and analysing transcription factor binding sites*.

Gilroy, K.L., and Austin, C.A. (2011) The impact of the C-terminal domain on the interaction of human DNA topoisomerase II α and β with DNA. *PLoS ONE* **6** (2): e14693.

Gómez-Herreros, F. (2019) DNA Double Strand Breaks and Chromosomal Translocations Induced by DNA Topoisomerase II. *Front Mol Biosci* **6:** 141.

Gregor, P.D., Sawadogo, M., and Roeder, R.G. (1990) The adenovirus major late transcription factor USF is a member of the helix-loop-helix group of regulatory proteins and binds to DNA as a dimer. *Genes Dev* **4** (10): 1730–1740.

Grisendi, S., Mecucci, C., Falini, B., and Pandolfi, P.P. (2006) Nucleophosmin and cancer. *Nat Rev Cancer* **6** (7): 493–505.

Groenen, P.M., Garcia, E., Debeer, P., Devriendt, K., Fryns, J.P., and van de Ven, W.J. (1996) Structure, sequence, and chromosome 19 localization of human USF2 and its rearrangement in a patient with multicystic renal dysplasia. *Genomics* **38** (2): 141–148.

Grue, P., Grässer, A., Sehested, M., Jensen, P.B., Uhse, A., Straub, T., *et al.* (1998) Essential mitotic functions of DNA topoisomerase IIalpha are not adopted by topoisomerase IIbeta in human H69 cells. *J Biol Chem* **273** (50): 33660–33666.

Gupta, K., Sari-Ak, D., Haffke, M., Trowitzsch, S., and Berger, I. (2016) Zooming in on Transcription Preinitiation. *Journal of Molecular Biology* **428** (12): 2581–2591.

Haber, J.E. (2000) Partners and pathways. *Trends in Genetics* **16** (6): 259–264.

Hadsell, D.L., Bonnette, S., George, J., Torres, D., Klimentidis, Y., Klementidis, Y., *et al.* (2003) Diminished milk synthesis in upstream stimulatory factor 2 null mice is associated with decreased circulating oxytocin and decreased mammary gland expression of eukaryotic initiation factors 4E and 4G. *Mol Endocrinol* **17** (11): 2251–2267.

Haffner, M.C., Aryee, M.J., Toubaji, A., Esopi, D.M., Albadine, R., Gurel, B., *et al.* (2010) Androgen-induced TOP2B-mediated double-strand breaks and prostate cancer gene rearrangements. *Nat Genet* **42** (8): 668–675.

Hanahan, D. (2022) Hallmarks of Cancer: New Dimensions. *Cancer Discov* **12** (1): 31–46.

Hanahan, D., and Weinberg, R.A. (2000) The hallmarks of cancer. *Cell* **100** (1): 57–70.

Hanahan, D., and Weinberg, R.A. (2011) Hallmarks of cancer: The next generation. *Cell* **144** (5): 646–674.

Hande, K. (1998) Etoposide: four decades of development of a topoisomerase II inhibitor. *Eur J Cancer* **34** (10): 1514–1521.

Heck, M.M., and Earnshaw, W.C. (1986) Topoisomerase II: A specific marker for cell proliferation. *J Cell Biol* **103** (6 Pt 2): 2569–2581.

Heck, M.M., Hittelman, W.N., and Earnshaw, W.C. (1988) Differential expression of DNA topoisomerases I and II during the eukaryotic cell cycle. *Proc Natl Acad Sci U S A* **85** (4): 1086–1090.

Heery, D.M., Kalkhoven, E., Hoare, S., and Parker, M.G. (1997) Heery et al 1997_A signature motif in transcriptional co-activators mediates binding to nuclear receptors // A signature motif in transcriptional co-activators mediates binding to nuclear receptors. *Nature* **387** (6634): 733–736.

Heiselmayer, C. (2018) Identification and characterization of novel Taspase1 target proteins. *Dissertation (University Duisburg-Essen)*.

Henkel, T., Zabel, U., van Zee, K., Müller, J.M., Fanning, E., and Baeuerle, P.A. (1992) Intramolecular masking of the nuclear location signal and dimerization domain in the precursor for the p50 NF-κB subunit. *Cell* **68** (6): 1121–1133.

Hensel, A., Stahl, P., Moews, L., König, L., Patwardhan, R., Höing, A., *et al.* (2022) The Taspase1/Myosin1f-axis regulates filopodia dynamics. *iScience* **25** (6): 104355.

Hess, J.L. (2004) MLL: a histone methyltransferase disrupted in leukemia. *Trends in Molecular Medicine* **10** (10): 500–507.

Hess, R.A., Bunick, D., Lee, K.H., Bahr, J., Taylor, J.A., Korach, K.S., and Lubahn, D.B. (1997) A role for oestrogens in the male reproductive system. *Nature* **390** (6659): 509–512.

Hiyama, H., Iavarone, A., and Reeves, S.A. (1998) Regulation of the cdk inhibitor p21 gene during cell cycle progression is under the control of the transcription factor E2F. *Oncogene* **16** (12): 1513–1523.

Hoeller, D., Hecker, C.-M., and Dikic, I. (2006) Ubiquitin and ubiquitin-like proteins in cancer pathogenesis. *Nat Rev Cancer* **6** (10): 776–788.

Høiby, T., Mitsiou, D.J., Zhou, H., Erdjument-Bromage, H., Tempst, P., and Stunnenberg, H.G. (2004) Cleavage and proteasome-mediated degradation of the basal transcription factor TFIIA // Cleavage and proteasome-mediated degradation of the basal transcription factor TFIIA. *EMBO J* **23** (15): 3083–3091.

Høiby, T., Zhou, H., Mitsiou, D.J., and Stunnenberg, H.G. (2007) A facelift for the general transcription factor TFIIA. *Biochim Biophys Acta* **1769** (7-8): 429–436.

Höing, A., Zimmermann, A., Moews, L., Killa, M., Heimann, M., Hensel, A., *et al.* (2022) A Bivalent Supramolecular GCP Ligand Enables Blocking of the Taspase1/Importin α Interaction. *ChemMedChem* **17** (1): e202100640.

Hsiang, Y.H., Wu, H.Y., and Liu, L.F. (1988) Proliferation-dependent regulation of DNA topoisomerase II in cultured human cells. *Cancer Res* **48** (11): 3230–3235.

Hsieh, J.J.-D., Cheng, E.H.-Y., and Korsmeyer, S.J. (2003a) Taspase1: a threonine aspartase required for cleavage of MLL and proper HOX gene expression. *Cell* **115** (3): 293–303.

Hsieh, J.J.-D., Ernst, P., Erdjument-Bromage, H., Tempst, P., and Korsmeyer, S.J. (2003b) Proteolytic cleavage of MLL generates a complex of N- and C-terminal fragments that confers protein stability and subnuclear localization. *Mol Cell Biol* **23** (1): 186–194.

Hughes, C.M., Rozenblatt-Rosen, O., Milne, T.A., Copeland, T.D., Levine, S.S., Lee, J.C., *et al.* (2004) Menin Associates with a Trithorax Family Histone Methyltransferase Complex and with the Hoxc8 Locus. *Mol Cell* **13** (4): 587–597.

Imbalzano, A.N., Zaret, K.S., and Kingston, R.E. (1994) Transcription factor (TF) IIB and TFIIA can independently increase the affinity of the TATA-binding protein for DNA. *Journal of Biological Chemistry* **269** (11): 8280–8286.

Jenkins, J.R., Ayton, P., Jones, T., Davies, S.L., Simmons, D.L., Harris, A.L., *et al.* (1992) Isolation of cDNA clones encoding the beta isozyme of human DNA topoisomerase II and localisation of the gene to chromosome 3p24. *Nucleic Acids Res* **20** (21): 5587–5592.

Jensen, A.D., and Svejstrup, J.Q. (1996) Purification and characterization of human topoisomerase I mutants. *Eur J Biochem* **236** (2): 389–394.

Jensen, P.B., Sørensen, B.S., Demant, E.J., Sehested, M., Jensen, P.S., Vindeløv, L., and Hansen, H.H. (1990) Antagonistic effect of aclarubicin on the cytotoxicity of etoposide and 4'-(9-acridinylamino)methanesulfon-m-anisidide in human small cell lung cancer cell lines and on topoisomerase II-mediated DNA cleavage. *Cancer Res* **50** (11): 3311–3316.

Ju, B.-G., Lunyak, V.V., Perissi, V., Garcia-Bassets, I., Rose, D.W., Glass, C.K., and Rosenfeld, M.G. (2006) A topoisomerase IIbeta-mediated dsDNA break required for regulated transcription. *Science* **312** (5781): 1798–1802.

Ju, B.-G., and Rosenfeld, M.G. (2006) A Breaking Strategy for Topoisomerase IIβ/PARP-1-Dependent Regulated Transcription // A breaking strategy for topoisomerase IIbeta/PARP-1-dependent regulated transcription. *Cell Cycle* **5** (22): 2557–2560.

Kane, R.C., Bross, P.F., Farrell, A.T., and Pazdur, R. (2003) Velcade: U.S. FDA approval for the treatment of multiple myeloma progressing on prior therapy. *Oncologist* **8** (6): 508–513.

Kane, R.C., Dagher, R., Farrell, A., Ko, C.-W., Sridhara, R., Justice, R., and Pazdur, R. (2007) Bortezomib for the treatment of mantle cell lymphoma. *Clin Cancer Res* **13** (18 Pt 1): 5291–5294.

Kashima, H., Shiozawa, T., Miyamoto, T., Suzuki, A., Uchikawa, J., Kurai, M., and Konishi, I. (2009) Autocrine stimulation of IGF1 in estrogen-induced growth of endometrial carcinoma cells: involvement of the mitogen-activated protein kinase pathway followed by up-regulation of cyclin D1 and cyclin E. *Endocr Relat Cancer* **16** (1): 113–122.

Katzenellenbogen, B.S. (1996) Katzenellenbogen 1996_Estrogen receptors bioactivities and interactions with cell signaling pathways // Estrogen receptors: bioactivities and interactions with cell signaling pathways. *Biol Reprod* **54** (2): 287–293.

Katzenellenbogen, B.S., Kendra, K.L., Norman, M.J., and Berthois, Y. (1987) Proliferation, hormonal responsiveness, and estrogen receptor content of MCF-7 human breast cancer cells grown in the short-term and long-term absence of estrogens. *Cancer Res* **47** (16): 4355–4360.

Kel, A.E., Gössling, E., Reuter, I., Cheremushkin, E., Kel-Margoulis, O.V., and Wingender, E. (2003) MATCH: A tool for searching transcription factor binding sites in DNA sequences. *Nucleic Acids Res* **31** (13): 3576–3579.

Kellner, U., Rudolph, P., and Parwaresch, R. (2000) Human DNA-Topoisomerases - Diagnostic and Therapeutic Implications for Cancer. *Onkologie* **23** (5): 424–430.

Khan, J.A., Dunn, B.M., and Tong, L. (2005) Crystal structure of human Taspase1, a crucial protease regulating the function of MLL. *Structure* **13** (10): 1443–1452.

Khélifa, T., Casabianca-Pignède, M.R., René, B., and Jacquemin-Sablon, A. (1994) Expression of topoisomerases II alpha and beta in Chinese hamster lung cells resistant to topoisomerase II inhibitors. *Mol Pharmacol* **46** (2): 323–328.

Klinge, C.M. (2001) Estrogen receptor interaction with estrogen response elements. *Nucleic Acids Res* **29** (14): 2905–2919.

Knauer, S.K., Fetz, V., Rabenstein, J., Friedl, S., Hofmann, B., Sabiani, S., *et al.* (2011) Bioassays to monitor Taspase1 function for the identification of pharmacogenetic inhibitors. *PLoS ONE* **6** (5): e18253.

Koblinski, J.E., Ahram, M., and Sloane, B.F. (2000) Unraveling the role of proteases in cancer. *Clinica Chimica Acta* **291** (2): 113–135.

Kopitar-Jerala, N. (2012) The role of cysteine proteinases and their inhibitors in the host-pathogen cross talk. *Curr Protein Pept Sci* **13** (8): 767–775.

Korach, K.S. (1994) Insights from the study of animals lacking functional estrogen receptor. *Science* **266** (5190): 1524–1527.

Korgaonkar, C., Hagen, J., van Tompkins, Frazier, A.A., Allamargot, C., Quelle, F.W., and Quelle, D.E. (2005) Nucleophosmin (B23) targets ARF to nucleoli and inhibits its function. *Mol Cell Biol* **25** (4): 1258–1271.

Kossatz, U., and Malek, N.P. (2007) p27: tumor suppressor and oncogene …? *Cell Res* **17** (10): 832–833.

Kotake, Y., Zeng, Y., and Xiong, Y. (2009) DDB1-CUL4 and MLL1 mediate oncogene-induced p16INK4a activation. *Cancer Res* **69** (5): 1809–1814.

Krivtsov, A.V., and Armstrong, S.A. (2007) MLL translocations, histone modifications and leukaemia stem-cell development. *Nat Rev Cancer* **7** (11): 823–833.

Kuo, M.-L., Besten, W. den, Thomas, M.C., and Sherr, C.J. (2008) Arf-induced turnover of the nucleolar nucleophosmin-associated SUMO-2/3 protease Senp3. *Cell Cycle* **7** (21): 3378–3387.

La, P., Desmond, A., Hou, Z., Silva, A.C., Schnepp, R.W., and Hua, X. (2006) Tumor suppressor menin: the essential role of nuclear localization signal domains in coordinating gene expression. *Oncogene* **25** (25): 3537–3546.

LaCasse, E.C., and Lefebvre, Y.A. (1995) Nuclear localization signals overlap DNA- or RNA-binding domains in nucleic acid-binding proteins. *Nucleic Acids Res* **23** (10): 1647–1656.

Lagrange, T., Kim, T.K., Orphanides, G., Ebright, Y.W., Ebright, R.H., and Reinberg, D. (1996) Lagrange et al 1996_High-resolution mapping of nucleoprotein complexes by site-specific protein-DNA photocrosslinking organization of the human TBP-TFIIA-TFIIB-DNA quaternary complex // High-resolution mapping of nucleoprotein complexes by site-specific protein-DNA photocrosslinking: organization of the

human TBP-TFIIA-TFIIB-DNA quaternary complex. *Proc Natl Acad Sci U S A* **93** (20): 10620–10625.

Lah, T.T., Durán Alonso, M.B., and van Noorden, C.J.F. (2006) Antiprotease therapy in cancer: hot or not? *Expert Opin Biol Ther* **6** (3): 257–279.

Landgraf, P., Wahle, P., Pape, H.-C., Gundelfinger, E.D., and Kreutz, M.R. (2008) The survival-promoting peptide Y-P30 enhances binding of pleiotrophin to syndecan-2 and -3 and supports its neuritogenic activity. *J Biol Chem* **283** (36): 25036–25045.

Law, R.H.P., Zhang, Q., McGowan, S., Buckle, A.M., Silverman, G.A., Wong, W., *et al.* (2006) An overview of the serpin superfamily. *Genome Biol* **7** (5): 216.

Lee, J.T., Chen, D.Y., Yang, Z., Ramos, A.D., Hsieh, J.J.-D., and Bogyo, M. (2009) Design, syntheses, and evaluation of Taspase1 inhibitors. *Bioorg Med Chem Lett* **19** (17): 5086–5090.

Li, Y.P., Busch, R.K., Valdez, B.C., and Busch, H. (1996) C23 interacts with B23, a putative nucleolar-localization-signal-binding protein. *Eur J Biochem* **237** (1): 153–158.

Lieber, M.R. (2008) The mechanism of human nonhomologous DNA end joining. *J Biol Chem* **283** (1): 1–5.

Liggett, W.H., and Sidransky, D. (1998) Role of the p16 tumor suppressor gene in cancer. *J Clin Oncol* **16** (3): 1197–1206.

Lin, C.Y., Liang, Y.C., and Yung, B.Y.-M. (2006) Nucleophosmin/B23 regulates transcriptional activation of E2F1 via modulating the promoter binding of NF-kappaB, E2F1 and pRB. *Cell Signal* **18** (11): 2041–2048.

Liu, H., Cheng, E.H.Y., and Hsieh, J.J.D. (2009) MLL fusions: pathways to leukemia. *Cancer Biol Ther* **8** (13): 1204–1211.

Liu, X., Kraus, W.L., and Bai, X. (2015) Ready, pause, go: regulation of RNA polymerase II pausing and release by cellular signaling pathways. *Trends Biochem Sci* **40** (9): 516–525.

Look, A.T. (1997) Oncogenic transcription factors in the human acute leukemias. *Science* **278** (5340): 1059–1064.

López-Otín, C., and Bond, J.S. (2008) Proteases: multifunctional enzymes in life and disease. *J Biol Chem* **283** (45): 30433–30437.

López-Otín, C., and Matrisian, L.M. (2007) Emerging roles of proteases in tumour suppression. *Nat Rev Cancer* **7** (10): 800–808.

López-Otín, C., and Overall, C.M. (2002) Protease degradomics: a new challenge for proteomics. *Nat Rev Mol Cell Biol* **3** (7): 509–519.

Lubahn, D.B., Moyer, J.S., Golding, T.S., Couse, J.F., Korach, K.S., and Smithies, O. (1993) Alteration of reproductive function but not prenatal sexual development after insertional disruption of the mouse estrogen receptor gene. *Proc Natl Acad Sci U S A* **90** (23): 11162–11166.

Luo, J., Solimini, N.L., and Elledge, S.J. (2009) Principles of cancer therapy: oncogene and non-oncogene addiction. *Cell* **136** (5): 823–837.

Luo, X., and Sawadogo, M. (1996) Functional domains of the transcription factor USF2: atypical nuclear localization signals and context-dependent transcriptional activation domains. *Mol Cell Biol* **16** (4): 1367–1375.

Lyu, Y.L., Lin, C.-P., Azarova, A.M., Cai, L., Wang, J.C., and Liu, L.F. (2006) Role of topoisomerase IIbeta in the expression of developmentally regulated genes. *Mol Cell Biol* **26** (21): 7929–7941.

Lyu, Y.L., and Wang, J.C. (2003) Aberrant lamination in the cerebral cortex of mouse embryos lacking DNA topoisomerase IIbeta. *Proc Natl Acad Sci U S A* **100** (12): 7123–7128.

Madabhushi, R. (2018) The Roles of DNA Topoisomerase IIβ in Transcription. *Int J Mol Sci* **19** (7).

Madabhushi, R., Gao, F., Pfenning, A.R., Pan, L., Yamakawa, S., Seo, J., *et al.* (2015) Activity-Induced DNA Breaks Govern the Expression of Neuronal Early-Response Genes. *Cell* **161** (7): 1592–1605.

Maki, K., Mitani, K., Yamagata, T., Kurokawa, M., Kanda, Y., Yazaki, Y., and Hirai, H. (1999) Transcriptional Inhibition of p53 by the MLL/MEN Chimeric Protein Found in Myeloid Leukemia. *Blood* **93** (10): 3216–3224.

Mangelsdorf, D.J., Thummel, C., Beato, M., Herrlich, P., Schütz, G., Umesono, K., *et al.* (1995) The nuclear receptor superfamily: the second decade. *Cell* **83** (6): 835–839.

Mason, S.D., and Joyce, J.A. (2011) Proteolytic networks in cancer. *Trends Cell Biol* **21** (4): 228–237.

Mayeur, G.L., Kung, W.-J., Martinez, A., Izumiya, C., Chen, D.J., and Kung, H.-J. (2005) Ku is a novel transcriptional recycling coactivator of the androgen receptor in prostate cancer cells. *J Biol Chem* **280** (11): 10827–10833.

McClendon, A.K., and Osheroff, N. (2006) The geometry of DNA supercoils modulates topoisomerase-mediated DNA cleavage and enzyme response to anticancer drugs. *Biochemistry* **45** (9): 3040–3050.

McClendon, A.K., and Osheroff, N. (2007) DNA topoisomerase II, genotoxicity, and cancer. *Mutat Res* **623** (1-2): 83–97.

McClendon, A.K., Rodriguez, A.C., and Osheroff, N. (2005) Human topoisomerase IIalpha rapidly relaxes positively supercoiled DNA: implications for enzyme action ahead of replication forks. *J Biol Chem* **280** (47): 39337–39345.

McNamara, S., Wang, H., Hanna, N., and Miller, W.H. (2008) Topoisomerase IIbeta negatively modulates retinoic acid receptor alpha function: a novel mechanism of retinoic acid resistance. *Mol Cell Biol* **28** (6): 2066–2077.

Meczes, E.L., Gilroy, K.L., West, K.L., and Austin, C.A. (2008) The impact of the human DNA topoisomerase II C-terminal domain on activity. *PLoS ONE* **3** (3): e1754.

Meyer, C., Burmeister, T., Gröger, D., Tsaur, G., Fechina, L., Renneville, A., *et al.* (2018) The MLL recombinome of acute leukemias in 2017. *Leukemia* **32** (2): 273–284.

Meyer, C., Kowarz, E., Hofmann, J., Renneville, A., Zuna, J., Trka, J., *et al.* (2009) New insights to the MLL recombinome of acute leukemias. *Leukemia* **23** (8): 1490–1499.

Meyer, C., Schneider, B., Jakob, S., Strehl, S., Attarbaschi, A., Schnittger, S., *et al.* (2006) Meyer et al 2006_The MLL recombinome of acute leukemias // The MLL recombinome of acute leukemias. *Leukemia* **20** (5): 777–784.

Milne, T.A., Briggs, S.D., Brock, H.W., Martin, M.E., Gibbs, D., Allis, C.D., and Hess, J.L. (2002) MLL targets SET domain methyltransferase activity to Hox gene promoters. *Mol Cell* **10** (5): 1107–1117.

Milne, T.A., Dou, Y., Martin, M.E., Brock, H.W., Roeder, R.G., and Hess, J.L. (2005a) MLL associates specifically with a subset of transcriptionally active target genes. *Proc Natl Acad Sci U S A* **102** (41): 14765–14770.

Milne, T.A., Hughes, C.M., Lloyd, R., Yang, Z., Rozenblatt-Rosen, O., Dou, Y., *et al.* (2005b) Menin and MLL cooperatively regulate expression of cyclin-dependent kinase inhibitors. *Proc Natl Acad Sci U S A* **102** (3): 749–754.

Mirski, S.E., Gerlach, J.H., and Cole, S.P. (1999) Sequence determinants of nuclear localization in the alpha and beta isoforms of human topoisomerase II. *Exp Cell Res* **251** (2): 329–339.

Mirski, S.E., Gerlach, J.H., Cummings, H.J., Zirngibl, R., Greer, P.A., and Cole, S.P. (1997) Bipartite nuclear localization signals in the C terminus of human topoisomerase II alpha. *Exp Cell Res* **237** (2): 452–455.

Morgan, B.A. (1997) Hox genes and embryonic development. *Poult Sci* **76** (1): 96–104.

Mueller, D., García-Cuéllar, M.-P., Bach, C., Buhl, S., Maethner, E., and Slany, R.K. (2009) Misguided transcriptional elongation causes mixed lineage leukemia. *PLoS Biol* **7** (11): e1000249.

Muller, M.T., Spitzner, J.R., DiDonato, J.A., Mehta, V.B., and Tsutsui, K. (1988) Single-strand DNA cleavages by eukaryotic topoisomerase II. *Biochemistry* **27** (22): 8369–8379.

Murano, K., Okuwaki, M., Hisaoka, M., and Nagata, K. (2008) Transcription regulation of the rRNA gene by a multifunctional nucleolar protein, B23/nucleophosmin, through its histone chaperone activity. *Mol Cell Biol* **28** (10): 3114–3126.

Myers, L.C., and Kornberg, R.D. (2000) Mediator of transcriptional regulation. *Annu Rev Biochem* **69:** 729–749.

Nakamura, T., Mori, T., Tada, S., Krajewski, W., Rozovskaia, T., Wassell, R., *et al.* (2002) ALL-1 is a histone methyltransferase that assembles a supercomplex of proteins involved in transcriptional regulation. *Mol Cell* **10** (5): 1119–1128.

Nelson, L.R., and Bulun, S.E. (2001) Estrogen production and action. *J Am Acad Dermatol* **45** (3 Suppl): S116-24.

Neurath, H., and Walsh, K.A. (1976) Role of proteolytic enzymes in biological regulation (a review). *Proc Natl Acad Sci U S A* **73** (11): 3825–3832.

Nicholson, D.W. (1999) Caspase structure, proteolytic substrates, and function during apoptotic cell death. *Cell Death Differ* **6** (11): 1028–1042.

Niizuma, H., Cheng, E.H., and Hsieh, J.J. (2015) Taspase 1: A protease with many biological surprises. *Mol Cell Oncol* **2** (4): e999513.

Nilson, I., Löchner, K., Siegler, G., Greil, J., Beck, J.D., Fey, G.H., and Marschalek, R. (1996) Exon/intron structure of the human ALL-1 (MLL) gene involved in translocations to chromosomal region 11q23 and acute leukaemias. *Br J Haematol* **93** (4): 966–972.

Nilsson, S., Mäkelä, S., Treuter, E., Tujague, M., Thomsen, J., Andersson, G., *et al.* (2001) Mechanisms of estrogen action. *Physiol Rev* **81** (4): 1535–1565.

Nitiss, J.L. (1998) Investigating the biological functions of DNA topoisomerases in eukaryotic cells. *Biochim Biophys Acta* **1400** (1-3): 63–81.

Nitiss, J.L. (2009) Targeting DNA topoisomerase II in cancer chemotherapy. *Nat Rev Cancer* **9** (5): 338–350.

O'Donnell, L., Robertson, K.M., Jones, M.E., and Simpson, E.R. (2001) Estrogen and spermatogenesis. *Endocr Rev* **22** (3): 289–318.

Oelgeschläger, T., Chiang, C.M., and Roeder, R.G. (1996) Topology and reorganization of a human TFIID-promoter complex. *Nature* **382** (6593): 735–738.

Okuwaki, M., Matsumoto, K., Tsujimoto, M., and Nagata, K. (2001) Function of nucleophosmin/B23, a nucleolar acidic protein, as a histone chaperone. *FEBS Lett* **506** (3): 272–276.

Oláh, J., Vincze, O., Virók, D., Simon, D., Bozsó, Z., Tõkési, N., *et al.* (2011) Interactions of pathological hallmark proteins: tubulin polymerization promoting protein/p25, beta-amyloid, and alpha-synuclein. *J Biol Chem* **286** (39): 34088–34100.

Orphanides, G., Lagrange, T., and Reinberg, D. (1996) The general transcription factors of RNA polymerase II. *Genes Dev* **10** (21): 2657–2683.

Osheroff, N., Zechiedrich, E.L., and Gale, K.C. (1991) Catalytic function of DNA topoisomerase II. *Bioessays* **13** (6): 269–273.

Oughtred, R., Rust, J., Chang, C., Breitkreutz, B.-J., Stark, C., Willems, A., *et al.* (2021) The BioGRID database: A comprehensive biomedical resource of curated protein, genetic, and chemical interactions. *Protein Sci* **30** (1): 187–200.

Ozer, J., Moore, P.A., Bolden, A.H., Lee, A., Rosen, C.A., and Lieberman, P.M. (1994) Molecular cloning of the small (gamma) subunit of human TFIIA reveals functions critical for activated transcription. *Genes Dev* **8** (19): 2324–2335.

Pedersen-Bjergaard, J., Andersen, M.K., and Johansson, B. (1998) Balanced chromosome aberrations in leukemias following chemotherapy with DNA-topoisomerase II inhibitors. *J Clin Oncol* **16** (5): 1897–1898.

Pommier, Y., Sun, Y., Huang, S.-Y.N., and Nitiss, J.L. (2016) Roles of eukaryotic topoisomerases in transcription, replication and genomic stability. *Nat Rev Mol Cell Biol* **17** (11): 703–721.

Qyang, Y., Luo, X., Lu, T., Ismail, P.M., Krylov, D., Vinson, C., and Sawadogo, M. (1999) Cell-type-dependent activity of the ubiquitous transcription factor USF in cellular proliferation and transcriptional activation. *Mol Cell Biol* **19** (2): 1508–1517.

Rasio, D., Schichman, S.A., Negrini, M., Canaani, E., and Croce, C.M. (1996) Complete exon structure of the ALL1 gene. *Cancer Res* **56** (8): 1766–1769.

Rawlings, N.D., and Barrett, A.J. (2020) MEROPS - the Peptidase Database: Release 12.2. [WWW document]. URL https://www.ebi.ac.uk/merops/cgi-bin/speccards?sp=sp001823;type=peptidase.

Rawlings, N.D., Barrett, A.J., Thomas, P.D., Huang, X., Bateman, A., and Finn, R.D. (2018) The MEROPS database of proteolytic enzymes, their substrates and

inhibitors in 2017 and a comparison with peptidases in the PANTHER database. *Nucleic Acids Res* **46** (D1): D624-D632.

Read, L.D., Keith, D., Slamon, D.J., and Katzenellenbogen, B.S. (1990) Hormonal modulation of HER-2/neu protooncogene messenger ribonucleic acid and p185 protein expression in human breast cancer cell lines. *Cancer Res* **50** (13): 3947–3951.

Reese, J.C. (2003) Basal transcription factors. *Current Opinion in Genetics & Development* **13** (2): 114–118.

Ringrose, L., and Paro, R. (2004) Epigenetic regulation of cellular memory by the Polycomb and Trithorax group proteins. *Annu Rev Genet* **38:** 413–443.

Robinson, M.J., Corbett, A.H., and Osheroff, N. (1993) Effects of topoisomerase II-targeted drugs on enzyme-mediated DNA cleavage and ATP hydrolysis: evidence for distinct drug interaction domains on topoisomerase II. *Biochemistry* **32** (14): 3638–3643.

Roca, J., and Wang, J.C. (1994) DNA transport by a type II DNA topoisomerase: Evidence in favor of a two-gate mechanism. *Cell* **77** (4): 609–616.

Rowley, J.D., and Olney, H.J. (2002) International workshop on the relationship of prior therapy to balanced chromosome aberrations in therapy-related myelodysplastic syndromes and acute leukemia: overview report. *Genes Chromosomes Cancer* **33** (4): 331–345.

Roy, A.L., Meisterernst, M., Pognonec, P., and Roeder, R.G. (1991) Cooperative interaction of an initiator-binding transcription initiation factor and the helix-loop-helix activator USF. *Nature* **354** (6350): 245–248.

Rozenblatt-Rosen, O., Rozovskaia, T., Burakov, D., Sedkov, Y., Tillib, S., Blechman, J., *et al.* (1998) The C-terminal SET domains of ALL-1 and TRITHORAX interact with the INI1 and SNR1 proteins, components of the SWI/SNF complex. *Proc Natl Acad Sci U S A* **95** (8): 4152–4157.

Ruggiero, R.J., and Likis, F.E. (2002) ESTROGEN: PHYSIOLOGY, PHARMACOLOGY, AND FORMULATIONS FOR REPLACEMENT THERAPY. *Journal of Midwifery & Women's Health* **47** (3): 130–138.

Russell, K.S., and Hung, M.C. (1992) Transcriptional repression of the neu protooncogene by estrogen stimulated estrogen receptor. *Cancer Res* **52** (23): 6624–6629.

Sabbah, M., Courilleau, D., Mester, J., and Redeuilh, G. (1999) Estrogen induction of the cyclin D1 promoter: involvement of a cAMP response-like element. *Proc Natl Acad Sci U S A* **96** (20): 11217–11222.

Sanger, F., and Coulson, A.R. (1975) A rapid method for determining sequences in DNA by primed synthesis with DNA polymerase. *Journal of Molecular Biology* **94** (3): 441–448.

Sano, K., Miyaji-Yamaguchi, M., Tsutsui, K.M., and Tsutsui, K. (2008) Topoisomerase IIbeta activates a subset of neuronal genes that are repressed in AT-rich genomic environment. *PLoS ONE* **3** (12): e4103.

Sasaki, M., Sugio, K., Kuwabara, Y., Koga, H., Nakagawa, M., Chen, T., *et al.* (2003) Alterations of tumor suppressor genes (Rb, p16, p27 and p53) and an increased FDG uptake in lung cancer. *Ann Nucl Med* **17** (3): 189–196.

Savkur, R.S., and Olson, M.O. (1998) Preferential cleavage in pre-ribosomal RNA byprotein B23 endoribonuclease. *Nucleic Acids Res* **26** (19): 4508–4515.

Sawadogo, M. (1988) Multiple forms of the human gene-specific transcription factor USF. II. DNA binding properties and transcriptional activity of the purified HeLa USF. *Journal of Biological Chemistry* **263** (24): 11994–12001.

Sawadogo, M., and Roeder, R.G. (1985) Interaction of a gene-specific transcription factor with the adenovirus major late promoter upstream of the TATA box region. *Cell* **43** (1): 165–175.

Sawadogo, M., van Dyke, M.W., Gregor, P.D., and Roeder, R.G. (1988) Multiple forms of the human gene-specific transcription factor USF. I. Complete purification and identification of USF from HeLa cell nuclei. *Journal of Biological Chemistry* **263** (24): 11985–11993.

Schuettengruber, B., Chourrout, D., Vervoort, M., Leblanc, B., and Cavalli, G. (2007) Genome regulation by polycomb and trithorax proteins. *Cell* **128** (4): 735–745.

Sehested, M., and Jensen, P.B. (1996) Mapping of DNA topoisomerase II poisons (etoposide, clerocidin) and catalytic inhibitors (aclarubicin, ICRF-187) to four distinct steps in the topoisomerase II catalytic cycle. *Biochem Pharmacol* **51** (7): 879–886.

Shang, Y., Hu, X., DiRenzo, J., Lazar, M.A., and Brown, M. (2000) Cofactor dynamics and sufficiency in estrogen receptor-regulated transcription. *Cell* **103** (6): 843–852.

Sherr, C.J. (2001) The INK4a/ARF network in tumour suppression. *Nat Rev Mol Cell Biol* **2** (10): 731–737.

Sirito, M., Lin, Q., Deng, J.M., Behringer, R.R., and Sawadogo, M. (1998) Overlapping roles and asymmetrical cross-regulation of the USF proteins in mice. *Proc Natl Acad Sci U S A* **95** (7): 3758–3763.

Sirito, M., Lin, Q., Maity, T., and Sawadogo, M. (1994) Ubiquitous expression of the 43- and 44-kDa forms of transcription factor USF in mammalian cells. *Nucleic Acids Res* **22** (3): 427–433.

Sirito, M., Walker, S., Lin, Q., Kozlowski, M.T., Klein, W.H., and Sawadogo, M. (1992) Members of the USF family of helix-loop-helix proteins bind DNA as homo- as well as heterodimers. *Gene Expr* **2** (3): 231–240.

Skaar, T.C., Prasad, S.C., Sharareh, S., Lippman, M.E., Brünner, N., and Clarke, R. (1998) Two-dimensional gel electrophoresis analyses identify nucleophosmin as an estrogen regulated protein associated with acquired estrogen-independence in human breast cancer cells. *The Journal of Steroid Biochemistry and Molecular Biology* **67** (5-6): 391–402.

Slany, R.K. (2009) The molecular biology of mixed lineage leukemia. *Haematologica* **94** (7): 984–993.

Sng, J.-H., Heaton, V.J., Bell, M., Maini, P., Austin, C.A., and Fisher, L. (1999) Molecular cloning and characterization of the human topoisomerase IIα and IIβ genes: evidence for isoform evolution through gene duplication 1Sequences described here have been submitted to the EMBL/GenBank databases under

accession nos. AJ011721–AJ011732 and AJ011741–AJ011758. Part of this work was presented as a poster at the Fourth Conference on DNA Topoisomerases in Therapy, New York, 1992: J.-H. Sng, C.A. Austin, L.M. Fisher. Cloning the human topoisomerase IIα gene. Abstract P03. 1. *Biochimica et Biophysica Acta (BBA) - Gene Structure and Expression* **1444** (3): 395–406.

Sørensen, B.S., Sinding, J., Andersen, A.H., Alsner, J., Jensen, P.B., and Westergaard, O. (1992) Mode of action of topoisomerase II-targeting agents at a specific DNA sequence. *Journal of Molecular Biology* **228** (3): 778–786.

Spitzner, J.R., and Muller, M.T. (1988) A consensus sequence for cleavage by vertebrate DNA topoisomerase II. *Nucleic Acids Res* **16** (12): 5533–5556.

Sternlicht, M.D., and Werb, Z. (2001) How matrix metalloproteinases regulate cell behavior. *Annu Rev Cell Dev Biol* **17:** 463–516.

Storre, J., Elsässer, H.-P., Fuchs, M., Ullmann, D., Livingston, D.M., and Gaubatz, S. (2002) Homeotic transformations of the axial skeleton that accompany a targeted deletion of E2f6. *EMBO Rep* **3** (7): 695–700.

Strissel, P.L., Strick, R., Tomek, R.J., Roe, B.A., Rowley, J.D., and Zeleznik-Le, N.J. (2000) DNA structural properties of AF9 are similar to MLL and could act as recombination hot spots resulting in MLL/AF9 translocations and leukemogenesis. *Hum Mol Genet* **9** (11): 1671–1679.

Szijan, I., Parma, D.L., and Engel, N.I. (1992) Expression of c-myc and c-fos protooncogenes in the anterior pituitary gland of the rat. Effect of estrogen. *Horm Metab Res* **24** (4): 154–157.

Takeda, S., Chen, D.Y., Westergard, T.D., Fisher, J.K., Rubens, J.A., Sasagawa, S., *et al.* (2006) Proteolysis of MLL family proteins is essential for taspase1-orchestrated cell cycle progression. *Genes Dev* **20** (17): 2397–2409.

Takeda, S., Sasagawa, S., Oyama, T., Searleman, A.C., Westergard, T.D., Cheng, E.H., and Hsieh, J.J. (2015) Taspase1-dependent TFIIA cleavage coordinates head morphogenesis by limiting Cdkn2a locus transcription. *J Clin Invest* **125** (3): 1203–1214.

Taylor, H.S. (2000) The role of HOX genes in the development and function of the female reproductive tract. *Semin Reprod Med* **18** (1): 81–89.

Teitz, T., Wei, T., Valentine, M.B., Vanin, E.F., Grenet, J., Valentine, V.A., *et al.* (2000) Caspase 8 is deleted or silenced preferentially in childhood neuroblastomas with amplification of MYCN. *Nat Med* **6** (5): 529–535.

Tenney, K., and Shilatifard, A. (2005) A COMPASS in the voyage of defining the role of trithorax/MLL-containing complexes: linking leukemogensis to covalent modifications of chromatin. *J Cell Biochem* **95** (3): 429–436.

The UniProt Consortium (2021) UniProt: the universal protein knowledgebase in 2021. *Nucleic Acids Res* **49** (D1): D480-D489.

Thomas, M.C., and Chiang, C.-M. (2006) The general transcription machinery and general cofactors. *Crit Rev Biochem Mol Biol* **41** (3): 105–178.

Thompson, L.H., and Schild, D. (2001) Homologous recombinational repair of DNA ensures mammalian chromosome stability. *Mutation Research/Fundamental and Molecular Mechanisms of Mutagenesis* **477** (1-2): 131–153.

Trotter, K.W., King, H.A., and Archer, T.K. (2015) Glucocorticoid Receptor Transcriptional Activation via the BRG1-Dependent Recruitment of TOP2β and Ku70/86. *Mol Cell Biol* **35** (16): 2799–2817.

Tsai-Pflugfelder, M., Liu, L.F., Liu, A.A., Tewey, K.M., Whang-Peng, J., Knutsen, T., *et al.* (1988) Cloning and sequencing of cDNA encoding human DNA topoisomerase II and localization of the gene to chromosome region 17q21-22. *Proc Natl Acad Sci U S A* **85** (19): 7177–7181.

Turk, B. (2006) Targeting proteases: successes, failures and future prospects. *Nat Rev Drug Discov* **5** (9): 785–799.

Tyagi, S., Chabes, A.L., Wysocka, J., and Herr, W. (2007) E2F activation of S phase promoters via association with HCF-1 and the MLL family of histone H3K4 methyltransferases. *Mol Cell* **27** (1): 107–119.

Vallet, V.S., Henrion, A.A., Bucchini, D., Casado, M., Raymondjean, M., Kahn, A., and Vaulont, S. (1997) Glucose-dependent liver gene expression in upstream stimulatory factor 2 -/- mice. *J Biol Chem* **272** (35): 21944–21949.

van den Boom, J., Hensel, A., Trusch, F., Matena, A., Siemer, S., Guel, D., *et al.* (2020) The other side of the corona: nanoparticles inhibit the protease taspase1 in a size-dependent manner. *Nanoscale* **12** (37): 19093–19103.

van den Boom, J., Mamić, M., Baccelliere, D., Zweerink, S., Kaschani, F., Knauer, S., *et al.* (2014) Peptidyl succinimidyl peptides as taspase 1 inhibitors. *Chembiochem* **15** (15): 2233–2237.

van den Boom, J., Trusch, F., Hoppstock, L., Beuck, C., and Bayer, P. (2016) Structural Characterization of the Loop at the Alpha-Subunit C-Terminus of the Mixed Lineage Leukemia Protein Activating Protease Taspase1. *PLoS ONE* **11** (3): e0151431.

van der Burg, B., van Selm-Miltenburg, A.J., Laat, S.W. de, and van Zoelen, E.J. (1989) Direct effects of estrogen on c-fos and c-myc protooncogene expression and cellular proliferation in human breast cancer cells. *Molecular and Cellular Endocrinology* **64** (2): 223–228.

Vandromme, M., Cavadore, J.C., Bonnieu, A., Froeschlé, A., Lamb, N., and Fernandez, A. (1995) Two nuclear localization signals present in the basic-helix 1 domains of MyoD promote its active nuclear translocation and can function independently. *Proc Natl Acad Sci U S A* **92** (10): 4646–4650.

Vann, K.R., Oviatt, A.A., and Osheroff, N. (2021) Topoisomerase II Poisons: Converting Essential Enzymes into Molecular Scissors. *Biochemistry* **60** (21): 1630–1641.

Vélez-Cruz, R., and Johnson, D.G. (2017) The Retinoblastoma (RB) Tumor Suppressor: Pushing Back against Genome Instability on Multiple Fronts. *Int J Mol Sci* **18** (8).

Vendrell, J.A., Magnino, F., Danis, E., Duchesne, M.J., Pinloche, S., Pons, M., *et al.* (2004) Estrogen regulation in human breast cancer cells of new downstream gene targets involved in estrogen metabolism, cell proliferation and cell transformation. *J Mol Endocrinol* **32** (2): 397–414.

Villamil, M.A., Liang, Q., Chen, J., Choi, Y.S., Hou, S., Lee, K.H., and Zhuang, Z. (2012) Serine phosphorylation is critical for the activation of ubiquitin-specific

protease 1 and its interaction with WD40-repeat protein UAF1. *Biochemistry* **51** (45): 9112–9123.

Vinogradov, A.E., and Anatskaya, O.V. (2017) DNA helix: the importance of being AT-rich. *Mamm Genome* **28** (9-10): 455–464.

Viollet, B., Lefrançois-Martinez, A.M., Henrion, A., Kahn, A., Raymondjean, M., and Martinez, A. (1996) Immunochemical characterization and transacting properties of upstream stimulatory factor isoforms. *J Biol Chem* **271** (3): 1405–1415.

Vizovisek, M., Ristanovic, D., Menghini, S., Christiansen, M.G., and Schuerle, S. (2021) The Tumor Proteolytic Landscape: A Challenging Frontier in Cancer Diagnosis and Therapy. *Int J Mol Sci* **22** (5).

Waladali, W., Luo, Y., Li, W.S., Zheng, M.X., and Hu, Q.L. (2009) 17Beta-estradiol affects the proliferation and apoptosis of rat bladder neck smooth muscle cells by modulating cell cycle transition and related proteins. *World J Urol* **27** (2): 241–248.

Wang, F., Li, P., Shao, Y., Li, Y., Zhang, K., Li, M., *et al.* (2020) Site-specific proteolytic cleavage prevents ubiquitination and degradation of human REV3L, the catalytic subunit of DNA polymerase ζ. *Nucleic Acids Res* **48** (7): 3619–3637.

Wang, J.C. (1996) DNA topoisomerases. *Annu Rev Biochem* **65:** 635–692.

Wang, J.C. (2002) Cellular roles of DNA topoisomerases: a molecular perspective. *Nat Rev Mol Cell Biol* **3** (6): 430–440.

Wang, T.J., Huang, M.S., Hong, C.Y., Tse, V., Silverberg, G.D., and Hsiao, M. (2001) Comparisons of tumor suppressor p53, p21, and p16 gene therapy effects on glioblastoma tumorigenicity in situ. *Biochem Biophys Res Commun* **287** (1): 173–180.

Wang, W., Budhu, A., Forgues, M., and Wang, X.W. (2005) Temporal and spatial control of nucleophosmin by the Ran-Crm1 complex in centrosome duplication. *Nat Cell Biol* **7** (8): 823–830.

Wiederschain, D., Kawai, H., Shilatifard, A., and Yuan, Z.-M. (2005) Multiple mixed lineage leukemia (MLL) fusion proteins suppress p53-mediated response to DNA damage. *J Biol Chem* **280** (26): 24315–24321.

Woessner, R.D., Mattern, M.R., Mirabelli, C.K., Johnson, R.K., and Drake, F.H. (1991) Proliferation- and cell cycle-dependent differences in expression of the 170 kilodalton and 180 kilodalton forms of topoisomerase II in NIH-3T3 cells. *Cell Growth Differ* **2** (4): 209–214.

Wong, R.H.F., Chang, I., Hudak, C.S.S., Hyun, S., Kwan, H.-Y., and Sul, H.S. (2009) A role of DNA-PK for the metabolic gene regulation in response to insulin. *Cell* **136** (6): 1056–1072.

Wünsch, D., Hahlbrock, A., Heiselmayer, C., Bäcker, S., Heun, P., Goesswein, D., *et al.* (2015) Fly versus man: evolutionary impairment of nucleolar targeting affects the degradome of Drosophila's Taspase1. *FASEB J* **29** (5): 1973–1985.

Xia, Z.-B., Anderson, M., Diaz, M.O., and Zeleznik-Le, N.J. (2003) MLL repression domain interacts with histone deacetylases, the polycomb group proteins HPC2 and BMI-1, and the corepressor C-terminal-binding protein. *Proc Natl Acad Sci U S A* **100** (14): 8342–8347.

Xia, Z.-B., Popovic, R., Chen, J., Theisler, C., Stuart, T., Santillan, D.A., *et al.* (2005) The MLL fusion gene, MLL-AF4, regulates cyclin-dependent kinase inhibitor CDKN1B (p27kip1) expression. *Proc Natl Acad Sci U S A* **102** (39): 14028–14033.

Yagi, H., Deguchi, K., Aono, A., Tani, Y., Kishimoto, T., and Komori, T. (1998) Growth Disturbance in Fetal Liver Hematopoiesis of Mll-Mutant Mice. *Blood* **92** (1): 108–117.

Yamaguchi, Y., Wada, T., Watanabe, D., Takagi, T., Hasegawa, J., and Handa, H. (1999) Structure and function of the human transcription elongation factor DSIF. *J Biol Chem* **274** (12): 8085–8092.

Yang, X., Li, W., Prescott, E.D., Burden, S.J., and Wang, J.C. (2000) DNA Topoisomerase IIβ and Neural Development // DNA topoisomerase IIbeta and neural development. *Science* **287** (5450): 131–134.

Yang, Z., Cheng, B., Song, J., Wan, Y., Wang, Q., Cheng, B., and Chen, X. (2007) Estrogen accelerates G1 to S phase transition and induces a G2/M phase-predominant apoptosis in synthetic vascular smooth muscle cells. *Int J Cardiol* **118** (3): 381–388.

Yokoyama, A., Kitabayashi, I., Ayton, P.M., Cleary, M.L., and Ohki, M. (2002) Leukemia proto-oncoprotein MLL is proteolytically processed into 2 fragments with opposite transcriptional properties. *Blood* **100** (10): 3710–3718.

Yokoyama, A., Somervaille, T., and Cleary, M.L. (2005) The Menin Tumor Suppressor Protein Is an Essential Oncogenic Cofactor for MLL-Associated Leukemogenesis. *Blood* **106** (11): 665.

Yokoyama, A., Wang, Z., Wysocka, J., Sanyal, M., Aufiero, D.J., Kitabayashi, I., *et al.* (2004) Leukemia proto-oncoprotein MLL forms a SET1-like histone methyltransferase complex with menin to regulate Hox gene expression. *Mol Cell Biol* **24** (13): 5639–5649.

Youn, J.-Y., Dunham, W.H., Hong, S.J., Knight, J.D.R., Bashkurov, M., Chen, G.I., *et al.* (2018) High-Density Proximity Mapping Reveals the Subcellular Organization of mRNA-Associated Granules and Bodies. *Mol Cell* **69** (3): 517-532.e11.

Yu, B.D., Hanson, R.D., Hess, J.L., Horning, S.E., and Korsmeyer, S.J. (1998) MLL, a mammalian trithorax-group gene, functions as a transcriptional maintenance factor in morphogenesis. *Proc Natl Acad Sci U S A* **95** (18): 10632–10636.

Yu, B.D., Hess, J.L., Horning, S.E., Brown, G.A., and Korsmeyer, S.J. (1995) Altered Hox expression and segmental identity in Mll-mutant mice. *Nature* **378** (6556): 505–508.

Yu, Y., Maggi, L.B., Brady, S.N., Apicelli, A.J., Dai, M.-S., Lu, H., and Weber, J.D. (2006) Nucleophosmin is essential for ribosomal protein L5 nuclear export. *Mol Cell Biol* **26** (10): 3798–3809.

Zeleznik-Le, N.J., Harden, A.M., and Rowley, J.D. (1994) 11q23 translocations split the "AT-hook" cruciform DNA-binding region and the transcriptional repression domain from the activation domain of the mixed-lineage leukemia (MLL) gene. *Proc Natl Acad Sci U S A* **91** (22): 10610–10614.

Zheng, R.-P., Wang, W., and Wei, C.-D. (2015) Bortezomib inhibits cell proliferation in prostate cancer. *Exp Ther Med* **10** (3): 1219–1223.

Zhou, H., Spicuglia, S., Hsieh, J.J.-D., Mitsiou, D.J., Høiby, T., Veenstra, G.J.C., *et al.* (2006) Uncleaved TFIIA is a substrate for taspase 1 and active in transcription. *Mol Cell Biol* **26** (7): 2728–2735.

Zhou, Y., Shen, J., Xia, L., and Wang, Y. (2014) Estrogen mediated expression of nucleophosmin 1 in human endometrial carcinoma clinical stages through estrogen receptor-α signaling. *Cancer Cell Int* **14** (1): 540.

Zhu, Y., Singh, B., Hewitt, S., Liu, A., Gomez, B., Wang, A., and Clarke, R. (2006) Expression patterns among interferon regulatory factor-1, human X-box binding protein-1, nuclear factor kappa B, nucleophosmin, estrogen receptor-alpha and progesterone receptor proteins in breast cancer tissue microarrays. *Int J Oncol* **28** (1): 67–76.

Ziemin-van der Poel, S., McCabe, N.R., Gill, H.J., Espinosa, R., Patel, Y., Harden, A., *et al.* (1991) Identification of a gene, MLL, that spans the breakpoint in 11q23 translocations associated with human leukemias. *Proc Natl Acad Sci U S A* **88** (23): 10735–10739.

6 APPENDIX

6.1 SUPPORTING INFORMATION

Table 6.1: Mass spectrometrically identified proteins in Taspase1-GFP complexes

-LOG (P-value)	Difference	Protein names	Gene names
1,4533	1,4459	Protein AATF	AATF
1,3894	0,7370	ATP-binding cassette sub-family D member 3	ABCD3
2,2353	2,5468	Activator of basal transcription 1	ABT1
2,2388	2,4690	Protein ELYS	AHCTF1
2,5335	3,0525	ATPase family AAA domain-containing protein 2	ATAD2
3,2639	1,9490	Bromodomain adjacent to zinc finger domain protein 1A	BAZ1A
1,5911	1,0452	Tyrosine-protein kinase BAZ1B	BAZ1B
3,5857	2,5714	Bromodomain adjacent to zinc finger domain protein 2A	BAZ2A
1,7551	1,4528	Bloom syndrome protein	BLM
2,3170	2,2029	Ribosome biogenesis protein BMS1 homolog	BMS1
2,4213	1,6777	Ribosome biogenesis protein BOP1	BOP1
2,2828	1,8470	Nucleosome-remodeling factor subunit BPTF	BPTF
3,1971	5,7335	Ribosome biogenesis protein BRX1 homolog	BRIX1
2,2387	1,7486	Bystin	BYSL
1,7886	1,6806	Leydig cell tumor 10 kDa protein homolog	C19orf53
2,0007	1,4325	Uncharacterized protein C7orf50	C7orf50
1,5284	0,8471	Chromobox protein homolog 3	CBX3
2,7491	2,9865	Chromobox protein homolog 5	CBX5
2,9865	1,8999	Cell division cycle and apoptosis regulator protein 1	CCAR1
2,3920	1,8936	Coiled-coil domain-containing protein 137	CCDC137
3,2868	3,1116	Coiled-coil domain-containing protein 86	CCDC86
2,9838	1,2425	Coiled-coil domain-containing protein 94	CCDC94
2,8792	2,3459	Tumor suppressor ARF	CDKN2A
3,1602	5,2704	CCAAT/enhancer-binding protein zeta	CEBPZ
3,4640	3,3583	Centromere protein V	CENPV
4,0012	1,6876	Chromatin assembly factor 1 subunit A	CHAF1A
1,6820	1,2356	Charged multivesicular body protein 4b	CHMP4B
2,7958	2,3254	Coilin	COIL
1,2392	1,2645	Transcriptional repressor CTCF	CTCF

-LOG (P-value)	Difference	Protein names	Gene names
1,5579	2,5362	Spliceosome-associated protein CWC15 homolog	CWC15
1,6575	2,3532	DDB1- and CUL4-associated factor 13	DCAF13
3,6214	4,1330	Probable ATP-dependent RNA helicase DDX10	DDX10
1,8640	1,1750	Probable ATP-dependent RNA helicase DDX17	DDX17
3,8437	2,3457	ATP-dependent RNA helicase DDX18	DDX18
3,2941	1,9227	Nucleolar RNA helicase 2	DDX21
2,2878	2,2877	ATP-dependent RNA helicase DDX24	DDX24
3,8272	5,7230	Probable ATP-dependent RNA helicase DDX27	DDX27
2,3555	2,3129	Probable ATP-dependent RNA helicase DDX31	DDX31
3,8412	2,2557	ATP-dependent RNA helicase DDX50	DDX50
2,6405	2,1053	ATP-dependent RNA helicase DDX51	DDX51
2,5235	1,3294	Probable ATP-dependent RNA helicase DDX52	DDX52
2,8915	4,0868	ATP-dependent RNA helicase DDX54	DDX54
2,4602	2,6282	Probable ATP-dependent RNA helicase DDX56	DDX56
2,9556	1,6690	Putative ATP-dependent RNA helicase DHX30	DHX30
1,4653	1,7830	Putative ATP-dependent RNA helicase DHX33	DHX33
1,4248	1,9336	Probable ATP-dependent RNA helicase DHX37	DHX37
1,7726	2,4872	DnaJ homolog subfamily C member 9	DNAJC9
2,9996	3,4663	Deoxynucleotidyltransferase terminal-interacting protein 2	DNTTIP2
2,1280	1,0841	Protein dpy-30 homolog	DPY30
4,8000	5,0413	Probable rRNA-processing protein EBP2	EBNA1BP2
1,9080	1,2859	Polycomb protein EED	EED
1,6631	1,4313	Histone-lysine N-methyltransferase EHMT1	EHMT1
2,8442	1,7448	Histone-lysine N-methyltransferase EHMT2	EHMT2
2,3417	1,6139	Eukaryotic translation initiation factor 6	EIF6
1,6847	1,6106	Emerin	EMD
2,0667	0,9847	Ribosomal RNA small subunit methyltransferase NEP1	EMG1
2,2262	3,3614	ESF1 homolog	ESF1
3,1632	2,4612	Exosome component 10	EXOSC10
2,9519	3,6399	Exosome complex component RRP4	EXOSC2
1,6117	2,1803	Exosome complex component RRP40	EXOSC3
1,9324	2,6287	Exosome complex component RRP41	EXOSC4
3,7153	2,4533	Exosome complex component MTR3	EXOSC6

-LOG (P-value)	Difference	Protein names	Gene names
1,9823	2,4380	Exosome complex component RRP42	EXOSC7
2,6942	2,5019	40S ribosomal protein S30	FAU
3,2244	4,7385	rRNA 2-O-methyltransferase fibrillarin	FBL
4,8024	4,8114	pre-rRNA processing protein FTSJ3	FTSJ3
2,2796	2,4053	RNA-binding protein FUS	FUS
1,7476	1,2681	Fragile X mental retardation syndrome-related protein 2	FXR2
2,3209	2,5170	Transcriptional repressor p66-alpha	GATAD2A
5,3776	5,7870	Nucleolar GTP-binding protein 2	GNL2
3,1080	4,4706	Guanine nucleotide-binding protein-like 3	GNL3
2,2115	0,7465	G patch domain-containing protein 4	GPATCH4
3,7024	1,5834	Glutamate-rich WD repeat-containing protein 1	GRWD1
1,6823	1,6750	General transcription factor 3C polypeptide 1	GTF3C1
1,8963	2,1141	General transcription factor 3C polypeptide 2	GTF3C2
3,1262	2,7694	Nucleolar GTP-binding protein 1	GTPBP4
1,4253	1,2334	Histone H1x	H1FX
2,3602	1,2364	Core histone macro-H2A.2;Histone H2A	H2AFY2
1,3256	3,6191	Histone H3;Histone H3.3	H3F3B;H3F3A
2,5558	3,2446	High mobility group protein HMG-I/HMG-Y	HMGA1
1,8784	1,3071	High mobility group protein HMGI-C	HMGA2
1,2209	1,3666	Non-histone chromosomal protein HMG-14	HMGN1
1,6388	1,4234	Heterogeneous nuclear ribonucleoprotein A0	HNRNPA0
2,5787	1,5488	Heterogeneous nuclear ribonucleoprotein A1	HNRNPA1
3,7621	1,8814	Heterogeneous nuclear ribonucleoproteins A2/B1	HNRNPA2B1
3,0915	1,6334	Heterogeneous nuclear ribonucleoprotein A3	HNRNPA3
4,3729	3,1751		HNRNPDL
1,4516	1,2002	Heterogeneous nuclear ribonucleoprotein H3	HNRNPH3
1,9890	0,5093	Heterogeneous nuclear ribonucleoprotein L	HNRNPL
6,3544	2,3546	Heterogeneous nuclear ribonucleoprotein R	HNRNPR
1,3737	0,8358	Heterogeneous nuclear ribonucleoprotein U	HNRNPU
3,1137	1,8892	Heterogeneous nuclear ribonucleoprotein U-like protein 1	HNRNPUL1
1,7421	2,1135	Protein Red	IK
2,9789	1,0759	Interleukin enhancer-binding factor 3	ILF3

-LOG (P-value)	Difference	Protein names	Gene names
1,3468	1,0357	U3 small nucleolar ribonucleoprotein protein IMP4	IMP4
2,0401	1,4577	Inner centromere protein	INCENP
1,7065	2,1915	Interferon-stimulated 20 kDa exonuclease-like 2	ISG20L2
3,8081	2,6055	KH domain-containing, RNA-binding, signal transduction-associated protein 1	KHDRBS1
3,0654	5,1239	Pumilio domain-containing protein KIAA0020	KIAA0020
2,6767	2,3267	Protein virilizer homolog	KIAA1429
2,5467	1,1927	Kinesin-like protein KIF18B	KIF18B
2,1445	2,0079	Protein KRI1 homolog	KRI1
2,6682	3,4815	KRR1 small subunit processome component homolog	KRR1
3,1549	1,5708	La-related protein 7	LARP7
3,3361	2,1252	Ribosomal biogenesis protein LAS1L	LAS1L
2,4959	2,3177	DNA ligase 3	LIG3
1,9398	1,3669	Protein lin-28 homolog B	LIN28B
2,2276	2,4426	Cell growth-regulating nucleolar protein	LYAR
3,0941	3,5466	Protein MAK16 homolog	MAK16
6,0013	5,0391	Mediator of DNA damage checkpoint protein 1	MDC1
2,1020	1,8919	Midasin	MDN1
3,7258	2,8227	Methyl-CpG-binding protein 2	MECP2
1,5049	0,7477	Mediator of RNA polymerase II transcription subunit 15	MED15
1,5297	1,0902	Mediator of RNA polymerase II transcription subunit 6	MED6
2,2304	3,6387	Antigen KI-67	MKI67
1,6823	1,8192	U3 small nucleolar ribonucleoprotein protein MPP10	MPHOSPH10
1,4856	1,2393	Myosin phosphatase Rho-interacting protein	MPRIP
1,4130	2,3333	mRNA turnover protein 4 homolog	MRTO4
1,6398	1,5918	DNA mismatch repair protein Msh2	MSH2
1,3441	0,9219	DNA mismatch repair protein Msh6	MSH6
1,7886	0,7443	Metastasis-associated protein MTA2	MTA2
2,4980	1,3658	Metal-response element-binding transcription factor 2	MTF2
3,4682	5,1108	Myb-binding protein 1A	MYBBP1A
2,3668	1,5688	Myosin-10	MYH10
1,9810	1,6852	Myosin-9	MYH9
2,0480	0,7459	Unconventional myosin-Ib	MYO1B
1,4272	4,6683	Myelin transcription factor 1-like protein	MYT1L
3,1142	0,7509	N-acetyltransferase 10	NAT10
2,9173	**3,6937**	**Nucleolin**	**NCL**

-LOG (P-value)	Difference	Protein names	Gene names
2,6296	1,1920	Neuroguidin	NGDN
3,3918	4,5364	MKI67 FHA domain-interacting nucleolar phosphoprotein	NIFK
2,3136	1,2635	60S ribosome subunit biogenesis protein NIP7 homolog	NIP7
1,2493	1,9966	NF-kappa-B-activating protein;NKAP-like protein	NKAP;NKAPL
1,3659	2,1529	Notchless protein homolog 1	NLE1
2,2462	0,9134	Nicotinamide/nicotinic acid mononucleotide adenylyltransferase 1	NMNAT1
2,1969	3,5726	Nucleolar complex protein 2 homolog	NOC2L
3,5683	2,4030	Nucleolar complex protein 3 homolog	NOC3L
2,1677	1,3241	Nucleolar complex protein 4 homolog	NOC4L
1,8872	2,7030	Nucleolar protein 10	NOL10
2,3551	1,0486	Nucleolar protein 11	NOL11
1,9948	1,1984	Nucleolar protein 6	NOL6
1,8760	2,8836	Nucleolar protein 7	NOL7
2,3551	2,3132	Nucleolar protein 8	NOL8
1,8825	2,4925	Polynucleotide 5-hydroxyl-kinase NOL9	NOL9
1,9142	2,9375	Nucleolar and coiled-body phosphoprotein 1	NOLC1
2,7865	4,0995	Non-POU domain-containing octamer-binding protein	NONO
2,9998	4,6736	Nucleolar protein 14	NOP14
3,2568	1,5258	Nucleolar protein 16	NOP16
4,0739	5,8043	Probable 28S rRNA (cytosine(4447)-C(5))-methyltransferase	NOP2
2,4831	3,0370	Nucleolar protein 56	NOP56
3,2937	**2,0602**	**Nucleophosmin**	**NPM1**
2,1155	1,4867	Nucleoplasmin-3	NPM3
2,6281	3,3155	Ribosome biogenesis protein NSA2 homolog	NSA2
1,8647	1,4105	E3 SUMO-protein ligase NSE2	NSMCE2
3,0715	2,4545	Nuclear mitotic apparatus protein 1	NUMA1
2,0293	1,2580	Nuclear valosin-containing protein-like	NVL
2,0972	2,8510	p21-activated protein kinase-interacting protein 1	PAK1IP1
3,2052	0,8923	Poly [ADP-ribose] polymerase 1	PARP1
1,7778	1,8535	Protein polybromo-1	PBRM1
2,0428	3,8468	Protein RRP5 homolog	PDCD11
3,1208	2,1211	Proline-, glutamic acid- and leucine-rich protein 1	PELP1
2,9570	1,1176	Pescadillo homolog	PES1
3,1393	1,1552	Prohibitin-2	PHB2
2,0600	0,8946	Histone lysine demethylase PHF8	PHF8
2,4179	3,2203	PH-interacting protein	PHIP

-LOG (P-value)	Difference	Protein names	Gene names
2,3744	2,0860	Ribonucleases P/MRP protein subunit POP1	POP1
4,9385	5,1363	Suppressor of SWI4 1 homolog	PPAN-P2RY11
1,4190	0,9349	Peptidyl-prolyl cis-trans isomerase A	PPIA
1,3919	2,2918	Serine/threonine-protein phosphatase PP1-beta catalytic subunit	PPP1CB
2,7391	0,6762	DNA-dependent protein kinase catalytic subunit	PRKDC
3,0218	2,8645	PC4 and SFRS1-interacting protein	PSIP1
3,7072	1,8511	Periodic tryptophan protein 1 homolog	PWP1
2,3078	1,6087	Periodic tryptophan protein 2 homolog	PWP2
1,2198	2,2100	GTP-binding nuclear protein Ran	RAN
1,4571	1,4034	Histone-binding protein RBBP4	RBBP4
2,2588	3,8934	RNA-binding protein 14	RBM14
1,9925	1,4997	Probable RNA-binding protein 19	RBM19
4,6944	2,0638	RNA-binding protein 28	RBM28
3,8715	4,6912	RNA-binding protein 34	RBM34
1,4482	1,8701	RNA-binding protein 8A	RBM8A
2,2848	3,0370	RNA-binding motif protein, X chromosome	RBMX
3,1362	2,7533	Regulator of chromosome condensation	RCC1
2,2262	1,6531	RNA exonuclease 4	REXO4
1,5457	0,9420	Replication factor C subunit 1	RFC1
1,2174	1,7923	Replication factor C subunit 2	RFC2
2,7269	1,1018	Telomere-associated protein RIF1	RIF1
2,6765	3,8658	Ribosome production factor 1	RPF1
2,7714	3,1937	Ribosome production factor 2 homolog	RPF2
2,6137	3,1016	60S ribosomal protein L10	RPL10
2,5289	1,0385	60S ribosomal protein L11	RPL11
2,4151	1,7471	60S ribosomal protein L13	RPL13
2,6098	3,8113	60S ribosomal protein L13a	RPL13A
2,7674	2,2360	60S ribosomal protein L14	RPL14
2,0396	3,2779	60S ribosomal protein L15	RPL15
3,5313	1,8920	60S ribosomal protein L18	RPL18
2,7361	3,8088	60S ribosomal protein L18a	RPL18A
2,8662	3,5085	60S ribosomal protein L21	RPL21
4,0759	5,4227	60S ribosomal protein L23a	RPL23A
2,2629	3,5709	60S ribosomal protein L26	RPL26
3,7918	2,1390	60S ribosomal protein L27	RPL27
4,8333	5,7166	60S ribosomal protein L27a	RPL27A
2,3571	1,6852	60S ribosomal protein L28	RPL28
3,4481	2,6418	60S ribosomal protein L3	RPL3
5,1083	4,7525	60S ribosomal protein L32	RPL32
1,9921	3,1082	60S ribosomal protein L34	RPL34
2,9679	2,7037	60S ribosomal protein L35a	RPL35A

-LOG (P-value)	Difference	Protein names	Gene names
2,4334	4,4540	60S ribosomal protein L36	RPL36
2,5703	2,3391	60S ribosomal protein L4	RPL4
2,9956	2,9257	60S ribosomal protein L5	RPL5
2,5501	3,6173	60S ribosomal protein L6	RPL6
3,3193	1,8135	60S ribosomal protein L7	RPL7
3,4192	2,6476	60S ribosomal protein L7a	RPL7A
1,4624	1,0244	60S ribosomal protein L7-like 1	RPL7L1
2,8245	3,2000	60S ribosomal protein L8	RPL8
3,3734	3,3316	60S acidic ribosomal protein P1	RPLP1
3,4208	1,8580	60S acidic ribosomal protein P2	RPLP2
2,2949	1,6955	Ribonuclease P protein subunit p30	RPP30
1,2985	2,0673	40S ribosomal protein S11	RPS11
2,7561	1,1397	40S ribosomal protein S14	RPS14
1,8700	1,7803	Active regulator of SIRT1	RPS19BP1
1,9480	0,8109	40S ribosomal protein S23	RPS23
1,8627	1,8852	40S ribosomal protein S24	RPS24
2,0512	1,9780	40S ribosomal protein S3a	RPS3A
2,2152	3,7698	40S ribosomal protein S6	RPS6
2,3653	2,2779	40S ribosomal protein S8	RPS8
2,7359	3,0458	Ribosomal RNA processing protein 1 homolog A	RRP1
3,1184	2,8782	RRP12-like protein	RRP12
2,9985	2,8537	RRP15-like protein	RRP15
4,1806	5,3675	Ribosomal RNA processing protein 1 homolog B	RRP1B
2,3326	1,7248	Ribosomal RNA processing protein 36 homolog	RRP36
1,9134	1,3803	Ribosomal RNA-processing protein 7 homolog A	RRP7A
2,3450	2,6344	Ribosomal RNA-processing protein 8	RRP8
1,9295	3,1653	U3 small nucleolar RNA-interacting protein 2	RRP9
2,6724	2,5263	Ribosome biogenesis regulatory protein homolog	RRS1
2,0376	2,2352	Round spermatid basic protein 1-like protein	RSBN1L
1,3579	1,5472	Remodeling and spacing factor 1	RSF1
2,9922	4,6573	Ribosomal L1 domain-containing protein 1	RSL1D1
1,5620	3,0653	Probable ribosome biogenesis protein RLP24	RSL24D1
1,3345	0,9517	tRNA-splicing ligase RtcB homolog	RTCB
4,9193	1,6924	Scaffold attachment factor B1	SAFB
1,4793	1,2945	U4/U6.U5 tri-snRNP-associated protein 1	SART1
1,8119	2,7092	Sentrin-specific protease 3	SENP3

-LOG (P-value)	Difference	Protein names	Gene names
1,7933	0,9076	Plasminogen activator inhibitor 1 RNA-binding protein	SERBP1
2,8286	1,3863	Splicing factor 3B subunit 2	SF3B2
1,5210	2,5622	Splicing factor 3B subunit 4	SF3B4
1,3828	0,9175	Transcription activator BRG1	SMARCA4
2,0230	0,6770	SWI/SNF complex subunit SMARCC1	SMARCC1
1,4402	1,2264	Structural maintenance of chromosomes protein 1A	SMC1A
2,9005	1,0818	Structural maintenance of chromosomes protein 5	SMC5
1,7436	2,1568	Structural maintenance of chromosomes flexible hinge domain-containing protein 1	SMCHD1
2,3830	2,8455	SNW domain-containing protein 1	SNW1
2,5907	1,7429	Spermatogenesis-associated protein 5	SPATA5
2,5672	2,2388	Msx2-interacting protein	SPEN
2,4393	1,5938	Serum response factor-binding protein 1	SRFBP1
1,6406	1,9874	Serine/arginine-rich splicing factor 9	SRSF9
1,4230	1,1621	Lupus La protein	SSB
3,2840	1,9000	FACT complex subunit SSRP1	SSRP1
2,7542	2,2523	Double-stranded RNA-binding protein Staufen homolog 1	STAU1
1,6098	0,9703	SURP and G-patch domain-containing protein 2	SUGP2
1,8460	1,4655	FACT complex subunit SPT16	SUPT16H
1,3450	1,6434	Heterogeneous nuclear ribonucleoprotein Q	SYNCRIP
2,6713	2,7237	TATA-binding protein-associated factor 2N	TAF15
7,3129	**10,4432**	**Threonine aspartase 1**	**TASP1**
2,2609	0,9266	Transducin beta-like protein 3	TBL3
1,7632	1,1928	Transcription elongation regulator 1	TCERG1
2,3202	1,4735	Testis-expressed sequence 10 protein	TEX10
3,9787	2,1365	Transcription factor A, mitochondrial	TFAM
3,1735	1,2028	Tight junction protein ZO-1	TJP1
1,5872	0,9450	Target of EGR1 protein 1	TOE1
3,4893	**2,1030**	**DNA topoisomerase 2-alpha**	**TOP2A**
1,9182	**3,3554**	**DNA topoisomerase 2-beta**	**TOP2B**
2,0187	0,9680	Tumor suppressor p53-binding protein 1	TP53BP1
2,7486	1,1862	TRMT1-like protein	TRMT1L
1,5322	2,2831	Nucleolar transcription factor 1	UBTF
6,8028	4,4660	Ubiquitin carboxyl-terminal hydrolase 36	USP36
3,1106	2,1976	Probable U3 small nucleolar RNA-associated protein 11	UTP11L
2,8875	2,3968	U3 small nucleolar RNA-associated protein 14 homolog A	UTP14A

-LOG (P-value)	Difference	Protein names	Gene names
1,8621	2,2077	U3 small nucleolar RNA-associated protein 15 homolog	UTP15
1,9902	3,4326	U3 small nucleolar RNA-associated protein 18 homolog	UTP18
2,6422	1,6148	Small subunit processome component 20 homolog	UTP20
2,7767	2,6975	Something about silencing protein 10	UTP3
2,2812	1,3586	U3 small nucleolar RNA-associated protein 6 homolog	UTP6
1,8716	2,4485	WW domain-binding protein 11	WBP11
3,0287	1,3139	Ribosome biogenesis protein WDR12	WDR12
2,8195	3,2388	WD repeat-containing protein 18	WDR18
3,4648	1,2625	WD repeat-containing protein 3	WDR3
2,9750	2,4686	pre-mRNA 3 end processing protein WDR33	WDR33
1,9633	0,7948	WD repeat-containing protein 36	WDR36
5,0338	1,0301	WD repeat-containing protein 43	WDR43
3,3921	2,6212	WD repeat-containing protein 46	WDR46
1,3990	1,0967	WD repeat-containing protein 5	WDR5
2,6216	1,2233	WD repeat-containing protein 74	WDR74
4,0020	0,8301	WD repeat-containing protein 76	WDR76
1,2599	1,0713	Protein Wiz	WIZ
2,3551	1,4047	DNA repair protein XRCC1	XRCC1
1,6563	0,8002	Nuclease-sensitive element-binding protein 1	YBX1
2,9222	1,4798	YTH domain-containing protein 1	YTHDC1
1,6568	1,5233	Zinc finger CCCH-type antiviral protein 1	ZC3HAV1
3,3099	2,5689	Zinc finger RNA-binding protein	ZFR
2,0564	1,6639	Zinc finger MYM-type protein 4	ZMYM4
1,6835	1,7883	Zinc finger protein 280C	ZNF280C
2,6580	2,7459	Zinc finger protein 638	ZNF638

6.2 LIST OF ABBREVIATIONS

aa	Amino acid
ACE	Analytics Core Facility Essen
AF9	ALL1-fused gene from chromosome 9 protein
ALF	TFIIA like factor
AML	Acute myeloid leukaemia
ANOVA	Analysis of variance
APP	Amyloid precursor protein
approx.	Approximately
APS	Ammonium persulfate
b-HLH	Basic helix-loop-helix
BSA	Bovine serum albumin
CDK	Cyclin-dependent kinase
CDKI	Cyclin-dependent kinase inhibitor
ChIP-seq	Chromatin immunoprecipitation-DNA sequencing
C-NHEJ	Classical non-homologous end-joining
co-IP	Co-immunoprecipitation
CS	Cleavage sites
Da	Dalton
DDR	DNA damage response
DMEM	Dulbecco’s Modified Eagle Medium
DNA	Deoxyribonucleic acid
dNTP	Deoxynucleotide triphosphate
DPBS	Dulbecco’s Phosphate-Buffered Saline
DSB	Double strand break
dsDNA	Double-stranded DNA

DTT	Dithiothreitol
E2	Estrogen/ 17β-estradiol
EDTA	Ethylenediaminetetraacetic acid
EMSA	Electrophoretic mobility shift assay
ER	Estrogen receptor
ERE	Estrogen response element
FCS	Fetal calf serum
FPLC	Fast protein liquid chromatography
GFP	Green fluorescent protein
GTF	General transcription factors
H3K4me	Histone H3 lysine 4 methylation
HBS	HEPES-Buffered Saline
HDAC3	Histone deacetylase 3
HMT	Histone methyltransferase
HR	Homologous recombination
HRP	Horseradish peroxidase
HSC	Hematopoietic stem cell
Hsp70	Human heat shock protein 70
ICCE	Imaging Center Campus Essen
IF	Immunofluorescence
IP	Immunoprecipitation
IPTG	Isopropyl b-D-1-thiogalactopyranoside
ITC	Isothermal titration calorimetry
LB	Luria-Bertani
LZ	Leucine zipper
MED4	Mediator complex subunit 4

MEF	Mouse embryonic fibroblast
MLL	Mixed lineage leukemia
MMP	Matrix metalloprotease
mRNA	Messenger RNA
MS	Mass spectrometry
NEB	New England BioLabs GmbH
NES	Nuclear export signal
NLS	Nuclear localization signal
NoLS	Nucleolar localization signal
NP40	Nonidet P40
NPM1	Nucleophosmin 1
NR	Nuclear receptor
Ntn	N-terminal nucleophile
Nuc	Nucleolin
oc	Open circle
OD	Optical density
Opti-MEM	Optimized Minimum Essential Medium
PAGE	Polyacrylamide gel electrophoresis
PARP1	Poly (ADP ribose) polymerase 1
PBS	Phosphate-buffered saline
PCR	Polymerase chain reaction
pH	Potentia Hydrogenii
PIC	Preinitiation complex
PLA	Proximity ligation assay
PMSF	Phenylmethanesulfonylfluoride
pol II	Polymerase II

POL2RA	DNA-directed RNA polymerase II subunit RPB1
Rb1	Retinoblastoma-associated protein 1
REV3L	Protein reversionless 3-like
RIPA	Radioimmunoprecipitation assay buffer
RNA	Ribonucleic acid
rpm	Round per minutes
RT	Room temperature
S5P	Phosphorylation at Serine 5
sc	Supercoiled
SDS	Sodium dodecylsulfate
SET	Su(var)3–9, Enhancer of zeste and trithorax
siRNA	Small interfering RNA
SPR	Surface resonance plasmon
ss	Single strand
TAE	Tris-acetate-EDTA
Taspase1	Threonine Aspartase 1
TBS	Tris-buffered saline
TBST	Tris-buffered saline/Tween
TE	Tris-EDTA buffer
TEMED	N,N,N’,N’-Tetramethylethylenediamine
TFIIA	Transcription factor IIA
Topo	Topoisomerase
Tris	Tris(hydroxymethyl)aminomethane
Tris-HCl	Tris hydrochloride
USF	Upstream stimulatory factor
USR	USF-specific region

UV	Ultraviolett
WB	Western blotting
WT	Wild type
γH2AX	Phosphorylated histone H2AX

6.3 LIST OF FIGURES

6.4 LIST OF TABLES

6.5 AMINO ACIDS

A	Ala	Alanine
C	Cys	Cysteine
D	Asp	Aspartate
E	Glu	Glutamate
F	Phe	Phenylalanine
G	Gly	Glycine
H	His	Histidine
I	Ile	Isoleucine
K	Lys	Lysine
L	Leu	Leucine
M	Met	Methionine
N	Asp	Asparagine
P	Pro	Proline
Q	Gln	Glutamine
R	Arg	Arginine
S	Ser	Serine
T	Thr	Threonine
V	Val	Valine
W	Trp	Tryptophan
Y	Tyr	Tyrosine

PUBLICATIONS

Oelschläger, L. (2019) Untersuchung des tumorrelevanten Proteins Survivin. Zugl.: Duisburg, Essen, Univ., Masterarbeit. Wiesbaden: Springer Spektrum (BestMasters).

Hensel, A., Stahl, P., **Moews, L**., König, L., Patwardhan, R., Höing, A.*, et al.* (2022) The Taspase1/Myosin1f-axis regulates filopodia dynamics. *iScience* **25** (6): 104355.

Höing, A., Zimmermann, A., **Moews, L**., Killa, M., Heimann, M., Hensel, A.*, et al.* (2022) A Bivalent Supramolecular GCP Ligand Enables Blocking of the Taspase1/Importin α Interaction. *ChemMedChem* **17** (1): e202100640.

Oelschläger, L., Stahl, P. Kaschani, F., Kaiser, M., Knauer, S.K., Hensel, A. Taspase1 facilitates Topoisomerase IIβ-mediated DNA breaks driving estrogen-induced transcription (*submitted to Life Science Alliance*)

LEBENSLAUF

Der Lebenslauf ist in der Online-Version aus Gründen des Datenschutzes nicht enthalten.

Der Lebenslauf ist in der Online-Version aus Gründen des Datenschutzes nicht enthalten.

EIDESSTATTLICHE ERKLÄRUNGEN

Erklärung:

Hiermit erkläre ich, gem. § 7 Abs. (2) d) + f) der Promotionsordnung der Fakultät für Biologie zur Erlangung des Dr. rer. nat., dass ich die vorliegende Dissertation selbstständig verfasst und mich keiner anderen als der angegebenen Hilfsmittel bedient, bei der Abfassung der Dissertation nur die angegebenen Hilfsmittel benutzt und alle wörtlich oder inhaltlich übernommenen Stellen als solche gekennzeichnet habe.

Essen, den _____ _____

Lisa Moews

Erklärung:

Hiermit erkläre ich, gem. § 7 Abs. (2) e) + g) der Promotionsordnung der Fakultät für Biologie zur Erlangung des Dr. rer. nat., dass ich keine anderen Promotionen bzw. Promotionsversuche in der Vergangenheit durchgeführt habe und dass diese Arbeit von keiner anderen Fakultät/Fachbereich abgelehnt worden ist.

Essen, den _____ _____

Lisa Moews

Erklärung:

Hiermit erkläre ich, gem. § 6 Abs. (2) g) der Promotionsordnung der Fakultät für Biologie zur Erlangung der Dr. rer. nat., dass ich das Arbeitsgebiet, dem das Thema „*Investigating the role of Threonine Aspartase 1 in estrogen-driven transcription*“ zuzuordnen ist, in Forschung und Lehre vertrete und den Antrag von *Lisa Moews geb. Oelschläger* befürworte und die Betreuung auch im Falle eines Weggangs, wenn nicht wichtige Gründe dem entgegenstehen, weiterführen werde.

Essen, den _____ _____

Prof. Dr. Shirley Knauer